

Aus dem Interfakultären Institut für Zellbiologie der Universität  
Tübingen

Abteilung Immunologie

**Identification of clinically relevant CD4<sup>+</sup> T-cell epitopes  
from HCMV antigens**

**Inaugural-Dissertation  
zur Erlangung des Doktorgrades  
der Medizin**

**der Medizinischen Fakultät  
der Eberhard Karls Universität  
zu Tübingen**

**vorgelegt von**

**Höttler, Alexander Frank**

**2022**

Dekan: Professor Dr. B. Pichler

1. Berichterstatter: Professor Dr. S. Stevanovic  
2. Berichterstatter: Professor Dr. Dr. K. Hamprecht  
3. Berichterstatter: Professorin Dr. B. Eiz-Vesper

Tag der Disputation: 29.11.2022

# Table of contents

Abbreviations

List of Figures

List of Tables

1	Introduction .....	1
1.1	Human cytomegalovirus.....	1
1.1.1	Virus structure.....	1
1.1.2	Viral genome.....	3
1.1.3	Infection and replication cycle.....	4
1.1.4	Latency and reactivation.....	5
1.2	Principles of T cell-mediated immunity .....	6
1.2.1	T-cell receptor.....	6
1.2.2	Major histocompatibility complex (MHC).....	7
1.3	Reverse immunology – <i>in silico</i> prediction of T-cell epitopes .....	12
1.4	Immune response to HCMV .....	13
1.4.1	T cell-mediated immune response.....	14
1.5	HCMV-associated diseases and therapeutic approaches.....	17
1.6	Aim of the project .....	22
2	Material.....	23
2.1	Devices .....	23
2.2	Software .....	24
2.3	General material.....	24
2.4	Enzymes and inhibitors .....	25
2.5	Chemicals .....	25
2.6	Buffers and solutions.....	26
2.7	Beads.....	26
2.8	Cell culture media and cytokines.....	26
2.9	Antibodies and dyes .....	27
3	Methods.....	28

3.1	Selection of T-cell epitope candidates by promiscuous epitope prediction .....	29
3.2	Fmoc solid-phase synthesis of epitope candidates for T-cell experiments .....	33
3.3	PBMC isolation from buffy coats .....	33
3.3.1	Experimental procedure: PBMC isolation from buffy coats .....	35
3.4	Cell counting .....	36
3.5	Cell thawing .....	36
3.6	Cell culture and 12-day peptide stimulation .....	36
3.7	Epitope screening by the IFN $\gamma$ ELISpot assay .....	37
3.7.1	Evaluation criteria of ELISpot results .....	41
3.7.2	Experimental procedure: ELISpot after 12-day peptide stimulation ...	42
3.8	Epitope validation by intracellular cytokine staining .....	44
3.8.1	Experimental procedure: intracellular cytokine staining .....	46
3.9	Protein sequence alignment .....	47
4	Results .....	48
4.1	Identification of T-cell epitopes by the IFN $\gamma$ ELISpot assay .....	48
4.2	Identified T-cell epitopes originate from a broad antigen spectrum .....	56
4.3	Validation of T-cell epitopes by intracellular cytokine staining .....	57
4.4	Prediction of promiscuous CD4 <sup>+</sup> T-cell epitopes from HCMV antigens ....	62
4.5	Generation of peptide pools containing validated CD4 <sup>+</sup> T-cell epitopes ...	63
4.6	Epitopes and peptide pools tested in <i>ex vivo</i> ELISpot assays .....	67
4.7	Dominant epitopes tested in PBMC cultures of HCMV-seronegative blood donors .....	71
4.8	Alignment of the source protein sequences of dominant epitopes with correspondent protein sequences of the HCMV strain Merlin .....	72
5	Discussion .....	73
5.1	Identification of T-cell epitopes by the IFN $\gamma$ ELISpot assay .....	73
5.2	Identified T-cell epitopes originate from a broad antigen spectrum .....	74
5.3	Validation of T-cell epitopes by ICS .....	77



5.4	Prediction of promiscuous CD4 <sup>+</sup> T-cell epitopes from HCMV antigens ....	78
5.5	Generation of peptide pools containing validated CD4 <sup>+</sup> T-cell epitopes ...	81
5.6	Epitopes and peptide pools tested in <i>ex vivo</i> ELISpot assays.....	83
5.7	Dominant epitopes tested in PBMC cultures of HCMV-seronegative blood donors .....	84
5.8	Alignment of the source protein sequences of dominant epitopes with correspondent protein sequences of the HCMV strain Merlin .....	85
5.9	Conclusion and outlook .....	87
6	Summary .....	88
7	Zusammenfassung .....	89
8	Appendix.....	90
9	References .....	100
10	Erklärung zum Eigenanteil.....	120
11	Publications .....	121
11.1	Poster presentation .....	121
12	Danksagung .....	122

## Abbreviations

15-mer *15-aa-long peptide*

aa *amino acid*

APC *antigen-presenting cell, allophycocyanin*

BSA *bovine serum albumin*

CD *cluster of differentiation*

CLIP *class II-associated invariant chain peptide*

CTL *cytotoxic T cells*

Cy *cyanine*

DMSO *dimethylsulfoxide*

E *early*

EDTA *ethylenediaminetetraacetic acid*

ELISpot *enzyme-linked immunospot assay*

*f.c.* *final concentration*

FACS *fluorescence activated cell sorting*

FCS *fetal calf serum*

FLNA *filamin-a*

FREP *frequently recognized epitope*

GMP *good manufacturing practice*

HCMV *human cytomegalovirus*

HCMVA *HCMV strain AD169*

HCMVM *HCMV strain Merlin*

HLA *human leukocyte antigen*

HPLC *high-performance liquid chromatography*

HSCT *hematopoietic stem cell transplantation*

ICS *intracellular cytokine staining*

IE *immediate-early*

IFN $\gamma$  *interferon  $\gamma$*

IL-2 *interleukin-2*

L *late*

LCK *lymphocyte-specific protein tyrosine kinase*

MACS *magnetic-activated cell sorting*

MHC *major histocompatibility complex*  
MIEP *major immediate-early promoter*  
MIIC *MHC class II compartment*  
NK cell *natural killer cell*  
ORF *open reading frame, open reading frame*  
PBMC *peripheral blood mononuclear cell*  
PBS *phosphate-buffered saline*  
PE 27, *r-phycoerythrin*  
Pen/Strep *penicillin/streptomycin*  
PHA *phytohemagglutinin*  
PLC *peptide loading complex*  
PMA *phorbol myristate acetate*  
RhCMV *rhesus macaque cytomegalovirus*  
rr *ELISpot recognition rate*  
SFC *spot-forming cells*  
SOT *solid organ transplantation*  
T<sub>CM</sub> *central memory T cell*  
TAP *transporter associated with antigen processing*  
TCM *T-cell medium*  
TCR *T-cell receptor*  
T<sub>EM</sub> *effector memory T cell*  
T<sub>H</sub> *T helper cell*  
TM *thawing medium*  
TNF *tumor necrosis factor*  
T<sub>RM</sub> *tissue-resident memory T cell*  
UL *unique long*  
US *unique short*

## List of Figures

FIGURE 1: STRUCTURE OF THE HCMV VIRION.....	3
FIGURE 2: THE MHC CLASS II ANTIGEN PRESENTATION PATHWAY. ....	10
FIGURE 3: SCHEMATIC OF THE BINDING GROOVE OF AN HLA CLASS II MOLECULE. .....	11
FIGURE 4: OVERVIEW OF APPLIED METHODS.....	28
FIGURE 5: EPITOPE SELECTION EXAMPLE FOR PROTEIN US4. ....	32
FIGURE 6: ISOLATION OF PBMCs FROM BUFFY COATS.....	34
FIGURE 7: SCHEMATIC OF AN ELISPOT ASSAY.....	40
FIGURE 8: GATING STRATEGY FOR ICS. ....	45
FIGURE 9: STANDARD SCREENING ELISPOT EXAMPLE. ....	49
FIGURE 10: RECOGNITION RATES OF PREDICTED PEPTIDES TESTED IN ELISPOT ASSAYS WITH A PRIOR 12-DAY STIMULATION. ....	55
FIGURE 11: ELISPOT RESULTS OF DOMINANT EPITOPES.....	56
FIGURE 12: ANTIGEN SPECTRUM OF PREDICTED DOMINANT AND SUBDOMINANT PEPTIDES. ....	57
FIGURE 13: VALIDATION OF CD4 <sup>+</sup> T-CELL EPITOPES BY ICS.....	61
FIGURE 14: PEPTIDE POOLS ACTIVATE THE VAST MAJORITY OF TESTED PBMC CULTURES.....	65
FIGURE 15: COMPARISON OF THE RECOGNITION RATES OF PEPTIDE POOL I AND II.....	66
FIGURE 16: EXPANSION OF EPITOPE-SPECIFIC T-CELL POPULATIONS THROUGH 12-DAY STIMULATION.....	68
FIGURE 17: EX VIVO T-CELL RESPONSES TO THE PEPTIDE POOLS.....	70
FIGURE 18: AMPLIFICATION OF T-CELL POPULATIONS BY 12-DAY STIMULATION WITH POOL I AND II. ....	70
FIGURE 19: DOMINANT EPITOPES WERE TESTED IN PBMC CULTURES OF HCMV- SERONEGATIVE DONORS. ....	71
FIGURE 20: EXEMPLARY ALIGNMENT OF TWO SOURCE PROTEIN SEQUENCES FROM HCMV STRAIN AD169 (HCMVA) AND MERLIN (HCMVM).....	72

FIGURE S1: ALGORITHM FOR THE DETECTION OF IDENTICAL CORE SEQUENCES AMONG PREDICTED PEPTIDES.....	90
FIGURE S2: SEQUENCE ALIGNMENT OF DOMINANT EPITOPES WITH THE HCMV STRAIN MERLIN. ....	99

## List of Tables

TABLE 1: ALLELE FREQUENCIES AT THE DRB1 GENE LOCUS.....	29
TABLE 2: POSITIVE POOL HLA CLASS II.....	39
TABLE 3: PEPTIDES TESTED IN ELISPOT ASSAYS SELECTED BY PROMISCUOUS EPITOPE PREDICTION.....	50
TABLE 4: TESTED PEPTIDES ORIGINATING FROM THE LABORATORY STOCK.....	53
TABLE 5: PEPTIDES TESTED IN ICS.....	58
TABLE 6: COMPOSITION OF PEPTIDE POOL I. ....	64
TABLE 7: ELISPOT RESULTS OF THE PEPTIDE POOLS.....	64
TABLE 8: PEPTIDES TESTED IN EX VIVO ELISPOT ASSAYS.....	69
TABLE S1: PREDICTED PROMISCUOUS EPITOPE CANDIDATES FROM THE SINGLE- PROTEIN PREDICTION. ....	91
TABLE S2: PREDICTED PROMISCUOUS EPITOPE CANDIDATES FROM THE WHOLE- PROTEOME PREDICTION.....	95

## **1 Introduction**

### **1.1 Human cytomegalovirus**

The human cytomegalovirus (HCMV) or human betaherpesvirus-5 belongs to the subfamily of beta herpesviruses. Beta herpesviruses share common characteristics such as strict species specificity, a long replication time in culture, and a broad cell tropism for hematopoietic and epithelial cell types [1].

#### **1.1.1 Virus structure**

The virion consists of a capsid containing the double-stranded viral DNA, and a tegument layer that comprises proteins with different functions relevant for virus entry and initial steps of viral reproduction. The tegument is surrounded by a host cell-derived envelope comprising several viral glycoproteins that are responsible for establishing cell contact and mediating virus entry into the host cell [1]. The structure of the HCMV virion is depicted in Figure 1.

The icosahedral capsid is assembled of 162 capsomeres, hexamers and pentamers from the Major capsid protein (MCP), and is classified by the triangulation number 16 ( $T = 16$ ) [2-4]. Besides MCP, three proteins are part of the capsid: the minor capsid protein (mCP or triplex subunit 1), the minor capsid binding protein (triplex subunit 2), and the smallest capsid protein (SCP) [5]. Another essential component of the capsid is the portal protein (PORT), which enables DNA packaging into and release from the capsid together with two terminase subunits [6].

The tegument is an amorphous layer between the capsid and the envelope and contains more than half of all proteins of the infectious virion [7, 8]. They carry out various functions and are involved in infection and virus assembly [7]. The most abundant proteins are pp65, which is a major target for T cells, and pp150 [9, 10]. pp65 is the main constituent of extracellular virus particles and drives immune evasion in many different ways [11]. Pp150 is part of the inner tegument layer and

stabilizes the genome-containing capsid. Further, it could be relevant for the integration of essential tegument proteins into the virion [12]. Tegument proteins, like pp71, also trigger immediate-early gene expression by activating cellular transcription complexes [13].

Cytomegalovirus, like all other Herpesviridae, is enveloped by a lipid bilayer derived from the host cell. The virus uses endosomal membranes or parts of the ER-Golgi intermediate compartment (ERGIC) for envelopment [14, 15]. Further, host proteins of the endosomal sorting complex required for transport (ESCRT) serve the virus for maturation [16]. The envelope is equipped with several viral glycoproteins, two of which are indispensable for the virus to enter the cell: glycoprotein B (gB) [17] and the gH-gL dimer. Glycoprotein B mediates initial attachment to the cell by interacting with heparan sulfate glycosaminoglycans [18]. Moreover, it influences cell tropism and strain-specific infection efficiency via association to various receptor types [19-21]. GH-gL can form a complex with gO, which presumably mediates entry into fibroblasts. GH-gL can associate with UL128, UL130, and UL131, forming a pentameric complex that facilitates infection of endothelial and epithelial cells. The laboratory strain AD169, for instance, lacks the UL128-131 locus and, thus, lost endo- and epithelial cell tropism [22].

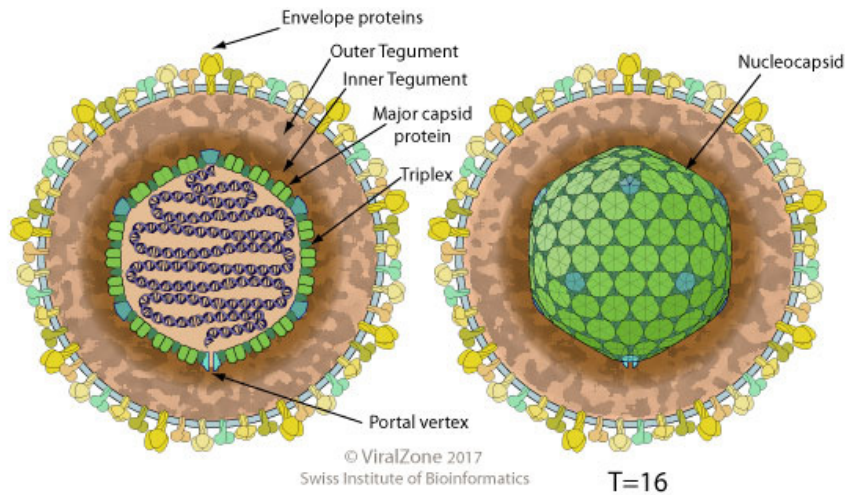


**Figure 1: Structure of the HCMV virion.** The virion of HCMV consists of a nucleocapsid containing the double-stranded viral DNA [1]. It comprises the major capsid protein, the minor capsid protein (triplex subunit 1), the minor capsid binding protein (triplex subunit 2), and the smallest capsid protein (not shown) [5]. The portal protein (portal vertex) mediates DNA entry [6]. It is enclosed by an envelope comprising different glycoproteins. The tegument layer is located between the capsid and the envelope [1]. Abbreviations: T, triangulation number. This figure was adopted from the Swiss Institute of Bioinformatics with permission [23].

### 1.1.2 Viral genome

HCMV has the largest genome among all herpesviruses. It is arranged according to a class E genome structure typical for herpesviruses. Therefore, it is made up of a unique long region (UL) and a unique short region (US). These are flanked by inverted repeats and long and short terminal/internal repeats (TRL, IRL, and TRS, IRS) [24]. Inversion of the UL and US regions, enabled by the flanking regions, results in four genetic isomers [25, 26]. Around 192, potentially protein-coding open reading frames (ORFs) have been estimated to be included in the HCMV genome [27]. By analyzing ribosome-protected mRNA fragments, the entire spectrum of HCMV translation products was assessed, resulting in 751 identified ORFs [28]. Complex transcription mechanisms contribute to a large number of ORFs [29]. How many of them are protein-coding remains elusive.



### **1.1.3 Infection and replication cycle**

HCMV enters the body through contact with the mucosal epithelium via body fluids like saliva or urine. Consecutive infection of monocyte-derived cells mediates hematogenous dissemination in the host organism [30]. Further, immunohistochemical analysis of tissue sections confirms tropism for mesenchymal cells, smooth muscle cells, hepatocytes, and granulocytes [31]. Notably, its tropism to vascular endothelial cells in immunocompromised individuals can lead to multiple organ damage [32, 33]. During the initiation of cell entry, envelope glycoproteins interact with host cell membrane receptors and cell surface heparan sulfate, which causes membrane merging and release of the capsid into the cytoplasm [18]. Subsequently, the nucleocapsid is transported into the nucleus exploiting cytoskeleton-dependent mechanisms [34]. The final step of viral entry is the transfer of the viral DNA into the nucleus [35]. Tegument proteins that are released simultaneously enable the transcription of immediate early genes and regulate the host cell defense (see 1.1.1).

Two phases of a viral infection can be distinguished: The lytic phase, defined as the expression of all viral genes in consecutive stages, and the latent phase going along with a strongly reduced transcription of viral proteins [36].

The consecutive gene expression stages in the lytic phase depend on different viral and host cell agents [37]. The conventional categories of viral proteins successively synthesized are immediate-early (IE), early (E), and late (L) [38]. Transcription of the major IE gene (UL 122 and 123) is regulated by the major immediate-early promoter (MIEP), which plays an essential role in latency and reactivation [39]. Gene products derived from this gene are crucial for gene expression in the subsequent stages. Moreover, they are responsible for the inhibition of the antiviral resistance mechanisms of the host cell and cell death [40, 41]. Proteins of the early gene class are mainly involved in DNA synthesis; they serve as structural components or contribute to immune evasion [42].

The majority of HCMV genes are expressed in the late phase of the lytic cycle. These genes encode for structural proteins of the virus or proteins that serve for virion maturation and egress from the cells, e.g., the tegument protein UL94 [43]. A novel approach, based on proteomics, defines five temporal classes of HCMV gene expression [44]. Through mass spectrometry analysis, proteomics provides a more profound insight into the whole spectrum of proteins present at different time points and discovers even low-abundant proteins [44].

#### ***1.1.4 Latency and reactivation***

After the primary infection with HCMV, the virus persists in the cells of the host, maintaining a status of latency, from which cycles of reactivation can occur. In contrast to lytic replication, the state of latency is characterized by the presence of episomal viral DNA in the nucleus without the production of infectious viral particles [45]. Active replication takes place in a broad spectrum of different cell types (see 1.1.3), but the latent persistence of viral DNA has been detected in myeloid-lineage cells only [46]. More precisely, CD34<sup>+</sup> and CD33<sup>+</sup> cells in the bone marrow serve as reservoirs for latent HCMV [47, 48]. These cells differentiate to CD14<sup>+</sup> monocytes that carry viral DNA [49]. Consequently, the virus is present during the stages of myeloid cell differentiation. This differentiation triggers HCMV reactivation in an interferon  $\gamma$  (IFN $\gamma$ )-dependent manner [50, 51].

During latency, epigenetic modifications of the viral DNA lead to altered gene expression. Specifically, the acetylation of histones that are bound to the MIEP leads to the inactivation of IE gene expression [52]. During cell differentiation, respective epigenetic modulation reactivates IE gene expression [53]. UL138, UL111A (IL-10 homolog), and LUNA are gene products associated with latency that may represent potential therapeutic targets [54-56]. However, recent studies revealed that lytic gene expression can be detected in latently infected myeloid cells, as well [57, 58]. These findings challenge the hypothesis of epigenetic silencing of lytic protein transcription in these cells. Single-cell analysis conducted by Shnayder et al. and

others elucidate this issue by suggesting progressive transcriptional repression of lytic viral gene expression over time [58]. Hence, changes in viral gene expression during latency seem to be rather quantitative [58, 59].

## **1.2 Principles of T cell-mediated immunity**

The innate immune system responds rapidly to pathogens but is unspecific. The adaptive immune response, on the other hand, recognizes antigens specifically. Thus, it controls infections or the growth of cancer cells more efficiently than the innate immune system. Further, it establishes immunological memory, enabling faster and stronger reactions facing a second exposure. T cells play a central role in the adaptive immunity. The underlying principle of how T cells detect their targets is the interaction of the T-cell receptor with specialized glycoproteins on the surface of the target cell, the so-called human leukocyte antigens (HLAs). Intracellular proteins or extracellular, phagocytosed proteins are processed into peptides that are loaded onto the HLA molecules. These HLA-peptide complexes can be recognized by T cells via their T-cell receptor (TCR).

T cells are grouped into two main categories according to the expression of the co-receptors CD4 and CD8 on the cell surface. CD4 is affine to the invariant chain of the HLA class II molecule and increases the sensitivity to activation when the TCR binds to an HLA-peptide complex. Correspondingly, CD8 binds to HLA class I molecules. The increase in sensitivity is accomplished by the lymphocyte-specific protein tyrosine kinase (LCK) that amplifies intracellular signaling upon T-cell activation [60].

### **1.2.1 T-cell receptor**

The structure of the T-cell receptor is generally equivalent to the Fab-segment of immunoglobulins. It is a heterodimer composed of an  $\alpha$ - and a  $\beta$ -chain. Most T cells express this  $\alpha:\beta$  T-cell receptor, but some detect antigen via a  $\gamma:\delta$  receptor, which is

a subject of ongoing research and not yet fully understood. Different regions within the T-cell receptor have been identified: a variable region, where the antigen binding takes place, a constant region, a stalk segment with a cysteine residue forming a disulfide bond between the two chains, a transmembrane domain, and a cytoplasmic tail [61].

T-cell progenitors migrate from the bone marrow to the thymus, where they are termed thymocytes, to pass several steps of selection. Before selective events occur, the germline gene configuration gets rearranged. Variable (V), diversity (D), and junction (J) segments of the  $\beta$ -chain are reorganized first, followed by rearrangement of the  $\alpha$ -chain. These sequential events result in  $CD4^+CD8^+CD3^+$  thymocytes ready to face a dual selection process that determines their further development to naïve T cells.

During positive selection, survival signals are sent to thymocytes that can recognize HLA-bound peptides. Secondly, thymocytes that recognize HLA-self-peptide complexes too strongly end up in apoptosis, which is described as negative selection [61].

### **1.2.2 Major histocompatibility complex (MHC)**

Antigen recognition by T cells is HLA-restricted, meaning that a T-cell receptor recognizes only complexes of HLA and peptide. This dual specificity of T-cell-antigen recognition allows the immune system to discriminate between self- and non-self-antigens. In contrast to antibodies, which neutralize or opsonize extracellular pathogens or bind to cell surfaces, T cells detect HLA-presented peptides derived from extracellular and intracellular antigens.

The gene locus coding for the protein units of the HLA molecules, and other linked proteins involved in antigen processing and epitope presentation, is located on chromosome 6 and comprises 224 gene loci [62, 63]. This group of genes is called the major histocompatibility complex. Beta-2 microglobulin and the invariant chain,

which associate with HLA molecules, are encoded on chromosome 5 and 15, respectively [64]. The coevolution of pathogens trying to escape antigen presentation on HLA molecules and of the antigen-presenting system resulted in an extraordinary polymorphism. The HLA genes are the most polymorphic in the human genome [63].

Moreover, the HLA locus is polygenic. Meaning, that the class I region encodes for three different  $\alpha$ -chains (A, B, C) and the class II region for three different pairs of  $\alpha$ - and  $\beta$ -chains (DR, DP, DQ). In some individuals, there is a third  $\beta$ -chain for HLA-DR, resulting in one more protein. Also, the two alleles for each gene are expressed codominantly [64].

HLA class III genes encode for the complement system and tumor necrosis factor (TNF) [65, 66].

HLA class I molecules are composed of an  $\alpha$ -chain divided into three different domains and  $\beta_2$ -microglobulin. The  $\alpha_1$  and  $\alpha_2$  domains are highly polymorphic as they form the peptide binding cleft. HLA class I molecules are expressed on the surface of nucleated cells, especially on hematopoietic cells [67]. The proteasome, a multicatalytic protease complex, continuously degrades ubiquitinated proteins into peptides that are then loaded onto HLA class I molecules. IFN $\gamma$ , released by T cells or other immune cells, triggers the transformation of the proteasome to an immunoproteasome [68]. Subsequently, the number of peptides able to be presented on HLA class I molecules increases, and the HLA class I expression itself is upregulated. The peptides are transported into the endoplasmic reticulum (ER) via the transporter associated with antigen processing (TAP). The TAP-associated peptide loading complex (PLC) consists of multiple chaperones that mediate the association of the  $\alpha$ -chain: $\beta_2$  heterodimer to TAP. The HLA class I molecule is held inside the ER until a high-affinity peptide binds and transport of the HLA class I-peptide complex to the cell surface can occur [69]. The peptides presented on HLA class I are typically eight to ten amino acids (aa) long [70]. However, it has been shown that 15-mers can also activate CD8<sup>+</sup> T cells [71]. It is assumed that peptidases

shorten these peptides allowing the binding to HLA class I molecules [72]. Moreover, work from several groups revealed that peptides longer than ten aa can bind to HLA class I molecules by bulging out of the binding groove and are recognized by CD8<sup>+</sup> T cells [73, 74].

The peptides are anchored at the second position of the peptide chain and the N- and C-terminus. Nonetheless, other anchor positions are relevant for peptide affinity, as well [75]. Consequently, each allelic variant of an HLA molecule has a specific peptide-binding motif [76].

HLA class II molecules are heterodimers consisting of an  $\alpha$ - and a  $\beta$ -chain that form the peptide-binding groove with their variable regions. They are expressed on antigen-presenting cells (APCs), like B cells, macrophages, dendritic cells, epithelial cells of the thymus, and activated T cells [77, 78]. Newly synthesized HLA class II polypeptide chains are transported into the ER, where an invariant chain binds to the molecule. The class II-associated invariant chain peptide (CLIP), as a domain of the invariant chain, blocks the peptide-binding groove until peptide loading occurs. A complex of three HLA molecules connected by an invariant chain trimer is transported to low-pH endosomal vesicles called the MHC class II compartment (MIIC). An extracellular antigen is internalized, e.g., by APCs and macrophages via phagocytosis, and is enclosed in early endosomes. Subsequently, acidification of these endosomes leads to the activation of proteases that cleave the proteins into peptides [77]. The endosomes fuse with the MIIC enabling the antigenic peptides to associate with the HLA class II molecules. The HLA class II molecule HLA-DM catalyzes the exchange of CLIP with antigenic peptides and maintains a peptide-receptive conformation of the HLA-molecule, allowing various peptides to associate and dissociate [79]. This way, only stable complexes of HLA and peptide are transported to the cell surface (Figure 2). This process mediated by HLA-DM and proteases inside the endosomes is called peptide editing and determines the selection of epitopes that are recognized by T cells [80]. HLA-DO, another HLA class

II molecule, interacts with HLA-DM and has an inhibitory effect on peptide editing [81].

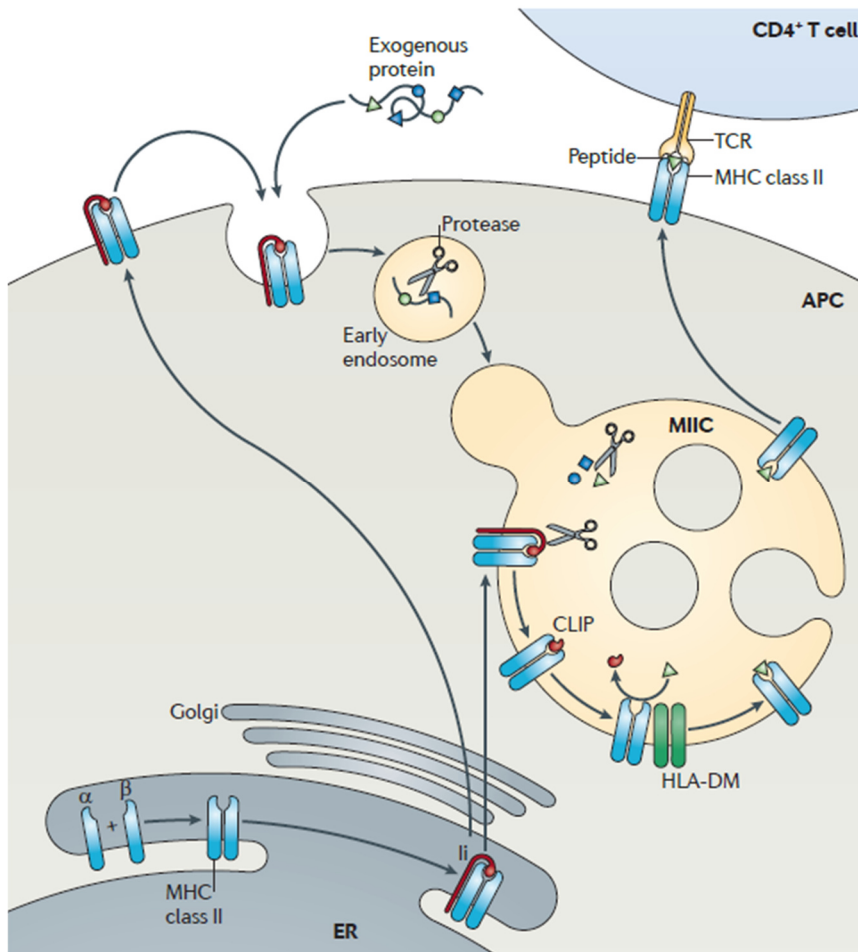


**Figure 2: The MHC class II antigen presentation pathway.** 1. The  $\alpha$ - and  $\beta$ -chain of the MHC class II molecule associate with the invariant chain in the ER. 2. The trimer is transported to the MHC class II compartment (MIIC). 3. Extracellular proteins are cleaved into peptides in early endosomes, and fuse with the MIIC. 4. There the class II-associated invariant chain peptide (CLIP) is replaced by a peptide to be presented, which is HLA-DM mediated. 5. Finally, the MHC-peptide complex is transported to the cell surface where it can be detected by a T cell *via* the T-cell receptor. Adopted with permission from [77] (license no. 5107690932157).

The binding groove of HLA class II molecules is open to the N- and C-terminus, which is a significant difference compared to HLA class I molecules. Peptides can protrude from the groove and can, therefore, be up to 28 aa long [82]. On average, HLA class II bound peptides are 15-18 aa long [83]. This variability in length makes the interpretation of pool sequencing data difficult. Further, promiscuous binding of peptides to several allelic variants of HLA class II molecules has been shown. This indicates that the aa side-chain requirements, and thus the allelic binding motifs, are not as strict as for HLA class I [83]. However, aa with specific chemical properties appear frequently at three or four anchor positions, depending on the HLA allotype. Binding pockets of the HLA class II molecules from the HLA-DRB1 gene locus are affine for specific aa side chains at positions 1, 4, 6, and 9 (Figure 3). In some cases, peptide side chains at position 7 of an HLA class II allotype influence the binding affinity as well. Thus, ligands of HLA-DR molecules have a nine-aa-long core sequence that is anchored in the peptide-binding groove [70, 84].

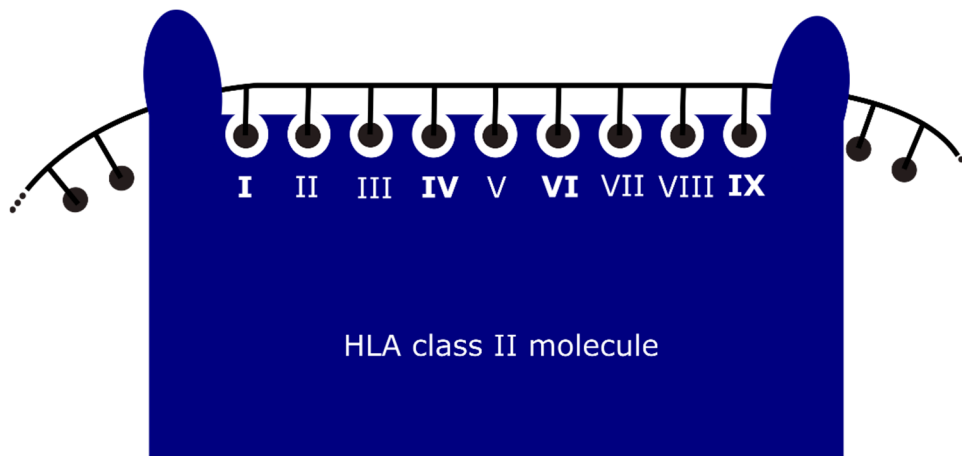


**Figure 3: Schematic of the binding groove of an HLA class II molecule.** This simplified schematic illustration demonstrates the basic principle of the HLA class II:peptide interaction. The binding groove of the HLA class II molecule is open to the N- and C-terminus. Thus, peptides of variable length can bind to the HLA molecule (black line – peptide chain). A core sequence of nine aa is anchored in the binding groove (black dots – aa residues, white spaces – binding pockets). Thereby, the anchor residues at the positions I, IV, VI and IX primarily determine the affinity [84]. This graphic was adapted from Rammensee et al. [85] with the publisher’s permission (order no. 1133087).



Since HLA class I molecules are loaded in the ER and HLA class II molecules in the endosomal compartment, the presentation of intracellular antigens typically occurs on HLA class I and that of extracellular antigens occurs on HLA class II. However, by cross-presentation extracellular antigens are presented to CD8<sup>+</sup> T cells via HLA class I [86]. The exact cross-presentation pathway has not been fully understood yet. In principle, two main mechanisms are discussed: The cytosolic pathway, where proteins escape the phagosome and are processed in the cytosol, and the vacuolar pathway, where proteins are cleaved and loaded on HLA class I molecules in the endosomal compartment [87].

Intracellular antigens can be presented on HLA class II molecules, as well. APCs can phagocytose virus-infected cells whereby intracellular proteins enter the HLA class II antigen presentation pathway. Another route of cross-presentation is mediated by autophagosomes, which include cell components for degeneration and fuse with lysosomes, which leads to peptide loading onto HLA class II molecules [88].

### **1.3 Reverse immunology – *in silico* prediction of T-cell epitopes**

Falk and coworkers discovered the allele-specific binding-motifs of HLA molecules, which has been the cornerstone for reverse immunology [76]. It is possible to predict T-cell epitopes *in silico* and test their immunogenicity in T-cell assays ever since. Rammensee et al. developed the prediction tool SYFPEITHI that is based on scoring matrices for numerous HLA allotypes [89]. The program assigns scores for aa at specific anchor positions in the peptide (-3 to 10). An aa that can be frequently found at an anchor position is assigned the value ten, for instance. Some non-anchoring aa are scored, as well, if they are supposed to influence the binding affinity [89]. The underlying binding-motifs of these scoring-matrices have been determined by a combined analysis of the HLA ultrastructure and the sequencing data of naturally presented HLA ligands. X-ray analysis of HLA crystals has given insight into the composition of the peptide-binding pockets. Using Edman degradation and mass

spectrometry combined with T-cell assays, Rammensee et al. decrypted the influence of different aa residues of a peptide on peptide-HLA interaction [90].

In 90% of the predictions by SYFPEITHI, the immunogenic epitopes can be found among the 2% highest scored epitope candidates for HLA class I. However, the accuracy of the prediction depends on comprehensive knowledge about the allele-specific motif and can be lower [89]. Anchors and interaction sites of HLA class II molecules allow greater variability among the epitopes [70, 91]. Further, these epitopes bind to several different HLA class II allotypes promiscuously [83]. Consequently, epitope prediction based on HLA class II motifs is challenging and has lower reliability than with HLA class I motifs [90].

#### **1.4 Immune response to HCMV**

Primary infection with cytomegalovirus remains silent in most cases due to the complementary control of viral replication by the innate and the adaptive immune system. Essential parts of the innate immune response to viral infection are initial cytokine release and natural killer cells (NK cells). Viral envelope glycoproteins interact with toll-like receptor two and thus lead to the secretion of inflammatory cytokines, which establishes an inflammatory environment [92]. NK cells play a role in the host defense against HCMV, especially in the early phases of the disease [93]. Experiments with HCMV-infected cell lines revealed sophisticated immune evasion strategies indicating that the circumvention of NK-cell attacks goes along with a significant survival advantage for the virus. HCMV uses HLA-E-dependent inhibition of NK-cells, for instance [94]. Additionally, it expresses a protein similar to an HLA class I molecule, UL18, that binds to inhibitory receptors [95]. pp65 can directly inhibit NK-cell cytotoxicity, as well [96].

Since HCMV is located predominantly in the intracellular compartment, humoral immunity can prevent transmission rather than control viral replication and dissemination. Maternal antibodies protect new-borns from severe HCMV-elicited damage, which explains why primary maternal infection during pregnancy has a

worse outcome for the child [97]. Moreover, the application of immune globulins in renal transplant settings reduces HCMV-induced diseases [98]. The main targets of antibodies are surface glycoproteins like gH and the gH/gL/UL128-131A complex [99, 100]. The magnitude of the humoral immunity in preventing disease and transmission is not understood yet.

T-cell-dependent immunity is, in contrast, fundamental for the control of HCMV replication.

### **1.4.1 T cell-mediated immune response**

#### 1.4.1.1 CD8<sup>+</sup> T cells

Numerous studies in mice showed that the control of HCMV replication is primarily regulated by CD8<sup>+</sup> cytotoxic T cells (CTLs) [101]. In humans, recovery of CTLs after hematopoietic stem cell transplantation (HSCT) is related to protection from HCMV disease [102]. Moreover, CD8<sup>+</sup> T cells can decrease the incidence of HCMV retinitis in HIV patients [103]. Together, these findings strongly suggest that CTL-dependent immunity is pivotal in combatting an HCMV infection. This is supported by the fact that HCMV has developed effective immune evasion mechanisms against CTL recognition and killing. The gene products of US2, US11, US3, and US6 complementarily inhibit antigen presentation on HLA class I molecules and therefore impair CTL-mediated killing [104-107]. Nonetheless, these strategies are not sufficient, since a study showed that pp65-derived epitopes were still presented despite the expression of the immune-evasive viral proteins [108]. pp65 itself has immune-evasive features and hampers antigen processing [109]. CD8<sup>+</sup> T-cell responses are directed to a broad spectrum of open reading frames (ORFs) targeting antigens of all expression stages [110]. The most immunodominant antigens are IE1 and pp65 [111, 112]. However, it is unclear if the strong responses to these proteins are most important for controlling an HCMV infection [113].

#### 1.4.1.2 CD4<sup>+</sup> T cells

Viruses are intracellular pathogens. Therefore, a primary mechanism of adaptive immune recognition is the intracellular processing of viral proteins to peptides that are loaded onto HLA class I molecules and recognized by CD8<sup>+</sup> T cells. Consequently, the research of the last decades mainly focused on how these cells control HCMV. Experiments with CD8<sup>+</sup> T cell-depleted mice, however, revealed that HCMV control could be achieved by CD4<sup>+</sup> T cells [114] in cooperation with other cell types [115]. Einsele et al. showed that the adoptive transfer of CD4<sup>+</sup> T cells could induce the expansion of CD8<sup>+</sup> T cells [116]. Thus, CD4<sup>+</sup> cells play a key role in the host's defense against HCMV. Several immune evasion strategies of HCMV support the significant role of CD4<sup>+</sup> T cells in virus control: pp65 induces the degradation of HLA class II molecules [117]. US2 and US3 interfere with the HLA class II pathway, as well [118, 119].

CD4<sup>+</sup> T cells can be further divided into several subsets. Naïve CD4<sup>+</sup> T cells recognize an antigen and differentiate depending on the surrounding cytokine milieu. Most CD4<sup>+</sup> T cells differentiate to distinct effector T helper (T<sub>H</sub>) cells. The CD4<sup>+</sup> immune response to a virus is dominated by T<sub>H</sub>1 cells that secrete IFN $\gamma$  and TNF to drive an inflammatory response and activate macrophages. Besides other subsets, there are cytolytic CD4<sup>+</sup> T cells expressing granzyme B, perforin, and FasL [120]. Hence, cytolytic CD4<sup>+</sup> T cells can directly combat virus-infected cells that express HLA class II molecules. Cytotoxic T cells of a CD4<sup>+</sup>CD28<sup>-</sup> phenotype expand during latent infection and convey HLA class II-dependent cytotoxicity [121].

T helper cells stimulate B cells to differentiate into antibody-secreting plasma cells and stimulate the CD8<sup>+</sup> T-cell response. Through the interaction of cell surface molecules with APCs and cytokine secretion, CD4<sup>+</sup> T cells contribute to the expansion of B cells, augment the CD8<sup>+</sup> T cell:APC contact and promote the expansion and functional development of CD8<sup>+</sup> T cells [122].

CD4<sup>+</sup> T cells against a broad spectrum of antigens can be detected in HCMV-positive donors. An analysis of 213 ORFs by Sylwester et al. recognized several frequently

targeted antigens of CD4<sup>+</sup> T cells: gB, pp65, MCP, CEP3, pp150, and UL153 [123]. The proportion of HCMV-specific cells from all CD4<sup>+</sup> T cells in peripheral blood is approximately ten percent but can expand to 40% [124].

#### 1.4.1.3 Memory T-cell compartment and memory inflation

After infection, selected primed naïve T cells and effector T cells differentiate into memory T cells. Unlike effector T cells, they express the IL-7 receptor, which is also expressed by naïve T cells. Memory T cells depend on stimulation with IL-15, IL-7, and contact to self-peptide:self-HLA complexes [125]. Memory T cells can be subdivided into three categories. Central memory T cells ( $T_{CM}$ ) expressing CCR7 circulate between the blood and the lymphatic tissue. Effector memory T cells ( $T_{EM}$ ) are CCR7 negative and traffic into the secondary lymphatic organs or non-lymphatic tissue. This subtype has the potential to develop into effector T cells rapidly. The third and most frequent type are tissue-resident memory T cells ( $T_{RM}$ ) that migrate into peripheral tissues and do not circulate back into the blood. These are also CCR7 negative [126]. IFN $\gamma$ , TNF, and interleukin-2 (IL-2) secreting cells dominate the memory compartment of CD4<sup>+</sup> T cells [127, 128].

The CD4<sup>+</sup> T-cell memory is composed of a small number of different clonotypes, which dominate the response to HCMV [129]. In rhesus macaque cytomegalovirus models (RhCMV), polyclonal T-cell populations were present in primarily infected monkeys shortly after the infection. These were extensively reduced to a few dominant clonotypes over time. Interestingly, the re-confrontation with RhCMV led to dominant T-cell responses of clonotypes that have diminished after the acute phase of the primary infection. Hence, continuous selection and recruitment of different clonotypes take place, while memory T cells of the early phases of infection persist. However, further research has to be conducted to understand the mechanisms of clonotypic selection during latent and lytic infection with HCMV [130].

The memory T-cell compartment against HCMV is dominated by  $T_{EM}$  cells. It was shown that gene expression during latency is relatively low compared to the lytic

phase, and reactivation of lytic replication occurs infrequently. Hence, low-level exposure of HCMV antigens in sporadic reactivation events to the immune system causes the maintenance of specific T cells [131].

HCMV-specific memory T cells, especially CD8<sup>+</sup> T cells, are present in extremely high numbers in older individuals [132]. CD4<sup>+</sup> HCMV-specific T cells in older people are less dependent on co-stimulation and produce less IL-2. HCMV seropositivity goes along with phenotypical changes of the overall CD4<sup>+</sup> T-cell repertoire, like an increased CD57 expression and a decreased CD28 and CD27 expression [133]. This way, CD4<sup>+</sup> T cells are developing towards end-stages of their differentiation, which restricts their proliferative capacity [134].

The process of immunosenescence, as a progressive low-grade pro-inflammatory status, weakening the function of the immune system is suggested to be associated with the memory inflation of HCMV-specific T cells [132]. However, Jackson et al. recently reviewed the existing studies on memory inflation. They question the body of evidence that led to the conclusion of memory inflation in humans since most of these findings originate from experiments in mice. They suggest more longitudinal studies investigating the long-term memory T-cell response to HCMV [135].

### **1.5 HCMV-associated diseases and therapeutic approaches**

There are three different ways of how an organism encounters a viral infection: primary infection, reinfection, and reactivation of the latent virus. Around 60% of the population is infected with HCMV; in developing countries, nearly 100% [136]. The virus is usually transmitted horizontally through contact to urine or saliva of infected individuals, especially children. Sexual intercourse can lead to infection with HCMV, as well [137]. Other ways of infection are HSCT or solid organ transplantation (SOT). Vertical transmission of HCMV from primarily infected pregnant women to the unborn happens in approximately one-third of the cases [138].

A reinfection with a different HCMV strain was shown to occur in approximately one-third of IgG-seropositive postpartum women in a longitudinal study during a 3-year follow-up [139]. Reactivation of HCMV in immunosuppressed patients that receive HSCT or SOT, or HIV-infected individuals, appears frequently and poses a significant risk for severe HCMV disease [140, 141].

Taken together, these numbers show that HCMV is a prevalent virus that harms large population groups. Moreover, recent studies revealed that HCMV seropositivity influences overall mortality and is a risk factor for ischaemic heart disease [142, 143].

As in other viruses, HCMV disease severity is closely related to viral load [144]. Productive replication of the virus is triggered by an inflammatory environment and sustained by insufficient control by the immune system, which can lead to end-organ damage. This is mediated either by direct cell destruction through the virus or immune-mediated tissue damage [1].

Infected neonates are diagnosed in 50% of the cases with microcephaly. Hearing loss and neurological abnormalities are regularly observed. Some develop multi-organ disease, and approximately 12% die in the first weeks [145].

In immunocompromised adults, HCMV disease can affect multiple organ systems. HCMV pneumonia, for instance, is a significant problem in patients who have received HSCT. Although mortality rates dropped due to pre-emptive antiviral chemotherapy with ganciclovir or foscarnet [146], HCMV-associated death in these patients is still high [147]. HCMV retinitis in HIV patients could be reduced by effective antiretroviral therapy and anti-HCMV therapy, but adverse effects on the overall mortality of these patients remain [148].

Antiviral prophylaxis with ganciclovir after HSCT is not beneficial regarding long-term survival rates. It increases the risk of late-onset HCMV disease instead [149]. Moreover, it goes along with severe side effects, as, e.g., myelotoxicity (thrombocytopenia, granulocytopenia), nephrotoxicity, and azoospermia [150]. Because of that reason, threshold-dependent pre-emptive chemotherapy is

seemingly superior to ganciclovir prophylaxis because it allows the generation of HCMV-specific immune cells [151].

New antiviral agents like maribavir and letermovir may improve the outcome of post-transplantation HCMV infection. Some clinical trials show improvement with less adverse effects [152], while others are rather sobering [153].

In addition to the adverse effects of standard anti-HCMV drugs, there is the problem of emerging resistance when treated over a longer time [154]. Consequently, it is necessary to develop effective therapies that have multiple targets and can prevent late-onset disease. Since the presence of HCMV-specific T cells is crucial for the control (see 1.2.3) of HCMV, it is reasonable to re-establish T-cell immunity.

HCMV-specific immunoglobulins were assessed as a prophylactic treatment for HCMV disease after HSCT. There were no benefits in patient survival or infection prevention [155-157]. Some studies successfully applied prophylactic HCMV-Ig therapy in a SOT setting [158]. Nonetheless, the American Society of Transplantation recommends using HCMV-Ig as an additional therapy for severe or resistant forms of HCMV disease only [159].

Since the impact of HCMV on the health of vulnerable patient groups, namely immunosuppressed and neonates, and because the economic costs of HCMV disease are high, lots of effort is invested in vaccine development. There still is no licensed vaccine available. However, there are some promising trials and forward-looking approaches. The envelope glycoprotein B is a primary target for vaccine development. Trials with recombinant, adjuvanted glycoprotein B have demonstrated the potential of such a vaccine to reduce maternal and congenital HCMV infection [160, 161]. Several other promising vaccines are investigated in clinical trials, e.g., DNA vaccines against gB and pp65 or disabled infectious single-cycle vaccines. Further, the pentameric gH complex is currently discussed as a vaccine candidate because it was shown to be a target for neutralizing antibodies [162].



Pioneering work from Riddell et al. proved that the adoptive transfer of HCMV-specific CD8<sup>+</sup> T cells is a safe and efficient method to reconstitute the T-cell response in the recipient [163]. Successively, numerous studies have been conducted confirming the feasibility and efficacy of this treatment [116, 164, 165]. Einsele et al. demonstrated that the adoptive transfer of CD4<sup>+</sup> T cells leads to CD4<sup>+</sup> and CD8<sup>+</sup> T-cell reconstitution resulting in dramatic viral clearance [116].

Two main approaches for the isolation of virus-specific T cells are established and in use under good manufacturing practice (GMP) conditions [166]. One is the isolation of IFN $\gamma$ -secreting cells upon stimulation with antigen or a peptide pool, which is simple to perform. The cytokine-producing cells are isolated with magnetic-activated cell sorting (MACS) [167]. The drawback of this technique is its low purity that could lead to graft vs. host reactions. However, there were no such reactions observed in a trial by Feuchtinger et al. [165]. Secondly, T cells can be isolated according to their T-cell receptor specificity. Via HLA streptamers loaded with peptide, bound T cells can be isolated using MACS. In this way, a pure cell product comprising “*minimally manipulated*” T cells is obtained [168, 169].

Another approach for obtaining virus-specific T cells for adoptive transfer is through EBV-transformed lymphoblastoid cell lines that are transduced with HCMV antigens [170]. Alternatively, the cell lines can be generated by cytokine activated monocytes loaded with peptide pools [171]. However, these procedures are time-consuming, which is a major limitation in treating acutely ill patients. The establishment of T-cell banks could facilitate an “*off the shelf*” therapy with HLA-matched HCMV-specific T cells [172]. They make transferable T cells readily available. In specific situations, it is not possible to transfer T cells from the transplant donor to the patient. Hence, the use of third-party donors is required. Here, T-cell banks of third-party donors with characterized HCMV-specific T-cell frequency and HLA-typing are especially valuable [173].

Several promising case reports and a clinical trial using the adoptive T-cell transfer to combat post SOT HCMV disease have been published in the last years. The

authors could prove that this approach can improve the clinical outcome and is feasible despite challenges like immunosuppression and the risk of graft rejection [174-176].

T-cell therapy, (peptide) vaccination, and other therapeutic assets can only be advanced by collecting comprehensive knowledge on T-cell target antigens. Thereby, the identification of novel T-cell epitopes enables pinpoint stimulation and isolation of epitope-specific T cells for these purposes.

Moreover, HCMV derived T-cell epitopes can be used for diagnostic purposes, as well. The status of cell-mediated immunity can guide clinicians when to stop antiviral chemotherapy, for instance, which can reduce the side effects of antiviral treatment and improve patient outcomes [177].

CD8<sup>+</sup> and CD4<sup>+</sup> T-cell epitopes have been mainly investigated for a few immunodominant antigens, i.e., pp65 and IE1 [9, 112, 178]. However, several studies revealed that the CD8<sup>+</sup> T cell response is not restricted to pp65 and IE1 but targets a broad antigen spectrum of HCMV [110, 179]. This also holds true for CD4<sup>+</sup> T cells [123]. A variety of different antigens have been investigated for CD8<sup>+</sup> epitopes ever since. The repertoire of CD4<sup>+</sup> epitopes is still limited to a little number of proteins in addition to pp65 [180] and IE1 [181]: DNBI [182], gB [183], gH [184], IE-2 [185], MCP [186], pp50 [187], pp150 [187].

## 1.6 Aim of the project

An infection with HCMV causes severe disease in immunocompromised patients. Immunotherapy represents a promising approach to re-establish virus-specific T-cell immunity and improve patient outcomes. Comprehensive knowledge of T-cell target antigens and T-cell epitopes is fundamental to improve these therapies. So far, CD4<sup>+</sup> T-cell epitopes have only been published for nine different proteins.

In this project, we aim to close this gap by screening 193 proteins from HCMV for frequently recognized promiscuous CD4<sup>+</sup> T-cell epitopes (FREPs) using an in-silico epitope prediction approach. We apply the enzyme-linked immunospot (ELISpot) assay to detect IFN $\gamma$  release in peripheral blood mononuclear cells (PBMCs) of healthy HCMV-seropositive blood donors as a response to HCMV epitope candidates. The reactive T cells are then assessed in flow cytometry by intracellular cytokine staining (ICS) to determine their functionality and differentiate between CD4<sup>+</sup> and CD8<sup>+</sup> T cells. Hence, we obtain a set of FREPs which can be used to generate a peptide pool. Ultimately, this peptide pool is used to reactivate HCMV-specific T cells in PBMC cultures from virtually every tested blood donor regardless of the HLA haplotype.

The set of novel epitopes and the peptide pool can be translated into the clinic to improve Immunotherapies, like the adoptive T-cell transfer.

## 2 Material

### 2.1 Devices

Cell culture hood Technoflow 3F150-II GS	Integra Biosciences (Fernwald, Germany)
Analytical balance XS105 DualRange	Mettler Toledo (Giessen, Germany)
Heraeus Centrifuge Megafuge 1.0R	Thermo Fisher Scientific (Waltham, USA)
Heraeus Centrifuge Labofuge 400	Thermo Fisher Scientific (Waltham, USA)
Heraeus Centrifuge Fresco 17	Thermo Fisher Scientific (Waltham, USA)
Centrifuge Spectrafuge mini	Labnet International, Inc. (Woodbridge, UK)
Neubauer improved counting chamber	Laboroptik (Bad Homburg, Germany)
ELISpot reader C.T.L. S6	Cellular Technology (Shaker Heights, USA)
Flow cytometer FACS Canto II	Becton Dickinson (Franklin Lakes, USA)
One-channel pipettes 2, 10, 100, 200, 1000 $\mu$ l	Abimed (Langenfeld, Germany)
Multi-channel pipette 200 $\mu$ l	Abimed (Langenfeld, Germany)
Pipet aid Pipetboy acu	Integra Biosciences (Fernwald, Germany)
Nalgene Mr. Frosty freezing container	Sigma-Aldrich (St.Louis, USA)
Sanyo Freezer MDF-593 -80°C	Sanyo Electric Biomedical (Tokyo, Japan)
Freezer GlassLine -20°C	Liebherr (Bulle, Switzerland)
Refrigerator GlassLine 4°C	Liebherr (Bulle, Switzerland)
Ice machine AF30	Scotsman (Milan, Italy)
CO <sub>2</sub> Incubator Heracell Vios 250i	Thermo Fisher Scientific (Schwerte, Germany)
Laboratory Microscope DMIL	Leica (Wetzlar, Germany)
MS1 Minishaker	IKA-works, Inc. (Wilmington, USA)
Water bath	GFL GmbH (Burgwedel, Germany)
Ultrasonic bath Sonorex Super RK 514 BH	Bandelin (Berlin, Germany)

## 2.2 Software

ImmunoSpot® Analysis software 5.1	Cellular Technology (Shaker Heights, USA)
FACSDiva software	Becton Dickinson (Franklin Lakes, USA)
FlowJo 10.0.7 software	Tree Star (Ashland, USA)
GraphPad Prism 6	GraphPad Software, San Diego USA
ImmunoCapture 6.1	Cellular Technology Ltd., Shaker Heights, USA
SYFPEITHI Vers.1 and 2	Department of Immunology, Tübingen, Germany; BMI, Heidelberg, Germany
Clustal Omega, Multiple Sequence Alignment	European Molecular Biology Laboratory, European Bioinformatics Institute (EMBL-EBI), Cambridgeshire, UK

## 2.3 General material

Tubes 15 ml, conical bottom, blue cap	Becton Dickinson (Franklin Lakes, USA)
Tubes 50 ml, conical bottom, blue cap, with and without support skirt	Greiner Bio-One (Frickenhausen, Germany)
FACS tubes 5 ml	Becton Dickinson (Franklin Lakes, USA)
Beaker 50 ml	Schott AG (Mainz, Germany)
Glass bottles (250 ml, 500 ml, 1l, 2l)	Schott AG (Mainz, Germany)
Needles (26 Ø 0.45 x 25 mm)	Braun (Melsungen, Germany)
Syringes 1 ml	Braun (Melsungen, Germany)
Syringes (10, 20, 50 ml)	Becton Dickinson (Franklin Lakes, USA)
Disposable serological pipettes (5, 10, 25, 50 ml)	Falcon, Corning Incorporated – Life Sciences, One Becton Circle, Durham, USA)
Pipette tips (10, 200, 1000 µl)	Starlab (Ahrensburg, Germany)
Safe-Lock reaction tubes (0,5/1,5/2 ml)	Eppendorf (Hamburg, Germany)
Millex®- GP, Sterile Syringe-driven Filter Unit 0.22µm, PES Membrane	Merck Millipore (Darmstadt, Germany)
Syringe Filter 0.22 µm Minisart®	Sartorius Stedim Biotech (Aubagne, France)
Cryotubes (2 ml)	Greiner Bio-One (Frickenhausen, Germany)

Polystyrene reservoirs Costar (50 ml)	Corning Incorporated (Corning, USA)
ELISpot plates 96-well MSHAN4B50	Merck Millipore (Darmstadt, Germany)
Cell culture flasks (250ml)	Greiner Bio-One (Frickenhausen, Germany)
Cell culture plates (6-well)	Greiner Bio-One (Frickenhausen, Germany)
Cell culture plates (96-well), U-bottom	Greiner Bio-One (Frickenhausen, Germany)
Cell culture plates Costar (96-well) 3799	Corning Incorporated (Corning, USA)
Surgical disposable scalpel	Braun (Melsungen, Germany)

## 2.4 Enzymes and inhibitors

DNAse I (grade II)	Roche (Basel, Switzerland)
ExtrAvidin® Alkaline Phosphatase	Sigma-Aldrich (St. Louis, USA)
Golgi-Stop (protein transport inhibitor)	Becton Dickinson (Franklin Lakes, USA)

## 2.5 Chemicals

Beta-Mercaptoethanol (14.3 M)	Carl Roth (Karlsruhe, Germany)
Biocoll Separating Solution	Biochrom (Berlin, Germany)
Bovine Serum Albumin [BSA]	Sigma-Aldrich (St. Louis, USA)
Brefeldin A (1 mg/ml in ethanol)	Sigma-Aldrich (St. Louis, USA)
Cytofix/Cytoperm	Becton Dickinson (Franklin Lakes, USA)
Dimethylsulfoxide (DMSO)	Merck (Darmstadt, Germany)
Ethylenediaminetetraacetic acid [EDTA]	Carl Roth (Karlsruhe, Germany)
Ethanol	Liquid Prod. (Flintsbach, Germany)
Fetal Calf Serum [FCS]	life technologies (Darmstadt, Germany)
Gentamicin sulfate (50 mg/ml)	Lonza (Cologne, Germany)
Human plasma (heat-inactivated)	in-house production (pooled)
Ionomycin (1 mM in DMSO)	Sigma-Aldrich (St. Louis, USA)
Penicillin (10 U/μl) Streptomycin (10 mg/ml)	Sigma-Aldrich (St. Louis, USA)
Phytohemagglutinine [PHA] (1 mg/ml)	Sigma-Aldrich (St. Louis, USA)
Saponin	Sigma-Aldrich (St. Louis, USA)
Sigmafast BCIP/NBT tablet	Sigma-Aldrich (St. Louis, USA)
Sodium azide	Merck (Darmstadt, Germany)
Tween® 20	Carl Roth (Karlsruhe, Germany)
Trypan blue	Merck (Darmstadt, Germany)

## 2.6 Buffers and solutions

Dulbecco's Phosphate Buffered Saline DPBS (1x) without CaCl <sub>2</sub> /MgCl <sub>2</sub>	Gibco – Thermo Fisher Scientific (Waltham, USA)
Phosphate Buffered Saline (PBS)	Claudia Falkenburger, Immunology Tübingen
FACS buffer	500 ml PBS (1x) with 2 mM EDTA, 2% FCS (10 ml), 0.02% sodium azide
PermWash buffer	500 ml DPBS (1x) with 0.5% BSA, 0.1% saponin and 0.02% sodium azide
PBS + BSA 0.5%	500 ml PBS (1x) + 2.5 g BSA
PBS + EDTA 2 mM	500 ml PBS (1x) + 2 ml EDTA (0.5 M)
PBS + Tween 0.05%	500 ml PBS (1x) + 500 µl Tween 20
Ethanol	70% in H <sub>2</sub> O <sub>dd</sub>
Trypan blue staining solution	0,05% in PBS (1x) + 0,02% sodium azide
β-Mercaptoethanol (100 mM)	1/14 in DPBS (1x)
DNase I (grade II)	10 mg/ml in DPBS (1x)
FACS-Clean, FACS-Rinse, FACS-Flow	Becton Dickinson (Franklin Lakes, USA)

## 2.7 Beads

Negative beads	life technologies (Darmstadt, Germany)
AbC™ capture beads mouse	life technologies (Darmstadt, Germany)
ArC™ reactive beads	Invitrogen (Carlsbad, USA)

## 2.8 Cell culture media and cytokines

Iscove's Modified Dulbecco's Medium (IMDM) with HEPES and L-Glutamine	Life Technologies, Thermo Fisher Scientific (Waltham, USA)
Thawing medium [TM]	IMDM (500 ml) 1% Pen/Strep (5 ml) 12.5 mg Gentamicin sulfate (250 µl) 50 µM β-Mercaptoethanol (250 µl) 1.5 mg DNase (150 µl)
T-cell medium [TCM]	IMDM (500 ml) 10% human plasma (50 ml) 1% Pen/Strep (5 ml) 12.5 mg Gentamicin sulfate (250 µl) 50 µM β-Mercaptoethanol (250 µl)
Freezing medium	FCS (45 ml) + 10% DMSO (5 ml)
Human recombinant IL-2 (65 U/µl)	R&D Systems (Minneapolis, USA)

## 2.9 Antibodies and dyes

mouse anti-human IFN $\gamma$ mAb1-D1K (1 mg/ml)	Mabtech AB (Nacka Strand, Sweden)
mouse anti-human IFN $\gamma$ Biotinylated mAb7-B6-1-Biotin (1 mg/ml)	Mabtech AB (Nacka Strand, Sweden)
mouse anti-human CD4 APC-Cy7	Biologend (San Diego, USA)
mouse anti-human TNF Pacific Blue	Biologend (San Diego, USA)
mouse anti-human IFN $\gamma$ PE	Biologend (San Diego, USA)
Aqua live/dead fluorescent reactive dye	life technologies (Darmstadt, Germany)
Mouse anti-human CD8 PE-Cy7	Beckman Coulter, Inc. (Brea, USA)



### 3 Methods

The experimental procedures applied in this project are described using the standard laboratory protocols developed by the working group of Prof. Dr. Stefan Stevanović (Department of Immunology, Tübingen). Any adaptations by the author are underlined and the original figures and reagents are given in brackets. Figure 4 provides an overview of the methods used in this project.

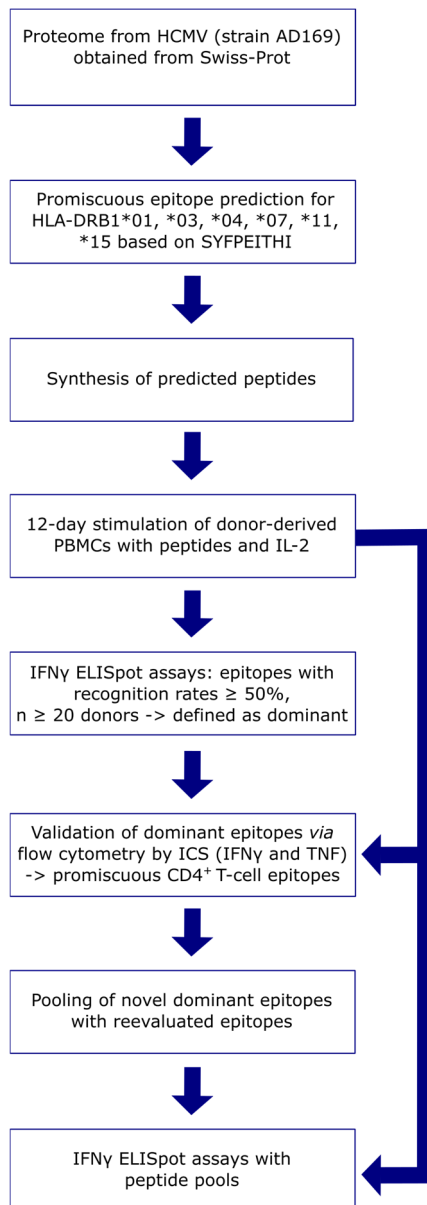


**Figure 4: Overview of applied methods. Adapted from [188].**

### 3.1 Selection of T-cell epitope candidates by promiscuous epitope prediction

The potential epitopes were selected by *in silico* prediction. Protein sequences were obtained from the reviewed Swiss-Prot section of the UniProt Knowledgebase [189]. All proteins in this work are named according to UniProt. All listed proteins of HCMV strain AD169 (193 entries) were screened for 15-aa-long peptides predicted to bind to multiple HLA class II allotypes promiscuously.

The online prediction tool SYFPEIHTI (Ver. 1.0) [89] was used to select epitope candidates with a high affinity to the most frequent alleles at the HLA-DRB1 gene locus in Germany (HLA-DRB1\*01, HLA-DRB1\*03, HLA-DRB1\*04, HLA-DRB1\*07, HLA-DRB1\*11, HLA-DRB1\*15), except for HLA-DRB1\*13 (Table 1) [190].

**Table 1: Allele frequencies at the DRB1 gene locus.** The allele frequency is given in decimals and represents the fraction of copies of the respective allele in the population sample. The number of copies is divided by the total number of chromosomes (2n). These data were obtained from allelefrequencies.net. The sample comprises 39,689 individuals (Germany pop 8) [190].

<u>Allele</u>	<u>Allele frequency</u>	<u>Allele</u>	<u>Allele frequency</u>
<b>DRB1*01:01</b>	0.0890	<b>DRB1*11:01</b>	0.0795
<b>DRB1*03:01</b>	0.1020	<b>DRB1*12:01</b>	0.0186
<b>DRB1*04:01</b>	0.0684	<b>DRB1*13:01</b>	0.0780
<b>DRB1*07:01</b>	0.1224	<b>DRB1*14:01</b>	0.0281
<b>DRB1*08:01</b>	0.0266	<b>DRB1*15:01</b>	0.1285
<b>DRB1*10:01</b>	0.0097	<b>DRB1*16:01</b>	0.0260

A single protein sequence was imported into SYFPEIHTI. The program evaluates every possible 15-aa-long peptide (15-mer) in the protein of interest and assigns a score (see 1.3). This is conducted for each HLA allotype separately. Next, the 2% best-scored epitope candidates of each HLA allotype are selected, which results in six peptide lists (Figure 5). Then, these lists are merged, and the predicted peptides of all six HLA allotypes together are sorted by their scores from high to low. Identical or similar peptides appear multiple times in the list, indicating potential promiscuous

binding of the peptide to different HLA allotypes. We assume that a nine-aa-long core sequence is fundamental for stable binding to the HLA molecule (see 1.2.2). Therefore, peptides are considered promiscuous binders if they include the respective core sequence. However, the core sequence of the selected epitope candidate should be shifted three aa at maximum to the N- or C-terminus in relation to other predicted peptides in the list. As a result, the binding cores of each predicted peptide that meets the mentioned criteria are included in the aa sequence of the selected epitope candidate.

This way, we selected potential epitopes that can bind promiscuously to five or six different HLA allotypes. These epitopes potentially activate T cells from a large part of the German population, as they bind to the most abundant HLA-DRB1 allotypes [188].

Similar core sequences were searched with an algorithm coded in python 3.0 (Figure S1).

The following secondary rules were applied for the epitope candidate selection:

1. Intermediate sequences were synthesized when a group of predicted peptides could not be covered by selecting one epitope candidate from the list.
2. Predicted peptides that appeared multiple times or were assigned higher scores were preferably selected.

The selection process described above was applied to every single protein separately. Therefore, we call it single-protein prediction. Since only the 2% highest-scored epitopes in a prediction for an HLA molecule are considered, proteins with short aa sequences can be underrepresented. In Figure 5, it is shown that only three peptides are selected for HLA-DRB1\*11, with 21 as the lowest score. In comparison, for a protein with a longer aa sequence, 25 peptides could be selected for HLA-DRB1\*11, and the lowest score could be below 21, for instance. Consequently, the

odds that epitopes from a long protein are selected are higher than for shorter proteins.

To disclose this bias in our prediction, we compared it with another approach. We took the sequence of the complete referenced proteome of HCMV AD169 from the UniProt database and conducted our prediction in the same way as described above. That means we treated the whole proteome like a single protein. This prediction process is referred to as whole-proteome prediction in this work. It bears the advantage that epitope candidates of all proteins are ranked together independent of the source proteins. All predicted peptides that were synthesized and tested in this project were determined with the single-protein prediction.

HLA-DRB1*01			HLA-DRB1*04			HLA-DRB1*11		
Pos.	Sequence	Score	Pos.	Sequence	Score	Pos.	Sequence	Score
65	PMRFINVKSHVSRPP	30	6	KRRYGFRTGISKPG	28	65	PMRFINVKSHVSRPP	23
38	TGTFRTAVSPPLTFS	26	38	TGTFRTAVSPPLTFS	28	102	CGLVVSRHGRAGGC	23
6	KRRYGFRTGISKPG	24	65	PMRFINVKSHVSRPP	28	101	RCGLVVSRHGRAGG	21
46	SPPLTFSSPPTSTVA	24	<b>HLA-DRB1*07</b>			<b>HLA-DRB1*15</b>		
48	PLTFSSPPTSTVATP	24	Pos.	Sequence	Score	Pos.	Sequenz	Score
60	ATPYFPMRFINVKSH	24	38	TGTFRTAVSPPLTFS	32	3	TCQKRRYGFRTGIS	24
68	FINVKSHVSRPPPLH	24	48	PLTFSSPPTSTVATP	26	42	RTAVSPPLTFSSPPT	24
75	VSRPPPLHGDPIIGH	24	6	KRRYGFRTGISKPG	18	62	PYFPMRFINVKSHVS	24
84	DIPIGHGTRVSRHV	24	9	YGFRTGISKPGPGLST	18	72	KSHVSRPPPLHGDIP	24
95	SRHVDDRCGLVVVSR	24	60	ATPYFPMRFINVKSH	18	78	PPPLHGDIPIGHGHT	24
<b>HLA-DRB1*03</b>			65	PMRFINVKSHVSRPP	18	95	SRHVDDRCGLVVVSR	24
Pos.	Sequence	Score	102	CGLVVSRHGRAGGC	18			
93	RVSRHVDDRCGLVVV	24	↓					
78	PPPLHGDIPIGHGHT	20						
101	RCGLVVSRHGRAGG	18						
104	LVVSRHGRAGGCLS	18						

Pos.	Sequence	Score	HLA
42	RTAVSPPLTFSSPPT	24	HLA-DRB1*15
46	SPPLTFSSPPTSTVA	24	HLA-DRB1*01
48	PLTFSSPPTSTVATP	26	HLA-DRB1*07
48	PLTFSSPPTSTVATP	24	HLA-DRB1*01
60	ATPYFPMRFINVKSH	24	HLA-DRB1*01
60	ATPYFPMRFINVKSH	18	HLA-DRB1*07
62	PYFPMRFINVKSHVS	24	HLA-DRB1*15
65	PMRFINVKSHVSRPP	30	HLA-DRB1*01
65	PMRFINVKSHVSRPP	28	HLA-DRB1*04
65	PMRFINVKSHVSRPP	23	HLA-DRB1*11
65	PMRFINVKSHVSRPP	18	HLA-DRB1*07
68	FINVKSHVSRPPPLH	24	HLA-DRB1*01
72	KSHVSRPPPLHGDIP	24	HLA-DRB1*15
75	VSRPPPLHGDPIIGH	24	HLA-DRB1*01
78	PPPLHGDIPIGHGHT	24	HLA-DRB1*15
78	PPPLHGDIPIGHGHT	20	HLA-DRB1*03

**Figure 5: Epitope selection example for protein US4.** “The upper tables list the 2% highest scored peptides for each of the HLA allotypes of interest. This protein is 119 aa long. Thus, there are 105 possible 15-mers. In this case, the 2% highest scores equal 2.1, so the three highest scored peptides were selected (all peptides with the smallest selected score value were considered, see HLA-DRB1\*01,03,07,15). The lower table lists all epitopes sorted by their position in the protein. The nine-aa-long binding-core (orange letters, green box, and blue box) is essential for the stable binding of a peptide to an HLA molecule. The binding core of the selected epitope candidate could be shifted three positions either to the N- or to the C-terminus. Accordingly, the peptide 62-76 (black arrow) potentially binds to five different HLA allotypes (in blue) since it contains the binding cores of seven peptides that are predicted binders to these HLA allotypes” [188].

### 3.2 Fmoc solid-phase synthesis of epitope candidates for T-cell experiments

The peptides selected for testing were synthesized by standard solid-phase peptide synthesis with Fmoc (fluorenylmethoxycarbonyl)-protection groups [191, 192] using Liberty Blue (CEM) and P11 (Activotec) synthesizers. Part of the peptides were kindly synthesized by Ulrich Wulle, Camille Supper and Stefan Stevanović.

After the chemical processing of the products, they were lyophilized and stored undissolved at 4°C. Qualitative and quantitative testing was performed by mass spectrometry and high-performance liquid chromatography (HPLC) by Marion Gauger, Monika Denk and Ulrich Wulle.

Peptides were lyophilized and dissolved in 20 mg/ml dimethylsulfoxide (DMSO). Depending on solubility, most peptides were diluted 1:10 in bidistilled H<sub>2</sub>O and stored at -80°C. For HCMV peptide pool I, 14 peptides at a concentration of 10 mg/ml were pooled to a concentration of 0.714 mg/ml per peptide in DMSO. HCMV peptide pool II contained 11 peptides of the pool I without the pp65-derived peptides (concentration 0.909mg/ml per peptide in DMSO). If peptides could not be dissolved entirely, aliquots were centrifuged, and the supernatant was used.

### 3.3 PBMC isolation from buffy coats

The synthesized peptides were subsequently tested in T-cell experiments. In order to obtain the cells for the assays, PBMCs were extracted from buffy coats of HCMV-seropositive individuals provided by the Institute for Clinical and Experimental Transfusion Medicine at the University Hospital of Tübingen (approved by the *Ethik-Kommission an der Medizinischen Fakultät der Eberhard-Karls-Universität und am Universitätsklinikum Tübingen*, Project No. 507/2017B01).

PBMCs were extracted from the buffy coats by ficoll density gradient centrifugation [193]. PBMCs are mainly composed of monocytes and lymphocytes. The blood was transferred from the buffy coat bag into a cell culture flask and diluted with phosphate-buffered saline (PBS). Subsequently, the blood solution was layered on

ficoll separating solution in a centrifugation tube. Centrifugation resulted in the separation of different cell types (Figure 6). After the aspiration of the PBMC layer and several washing steps, the segregated PBMCs could be counted. Then, the cells were suspended in a freezing medium (10% Dimethyl sulfoxide in fetal calf serum), aliquoted, and sorted into prechilled freezing containers filled with isopropanol, which enabled a continuous cooling rate of  $-1^{\circ}\text{C}$  per minute down to  $-80^{\circ}\text{C}$ , the final storage temperature. DMSO serves for cryopreservation by preventing the formation of ice crystals and dehydration of the cells [194].

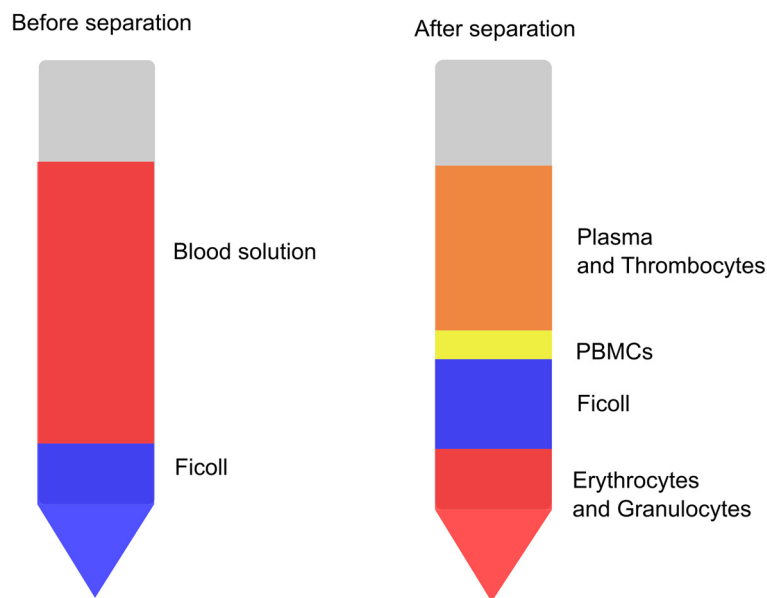


**Figure 6: Isolation of PBMCs from buffy coats.** The content of the buffy coat bag was diluted in PBS and carefully layered on ficoll separating solution. Density gradient centrifugation resulted in the separation of the different cell types. The erythrocytes and granulocytes have a higher density than the separating solution and settle down at the bottom of the tube. Above the ficoll layer, the PBMCs (monocytes and lymphocytes) remain. The plasma and the thrombocytes reside at the top.

### 3.3.1 Experimental procedure: PBMC isolation from buffy coats

The following description is adapted from the standard protocol (version 01\_2018) developed in the laboratory of Prof. Dr. Stefan Stevanović (Department of Immunology, Tübingen).

*The centrifugation steps are described for the „Megafuge“. Material for one bag of buffy coat: 60 ml Ficoll, 250 ml PBS(-Ca-Mg), 1x cell culture flask T75, 10 ml freezing medium, 5-15 cryovials, 6x 50 ml falcon tube, prechilled Mr.Frosty*

<p><b>1.</b></p> <ul style="list-style-type: none"> <li>– distribute 4x 15 ml Ficoll in 50 ml falcon tubes</li> <li>– transfer blood to the cell culture flask</li> <li>– fill up to 100 ml with PBS</li> <li>– stratify 25 ml of the blood mixture carefully on the Ficoll layer (keep tube flat)</li> <li>– wash cell culture flask at least 2x with 20 ml PBS in total, then distribute carefully 5 ml per tube</li> <li>– spin down: 2000 rpm, 20 min, room temperature (without break)</li> </ul> <p><b>2.</b></p> <ul style="list-style-type: none"> <li>– remove thrombocytes/PBS layer (top layer, yellowish), until approx. 10 ml of it remains above the PBMC layer</li> <li>– transfer lymphocyte layer (white layer in the middle directly above the Ficoll) to 2x50 ml falcons. Fill up these falcons to a total of 50 ml using PBS. Avoid the uptake of too much Ficoll, never collect erythrocytes!</li> <li>– spin down: 1500 rpm, 10 min, room temperature, with break</li> </ul> <p><b>3.</b></p> <ul style="list-style-type: none"> <li>– carefully discard the supernatant by using a pipette (careful: pellet can be loose!)</li> <li>– resuspend the pellet, fill up to a total of 50 ml with PBS.</li> <li>– spin down: 1300 rpm, 10 min, room temperature, with break</li> </ul>	<p><b>4.</b></p> <ul style="list-style-type: none"> <li>– resuspend cells very well, pool all cells of one donor in one falcon, wash the empty falcon 2x with PBS, fill up to a total of 50 ml per falcon</li> <li>– invert tubes several times, then take a sample for counting (approx. 20 µl)</li> </ul> <p><b>5.</b></p> <ul style="list-style-type: none"> <li>– Cell counting: <ul style="list-style-type: none"> <li>○ prepare 90 µl (1) and 10 µl (2) of trypan blue</li> <li>○ mix 10 µl of the cells in (1)</li> <li>○ mix 10 µl of (1) in (2)</li> <li>○ transfer (2) in counting chamber</li> </ul> </li> <li>– calculate total cell count, required volume of freezing medium and amount of aliquots needed</li> <li>– Freezing medium and prechilled Mr.Frosties available and ready to use?</li> <li>– print labels, label and prepare cryovials</li> <li>– spin down: 1100 rpm, 10 min, room temperature, with break</li> </ul> <p><b>6.</b></p> <ul style="list-style-type: none"> <li>– Freeze cells: Don't forget the labels! <ul style="list-style-type: none"> <li>○ Adjust the cell count downwards</li> </ul> </li> <li>➔ Freeze as many as possible (<math>1 \cdot 10^8</math>)/2 ml aliquots.</li> <li>➔ Dilute remaining (<math>1 \cdot 10^8</math>)/2 ml unit with 3 ml freezing medium, distribute 5x (<math>2 \cdot 10^7</math>)/1 ml for freezing</li> </ul>
--	--



### 3.4 Cell counting

Cell counting was performed with a Neubauer chamber. The bottom of the chamber is divided into four large squares. The cell suspension was diluted in trypan blue (for dilutions see respective standard protocol of the experiment) and then pipetted into the Neubauer chamber, which captures a volume of  $10^{-4}$  ml per square. Staining only permeable cells that are dead or impaired in their integrity, trypan blue allows visual counting of viable cells with a light microscope. The number of viable cells was counted in two squares. Next, the cell concentration of the suspension was calculated using the following formula:

$$\frac{\text{cells}}{\text{ml}} = \frac{\text{number of viable cells counted}}{\text{number of squares counted}} \times 10^4 \times \text{dilution factor}$$

### 3.5 Cell thawing

The cryovials were dipped into a water bath at 37°C for approximately one minute until they were partly thawed. Next, they were washed twice in thawing medium (TM). The cells were resuspended in T-cell medium (TCM) and transferred onto 6-well plates (see ELISpot standard protocol 3.7.2).

### 3.6 Cell culture and 12-day peptide stimulation

The PBMC samples for the T-cell assays were cultured for 12 days and stimulated with the peptides of interest and IL-2 [195].

One day after thawing, the cells were stimulated either with a peptide pool for ELISpot screening assays or single peptides for ICS. The peptide stock solutions were mixed with warm TCM and then added to the wells. Next, the positive control peptide was pipetted in just one of the three wells to avoid the domination of this T-cell population over the T cells responding to the peptides of interest.

The HLA molecules of antigen-presenting cells are loaded exogenously with the peptides since these are present at high concentrations. T cells recognize the HLA-peptide complexes, are reactivated and start proliferating.

On day three, six, and eight of the protocol, IL-2 was added. The cytokine initiates clonal expansion and differentiation of T cells [196]. Due to the pre-stimulation, T<sub>CM</sub> cells are recruited, proliferate, and differentiate to effector T cells that can secrete IFN $\gamma$  upon peptide exposure in ELISpot [195]. From day nine to day thirteen, the cells were cultured without cytokine stimuli. Thus, the cells could return to an activatable state for the second peptide stimulation in the ELISpot assay. The cells were supplied with fresh medium if necessary.

### **3.7 Epitope screening by the IFN $\gamma$ ELISpot assay**

The enzyme-linked immunospot assay was first described by Czerkinsky et al. for the enumeration of antibody-secreting cells [197]. A well-established tool for the quantification of activated lymphocytes emerged over time [198, 199]. The ELISpot assay has a high sensitivity, as it can reproducibly detect one antigen-specific T cell out of 100.000 PBMCs [200]. In this project, the activation of antigen-specific memory T cells was detected by measuring IFN $\gamma$  release.

A nitrocellulose membrane at the bottom of a 96-well plate was coated with a primary capture antibody. This antibody has a binding site for IFN $\gamma$ , which is released by T cells upon activation. After coating, several washing steps were performed. The remaining protein binding sites on the membrane were blocked by albumin, which is contained in the TCM. This prevents unspecific binding of the secondary antibody to the membrane.

In a standard ELISpot, PBMCs of eight different HCMV-seropositive blood donors were tested in duplicates for responses to nine different peptides each (see scheme in ELISpot standard protocol). Negative controls were the self-peptide FLNA<sub>1669-1683</sub> from human filamin-a (FLNA) or DMSO and medium control. The unspecific positive

control was the mitogen phytohaemagglutinin (PHA) [201, 202], which triggers a high IFN $\gamma$  release. For the screening assays, two different specific positive controls were used in addition to PHA. CAPSH\_ADE02<sub>23-32</sub> is a peptide originating from adenovirus and has been shown to activate CD4<sup>+</sup> T cells in PBMC cultures of many donors. The other positive control was a peptide pool containing various peptides of Epstein-Barr virus, adenovirus, and HCMV (Table 2).

After the cells were incubated with the peptides, the plates were washed to remove residual cells and cytokines. Next, a secondary biotinylated antibody, the detection antibody was added. It binds to IFN $\gamma$  at a different binding site. Thirdly, an avidin-alkaline phosphatase conjugate associates to the detection antibody. To indicate the localization of the phosphatase, BCIP/NBT was used. BCIP is transformed into a blue-colored product, and NBT reduces to purple diformazan [203]. Ideally, one spot represents one activated T cell, and the spot size correlates with the amount of cytokine released [204]. Figure 7 illustrates the functional principle of an ELISpot assay for a single T cell.

The dried plates were read out at an ImmunoSpot S5 analyzer and were counted automatically by ImmunoSpot® software.

**Table 2: Positive pool HLA class II.** This peptide pool consists of peptides that were tested by members of the Department of Immunology in Tübingen in ELISpot assays. The percentage of positively tested PBMC cultures is shown in the last column. For each peptide, activation of CD4<sup>+</sup> T cells was confirmed in ICS. Adapted from [188].

Batch number	Sequence	Source protein	Position	Positive (%)
165055	YQEFFWDANDIYRIF	pp65_HCMVA	510-524	61.0%
154048	PRPVSFRFLGNNNSILY	GP350_EBV9	268-282	75.0%
1093	IAEGLRALLARSHVERTTDE	EBN1_EBV	481-500	68.8%
1150	RRGTALAIQRCRLTPLSRLP	EBN1_EBV	521-540	62.5%
111223	RSPTVFYNIPPMPLPPSQL	EBNA2_EBV	277-295	75.0%
164609	TLLYLKYKRRSFID	E3GL_ADE06	140-154	65.0%
164534	RQVMDRIMSLTARNP-NH2	CAP3_ADE02	28-42	66.7%
184023	MHLWRAVVRHKNRLL	E1BS_ADE02	120-134	68.2%
164608	KNRLLLLSSVRPAII	E1BS_ADE02	130-144	70.0%
184024	TLVLAFVKTCAVLAA	LEAD_ADE02	32-46	70.8%
164529	RGIFCVVKQAKLTYE	E3145_ADE02	46-60	75.0%
164607	VSKFFHAFPSKLHDK	PKG1_ADE02	292-306	80.0%
164605	TFYLNHTFKKVAITF	CAPSH_ADE02	727-741	85.0%
174157	PQKFFAIKNLLLLPG	CAPSH_ADE05	563-577	85.7%

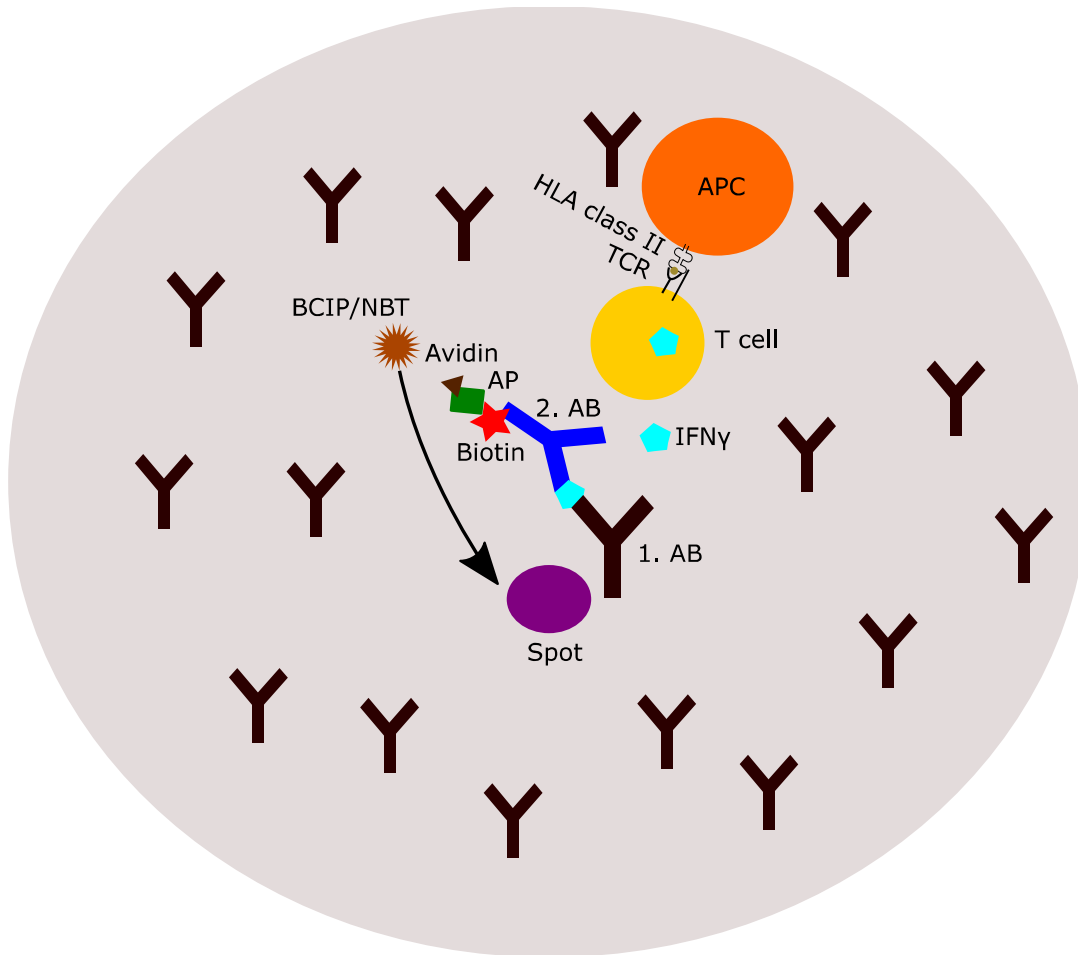


**Figure 7: Schematic of an ELISpot assay.** The well bottom of an ELISpot plate is shown. The nitrocellulose membrane is coated with a primary antibody (1. AB). The APC presents a peptide to the T cell via the HLA class II molecule, which is recognized by the T-cell receptor (TCR). The T cell gets activated and starts secreting IFN $\gamma$ , which can bind to the primary antibody. A biotinylated secondary antibody (2. AB) binds to the IFN $\gamma$ . Subsequently, the Enzyme-Avidin complex (AP - Alkaline phosphatase) converts the substrate BCIP/NBT to a visible purple spot on the membrane.

### **3.7.1 Evaluation criteria of ELISpot results**

The evaluation of the ELISpot results was based on empirical criteria, as described by Dubey et al. [205]. It was modified and adjusted to the experimental setting in our laboratory. An ELISpot result was evaluated as positive if the mean spot count of the duplicates in the test wells was more than three times higher than in the negative control wells. If one test well showed less than ten spots, the PBMC sample was excluded from the evaluation for the respective peptide to reduce the number of false-positive results. In case there were more than 300 spots counted in the negative control, data were not included in the further analysis. The response of epitope-specific T cells can be undetectable with such a high background activation. Besides, PBMC samples were excluded if the spot count difference of the duplicates exceeded the arithmetic mean to prevent false-positive results by accidental contamination of one well.

### 3.7.2 Experimental procedure: ELISpot after 12-day peptide stimulation

The following description is adapted from the standard protocol (version 01\_2018) developed in the laboratory of Prof. Dr. Stefan Stevanović (Department of Immunology, Tübingen).

<p><i>PBMCs from 8 Donors, 9 Peptides (+1 x negative control + 1 x positive control)</i></p> <p><b>Day 1: Thawing cells</b>  <i>Thaw <math>1 \times 10^8</math> cells per donor: for each stimulation, you should plan with <math>0.5 \times 10^6</math> cells/well, for the PHA positive control <math>0.25 \times 10^6</math> cells per well is sufficient</i></p> <ol style="list-style-type: none"> <li>1. Prepare a 15 ml-Falcon tube per donor with 10 ml cold TM. Add slightly thawed cells to the TM</li> <li>2. Spin down at 1,400 rpm, 7 min (Megafuge 1,0R) or 1,500 rpm (Labofuge 400), discard the supernatant</li> <li>3. Resuspend pellet in 10 ml of warm TM (37°C)</li> <li>4. <u>Incubate cells for 5-10 min at 37°C</u></li> <li>5. Spin down at 1,400 rpm, 7 min (Megafuge 1,0R) or 1,500 rpm (Labofuge 400), discard the supernatant</li> <li>6. Resuspend pellet in 6 ml TCM and distribute to 3 wells of a 6-well-plate (2 ml/well)</li> </ol> <p><i>Incubation at 37°C, 7.5% CO<sub>2</sub>, 24 hours min.</i></p> <p><b>Day 2: Pool stimulation</b>  <b>Stimulation of the cells with peptide mix in 6-well-plates</b></p> <ol style="list-style-type: none"> <li>1. Weigh 1.5-2.5 mg of a peptide, note the exact weight! Dissolve in DMSO (10%), then add sterile filtered ddH<sub>2</sub>O (90%). Concentration: <u>2 mg/ml</u> (1 mg/ml)</li> <li>2. Prepare a mix of peptide stocks in TCM with a final concentration of 1 µg/ml per peptide per well for HLA class I or 5 µg/ml for HLA class II peptides. Do not stimulate with HLA class I and II peptides in one well. Add 500 µl/well of this peptide pool (without positive control peptide) to the cells.</li> <li>3. The positive peptide is added in one of three wells per donor</li> </ol> <p><i>Incubation overnight at 37°C, 7.5% CO<sub>2</sub></i></p>	<p><b>Day 3, 6 and 8: IL-2 stimulation</b></p> <ol style="list-style-type: none"> <li>1. Concentration of the stock: 30,000 U/ml</li> <li>2. The final concentration of IL-2 in each well: 20 U/ml (caution, each day, the dilution is different!)</li> <li>3. Day 3 and 6: add 500 µl TCM with IL-2 per well</li> <li>4. Day 8: add 1 ml TCM with IL-2 per well</li> </ol> <p><i>Incubation 37°C, 7.5% CO<sub>2</sub></i></p> <p><b>Day 10: Feeding and coating plates</b></p> <ol style="list-style-type: none"> <li>1. Carefully discard 1 ml TCM per well and add 3 ml TCM per well.</li> <li>2. Incubation until day 13 at 37°C, 7.5% CO<sub>2</sub></li> <li>3. Coat plates: capture antibody human IFN<math>\gamma</math> (1 mg/ml) <math>\rightarrow</math> 1:500 in PBS (f.c. 2 µg/ml) <math>\rightarrow</math> 100 µl/well</li> <li>4. Incubate wrapped with plastic wrap at least o/n at 4°C</li> </ol> <p><b>Day 13: Loading</b></p> <ol style="list-style-type: none"> <li>1. Wash plates 2 x with sterile IMDM 200 µl/well</li> <li>2. Add <u>200 µl</u> (50 µl) TCM per well and incubate at least 2 h at 37°C, 7.5% CO<sub>2</sub> without bubbles!</li> </ol> <p><b>Prepare sterile cells and peptides</b></p> <ol style="list-style-type: none"> <li>3. Transfer cells from the 6-well-plates to a 50 ml-Falcon tube</li> <li>4. Spin down at 1,400 rpm, 7 min (Megafuge 1,0R) or 1,500 rpm (Labofuge 400)</li> <li>5. Discard supernatant</li> <li>6. Resuspend pellet in 10 ml TCM (or less, depending on the size of the pellet)</li> </ol> <p><b>Seed cells</b></p> <ol style="list-style-type: none"> <li>7. Count cells: dilute 1:10 in trypan blue</li> </ol>
---	--

8. Spin down at 1,400 rpm, 7 min (Megafuge 1,0R) or 1,500 rpm (Labofuge 400)

	Pep 1	Pep 2	...	Pep 9	+ co	- co	
Donor 1							PHA
Donor 1							TCM
Donor 2							PHA
Donor 2							TCM
Donor 3							...
Donor 3							
...							

9. Prepare peptides
- f.c. 1 µg/ml for HLA class I  
(→ 3 µl + 997 µl TCM per peptide)
  - f.c. 2.5 µg/ml for HLA class II
10. PHA: (f.c. 10 µg/ml) → 15 µl + 485 µl TCM
- Sterile loading of the cells on the 96-well plate**
- Discard TCM from blocking and add 50 µl warm TCM per well
  - Add 50 µl peptide or PHA dilution per well
  - Add 50 µl PBMCs (500,000 cells) per well

Mix by moving the plate carefully on the bench. Incubation: without bubbles, 20-22h (20-24 h) **without agitation** at 37°C

#### Day 14: Staining

##### Washing step:

- Wash plates 2 x with PBST 200 µl/well
- Wash plates 2 x with ddH<sub>2</sub>O 200 µl/well
- Wash plates 3 x with PBST 200 µl/well

##### Add detection antibody:

- biotinylated anti-human IFN $\gamma$  7-B6-1 (stock: 1 mg/ml, f.c. 0.3 µg/ml) → 1:3,000 in PBS/BSA → filter using a 0.22 µm filter → add 100 µl/well
- Incubation for 2h at room temperature in the dark (without bubbles)

##### Washing step:

- Wash plates 6 x with PBST 200 µl/well

##### Add alkaline phosphatase:

- ExtrAvidin alkaline phosphatase: 1:1,000 in PBS/BSA → 100 µl/well
- Incubation for 45-60 min at room temperature in the dark
- Dissolve 1 x BCIP/NBT tab (light-sensitive!) in 10 ml ddH<sub>2</sub>O in the dark

##### Washing step:

- Wash plates 3 x with PBST 200 µl/well
- Wash plates 3 x with PBS 200 µl/well

##### Final staining (BCIP/NBT):

- Filter substrate solution using 0.22 µm filter
- Add 50 µl chromogen-substrate-solution to each well
- Incubate 7-10 min in the dark
- Stop the reaction with running water; pull off underdrain on the back of the plates
- Pre-dry the plates by using dry, white cleaning paper (tap plate slightly)
- Dry overnight in the dark
  - hydrophilic MSHAN plates at room temperature (used in this project)
  - hydrophobic MSIP plates at 4°C
- Quick-dry protocol: place the plates onto the flow stream of a laminar hood

Store at room temperature in the dark.



### 3.8 Epitope validation by intracellular cytokine staining

Activated memory T cells secrete cytokines (e.g. TNF, IFN $\gamma$ ) that can be captured inside the cell by specific inhibitors. Staining of these intracellular cytokines and marking the surface molecules CD4 and CD8 allows the distinction of activated T-cell populations.

The ELISpot assay only detects IFN $\gamma$  secretion but allows no attribution to a specific cell type. Hence, peptides that could induce positively evaluated T-cell responses in more than 50% of all tested PBMC cultures ( $n_{\text{tested PBMC cultures}} \geq 20$ ) were validated by ICS. Peptides that are 15 aa long are frequently identified as HLA class II ligands and consequently activate CD4<sup>+</sup> T cells. However, it has been shown that 15-mers can also activate CD8<sup>+</sup> T cells [71, 73, 74]. If substrings of the tested peptide sequences were published as CD8<sup>+</sup> T-cell epitopes, we tried to test PBMC samples from donors with matching HLA class I typing in ICS. Since ICS is less sensitive than ELISpot, we chose PBMC samples with high spot counts in ELISpot for epitope validation in ICS [206].

The same 12-day peptide stimulation protocol as for the ELISpot assays was used with the following modifications:  $1 \times 10^7$  cells were thawed per donor and peptide. These were diluted in 2 ml of TCM and stimulated with test peptide and negative control peptide in a single well of a 6-well plate. The ICS was conducted in a 96-well plate with three wells per peptide and PBMC sample: one for the stimulation with the test peptide, one for the stimulation with the negative control peptide, and one for the positive control (PMA/ionomycin). Phorbol myristate acetate (PMA) and ionomycin are potent stimulators of the TNF and IFN $\gamma$  gene expression [207]. Eventually, Brefeldin A and Golgi-Stop® were added to each well. The ionophore monensin, which is contained in Golgi-Stop®, inhibits transport of cytokine vesicles from the Golgi-apparatus to the cell membrane [207]. Brefeldin A reverses the transport from the ER to the Golgi [208]. Together, these mechanisms capture the produced cytokines in the activated cell.

After the incubation period, the cells were treated first with a live/dead stain. Secondly, the extracellular molecules CD4 and CD8 were stained. Next, the cells were fixated and permeabilized using a solution of formaldehyde and saponin. Subsequently, TNF and IFN $\gamma$  were stained, and the plates were stored for a maximum of one day at 4°C until measuring by flow cytometry.

In flow cytometry, cells can be sorted by size and granularity based on a scattering pattern that results when a laser hits the cell. Moreover, specific cells can be detected by staining individual molecules with fluorescent antibodies. Figure 8 shows an example of the gating strategy for the experiments.

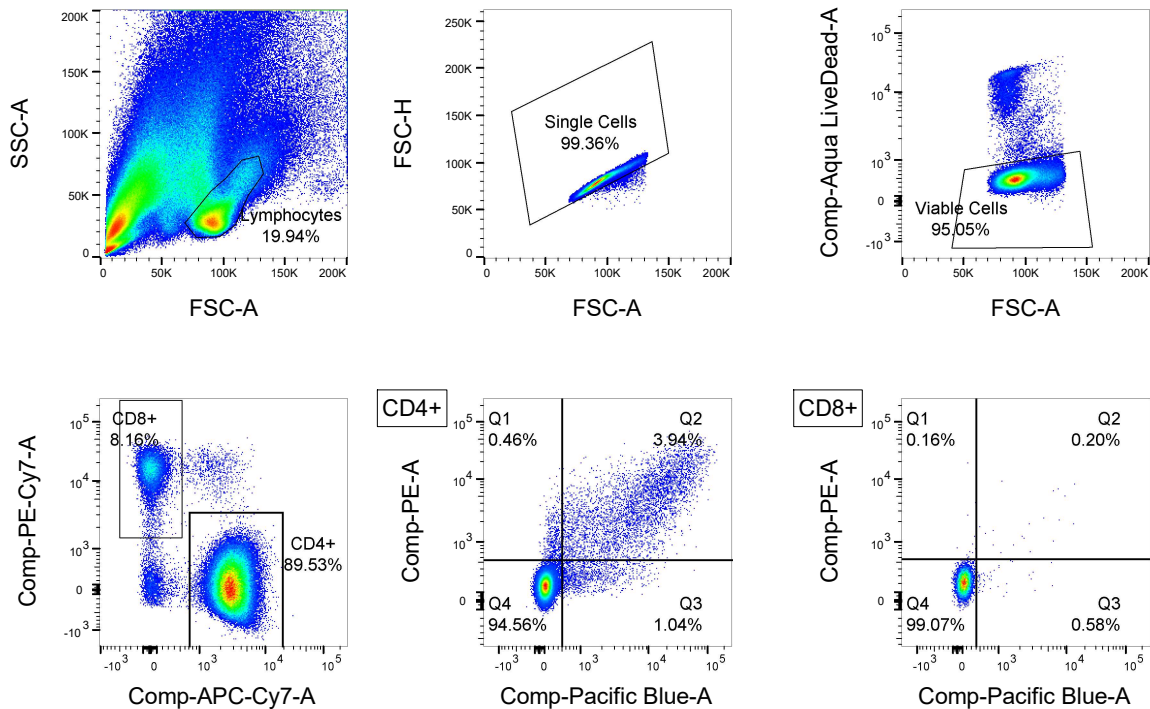


**Figure 8: Gating strategy for ICS.** The dot plots show the signal intensity for every measured event in flow cytometry. The PBMCs were gated on lymphocytes, single cells, viable cells (Comp-Aqua-LiveDead-A), CD4 (Comp-APC-Cy7-A) and CD8 (Comp-PE-Cy7-A), IFN $\gamma$  (Comp-PE-A), and TNF (Comp-Pacific Blue-A). Abbreviations: SSC, side scatter; FSC, forward scatter.

### 3.8.1 Experimental procedure: intracellular cytokine staining

The following description is adapted from the standard protocol (version 08/2016) developed in the laboratory of Prof. Dr. Stefan Stevanović (Department of Immunology, Tübingen).

<p><b>FACS buffer (=PFEA):</b> 500ml PBS + 2%FCS + 2mM EDTA  <b>Permwash buffer:</b> 500ml PBS + 0.1% Saponin S-7900 (0.5g) + 0.5% BSA</p> <p><b>Prepare cells:</b></p> <ul style="list-style-type: none"> <li>▪ Harvest cells from each donor, resuspend in TCM and count</li> <li>▪ Resuspend cells to <math>1-2 \times 10^7</math> cells/ml in TCM</li> <li>▪ Plate <u>200 <math>\mu</math>l</u> (50 <math>\mu</math>l) of cells (<math>1 \times 10^6</math> (0.5-<math>1 \times 10^6</math>) cells per well) in a 96-well plate (round bottom)</li> <li>▪ For each donor, you require:             <ul style="list-style-type: none"> <li>- 1 well positive control with PMA+Ionomycin</li> <li>- 1 well negative control with a negative peptide</li> <li>- 1 well for each peptide to be tested</li> </ul> </li> </ul> <p><b>Prepare peptides and positive controls</b> (peptide stock <u>2 mg/ml</u> (1mg/ml)):</p> <ul style="list-style-type: none"> <li>• Negative control (10 <math>\mu</math>g/ml final) per well: <u>0.75 <math>\mu</math>l</u> (1.5 <math>\mu</math>l) negative peptide + <u>49.25 <math>\mu</math>l</u> (48.5 <math>\mu</math>l) TCM</li> <li>• Test peptides (10 <math>\mu</math>g/ml final): per well: <u>0.75 <math>\mu</math>l</u> (1.5 <math>\mu</math>l) peptide + <u>49.25 <math>\mu</math>l</u> (48.5 <math>\mu</math>l) TCM</li> <li>• Positive control (PMA+ionomycin): per well: 0.75 <math>\mu</math>l PMA + 0.15 <math>\mu</math>l ionomycin + 49.1 <math>\mu</math>l TCM</li> </ul> <p><b>Prepare Brefeldin A + Golgi-Stop solution:</b></p> <ul style="list-style-type: none"> <li>• Brefeldin A (stock: 1 mg/ml) + Golgi-Stop (10 <math>\mu</math>g/ml final): per well: 1.5 <math>\mu</math>l Brefeldin A + 0.1 <math>\mu</math>l Golgi-Stop in 48.4 <math>\mu</math>l TCM</li> </ul> <p><b>Start reaction:</b></p> <ul style="list-style-type: none"> <li>• <u>Centrifuge (1800 rpm, 2 min, room temperature) and pour off</u></li> <li>• <u>Add to each well 50 <math>\mu</math>l of TCM</u></li> </ul>	<ul style="list-style-type: none"> <li>• Add to each well with 50 <math>\mu</math>l of cells             <ol style="list-style-type: none"> <li>1) 50 <math>\mu</math>l of peptide or PMA/Ionomycin</li> <li>2) 50 <math>\mu</math>l of Brefeldin A + Golgi-Stop solution (final volume: 150 <math>\mu</math>l per well)</li> </ol> </li> <li>• Mix by pipetting up and down</li> <li>▪ Incubate plate at 37°C for 12h</li> </ul> <p><b>Staining</b> (After 12h incubation (6-16h))</p> <p>All centrifugation steps: 1800 rpm, 2 min, 4°C</p> <ul style="list-style-type: none"> <li>▪ Centrifuge and pour off supernatant (once, with a dash)</li> <li>▪ Resuspend pellets in 150 <math>\mu</math>l <b>PBS-EDTA</b> per well</li> <li>▪ Centrifuge and pour off supernatant</li> <li>▪ Resuspend pellets in 150 <math>\mu</math>l <b>PBS-EDTA</b> per well</li> <li>▪ Centrifuge and pour off supernatant</li> </ul> <p><b>1. Live/dead staining</b></p> <ul style="list-style-type: none"> <li>▪ Dilute aqua live/dead stain in <b>PBS-EDTA</b> (2mM) 1:200 if the stain is older than 2 weeks (If it is fresher than 2 weeks, dilute 1:400). 50 <math>\mu</math>l per well is required.</li> <li>▪ Resuspend pellets in 50 <math>\mu</math>l diluted aqua live/dead per well</li> <li>▪ Incubate for 20 min at 4°C in the dark</li> <li>▪ Add 150 <math>\mu</math>l <b>PBS-EDTA</b> per well, centrifuge and pour off</li> </ul> <p><b>2. Staining of extracellular molecules (CD4, CD8):</b></p> <ul style="list-style-type: none"> <li>▪ Dilute antibodies in <b>FACS buffer</b> (for dilutions see below). 50 <math>\mu</math>l per well are required.</li> <li>▪ Incubate for 20 min at 4°C in the dark</li> <li>▪ Add 150 <math>\mu</math>l <b>FACS buffer</b> per well, centrifuge and pour off</li> </ul> <p><b>3. Permeabilizing:</b></p> <ul style="list-style-type: none"> <li>▪ Resuspend pellets in 100 <math>\mu</math>l <b>Cytoperm/Cytofix</b> per well</li> <li>▪ Incubate for 20 min at 4°C in the dark</li> <li>▪ Add 100 <math>\mu</math>l <b>Permwash buffer</b> per well, centrifuge and pour off</li> </ul>
---	--

<p><b>4. Staining of intracellular molecules (IFN<math>\gamma</math>, TNF):</b> Dilute antibodies in <b>Permash buffer</b> (for dilutions see below). 50 <math>\mu</math>l per well is required.</p> <ul style="list-style-type: none"> <li>▪ Resuspend pellets in 50 <math>\mu</math>l per well</li> <li>▪ Incubate for 20 min at 4°C in the dark</li> <li>• Add 150 <math>\mu</math>l <b>Permash buffer</b> per well, centrifuge and pour off</li> <li>▪ Repeat washing with 150 <math>\mu</math>l <b>Permash buffer</b> per well, centrifuge and pour off</li> <li>▪ <u>Wash with 150 <math>\mu</math>l <b>FACS buffer</b> per well, centrifuge and pour off</u></li> <li>▪ Resuspend pellet in 200 <math>\mu</math>l <b>FACS buffer</b></li> </ul> <p>→ Store cells for <u>1 day</u> (max. 3 days) in the dark at 4°C until measuring by FACS</p>	<p><b><u>Antibody combination:</u></b> <b>IFN<math>\gamma</math>-PE</b> (BD, 1:200) [...] <b>TNF-PacificBlue</b> (BD, 1:120) <b><u>CD8-PE-Cy7</u></b> (1:400) (CD8-FITC or <b>CD8-PerCP</b> (Biolegend, 1:100)) <b>CD4-APC-Cy7</b> (1:100) [...] <b>Aqua-Live-Dead</b></p>
---	--

### 3.9 Protein sequence alignment

The conservation of the identified epitope sequences between two different HCMV strains was assessed using the Multiple Sequence Alignment tool Clustal Omega [209]. The epitope source protein sequences of the standard HCMV laboratory strain AD169 were aligned with the correspondent sequences of the low-passage, wild-type prototype HCMV strain Merlin.

## 4 Results

### 4.1 Identification of T-cell epitopes by the IFN $\gamma$ ELISpot assay

We selected 169 epitope candidates with our promiscuous epitope prediction approach [188]. The epitope candidates were screened for immunogenicity in IFN $\gamma$  ELISpot assays. Nine peptides were tested against the PBMC cultures of eight different donors on two 96-well ELISpot-plates (Figure 9). In Table 3, the recognition rates, defined as the proportion of the tested PBMC cultures that secrete IFN $\gamma$  upon stimulation with the peptide, are listed for the predicted epitope candidates. US24<sub>255-269</sub>, UL36<sub>253-267</sub>, UL24<sub>201-215</sub>, and MCP<sub>515-529</sub> were recognized by more than 70% of the tested PBMC cultures each. Only three of the identified epitopes have already been published previously (as indicated in Table 3).

Throughout the project, it turned out that PBMC cultures recognized epitope candidates that reached the maximum prediction score (top score) for one of the HLA-DR allotypes of interest more frequently in ELISpot than the other epitope candidates (Figure 10). Hence, we narrowed testing to top scorers predicted for five HLA allotypes, and epitope candidates predicted for all six HLA allotypes [188]. The top scores were mostly reached for HLA-DRB1\*04 (data not shown).

In total, 103 predicted peptides were analyzed in ELISpot assays. Ten peptides were not synthesizable to a satisfying quality by our in-house facility. Peptides that were already published or available from previous projects in our laboratory ( $n = 26$ ) were assessed, as well. Table 4 lists all tested peptides that were taken from our laboratory stock and were not predicted. We confirmed several published epitopes, derived from the well-characterized immunodominant pp65 (Table 4). pp65<sub>109-123</sub>, for instance, triggered IFN $\gamma$  release in 82.6% of the tested PBMC cultures. Some peptides that were initially tested in HLA class I projects in our laboratory were assessed, as well. These peptides were predicted as CD8<sup>+</sup> T-cell epitopes but elicited CD4<sup>+</sup> T-cell responses in previous experiments. Here, VPAP<sub>253-267</sub>, for instance, was recognized by T cells of 76.2% of the tested PBMC samples [188].

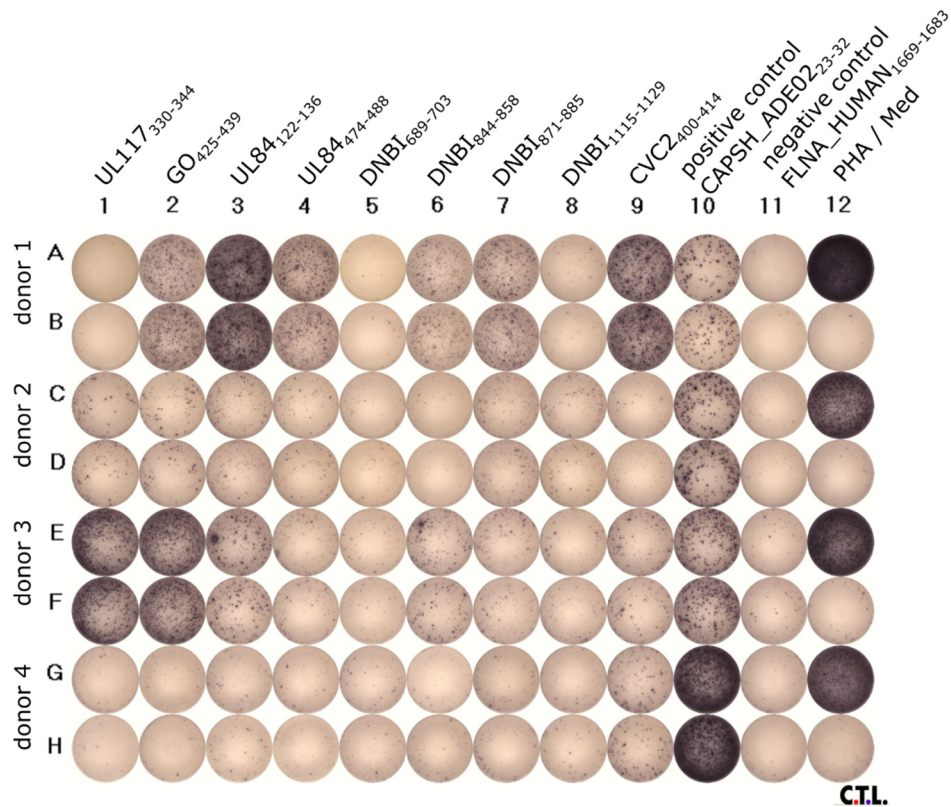


**Figure 9: Standard screening ELISpot example.** Here, an image of the colored membranes on the well bottoms of an ELISpot plate is shown. Each purple dot represents an IFN $\gamma$ -secreting cell. In one assay, nine different peptides (column 1-9) were tested against PBMC cultures of eight different donors in duplicates (rows) on two 96-well plates (only one plate shown). The adenovirus-derived peptide CAPSH\_ADE02<sub>23-32</sub> served as a positive control; human Filamin-A derived FLNA<sub>1669-1683</sub> as a negative control. Additionally, PHA, as an unspecific positive control, and medium control was applied.

**Table 3: Peptides tested in ELISpot assays selected by promiscuous epitope prediction.**

n<sub>td</sub>, number of tested PBMC cultures; rr, recognition rate; wpp, whole-proteome prediction; nt, not tested. Adapted from [188].

Protein <sub>position</sub>	Sequence	ELISpot		ICS	wpp
		n <sub>td</sub>	rr		
<b>US24</b> <sub>255-269</sub>	SRRWWWAVRANLATP	23	73.9	CD4	Yes
<b>UL36</b> <sub>253-267</sub>	QYVLVDTFGVVYGYD	23	73.9	CD4	yes (UL36 <sub>254-268</sub> )
<b>UL24</b> <sub>201-215</sub>	KRYFRPLLRAWSLGL	22	72.7	CD4 & CD8	Yes
<b>MCP</b> <sub>515-529</sub>	DFVVTDFYKVGNI TL	21	71.4	CD4	Yes
<b>TRM3</b> <sub>319-333</sub>	FNTILGFLAQNTTKI	23	69.6	CD4	Yes
<b>CVC2</b> <sub>400-414</sub>	RDDVLSLWSRRLLVG	22	63.6	CD4	Yes (CVC2 <sub>401-415</sub> )
<b>US4</b> <sub>62-76</sub>	PYFPMRFINVKSHVS	22	63.6	CD4	No
<b>UL34</b> <sub>219-233</sub>	NSFLHLLMNSGLDIA	22	63.6	CD4	Yes
<b>UL84</b> <sub>122-136</sub>	RDPFQILLSTPLQLG	24	62.5	CD4	Yes
<b>GO</b> <sub>425-439</sub>	LLFLDEIRNFSLRSP	24	62.5	CD4	Yes
<b>MCP</b> <sub>570-584</sub>	FHELRTWEIMEHMRL	20	60.0	CD4	No
<b>HHLF1 &amp; IRS1</b> <sub>214-228</sub>	FRVFVYDLANNTLIL	22	59.1	CD4	No
<b>CVC2</b> <sub>595-609</sub>	EHGLGRLLSVTLPRH	26	57.7	CD4	Yes (CVC2 <sub>598-612</sub> )
<b>PORTL</b> <sub>246-260</sub>	VRVFKKVRSERLEAQ	23	56.5	CD4	Yes
<b>DPOL</b> <sub>67-81</sub>	LMFYREIKHLLSHDM	23	56.5	CD4	Yes
<b>HEPA</b> <sub>488-502</sub>	FWQIQSLLGYISEHV	24	54.2	CD4	No
<b>US8</b> <sub>191-205</sub>	MVLLLGYVLARTVYR	24	50.0	CD4	No
<b>UL52</b> <sub>240-254</sub>	LIIMSEFTHLLQQHF	31	48.4	nt	Yes
<b>IE1</b> <sub>313-327</sub>	CCYVLEETSVMLAKR <sup>a</sup>	23	47.8	CD4	Yes (IE1 <sub>314-328</sub> )
<b>NEC2</b> <sub>103-117</sub>	FNVLKVNESLIVTLK	23	47.8	nt	No
<b>YHR1</b> <sub>50-64</sub>	VLRFVVRDLDLPR	21	47.6	CD4	No
<b>UL61</b> <sub>384-398</sub>	GFIGFQMPRLGGRSG	22	45.5	CD4	No
<b>UL49</b> <sub>197-211</sub>	RFLFGVDLRLPVLHP	22	45.5	CD4	Yes (UL49 <sub>197-211</sub> )
<b>EP84</b> <sub>347-361</sub>	ALLPIERGAVVSSP	22	45.5	CD4	no
<b>MCP</b> <sub>621-635</sub>	VDAFLLRITFVARCI	20	45.0	nt	Yes
<b>UL31</b> <sub>203-217</sub>	GYKYDWSNVVTPKAA	23	43.5	CD4	No
<b>DUT</b> <sub>311-325</sub>	RFTYLPVGSHPGLQGM	21	42.9	nt	Yes
<b>UL40</b> <sub>196-210</sub>	FSSFYSQIARSLGVL	14	42.9	nt	No
<b>UL78</b> <sub>272-286</sub>	IMDYVELATRLLTM	13	38.5	nt	Yes (UL78 <sub>274-288</sub> )
<b>HEPA</b> <sub>706-720</sub>	YREILFRFVARRNDV	14	35.7	nt	Yes (HEPA <sub>709-723</sub> )
<b>DPOL</b> <sub>988-1002</sub>	CEFVKGVTRDVL SLL	24	33.3	nt	Yes
<b>UL20</b> <sub>190-204</sub>	FMDYVILTPLAVLTC	15	33.3	nt	No
<b>UL81</b> <sub>73-87</sub>	LYLFLNNKNTETLII	21	33.3	CD4	No
<b>RIR1</b> <sub>341-355</sub>	IYRFHLDARFEGEVL	22	31.8	nt	No

<b>DNBI</b> <sub>871-885</sub>	VKFLVAVTADYQEHD	16	31.3	nt	No
<b>UL11</b> <sub>133-147</sub>	CYYVYVTQNGTLPTT	16	31.3	nt	Yes
<b>AN</b> <sub>238-252</sub>	LGLLIDPTSGLLGAS	16	31.3	nt	Yes (AN <sub>239-253</sub> )
<b>UL117</b> <sub>330-344</sub>	VATFKFFHQDPNRVL	16	31.3	nt	yes
<b>HEPA</b> <sub>438-452</sub>	VLIVDLVERVLAKCV	17	29.4	CD4	No
<b>HEPA</b> <sub>150-164</sub>	LSLFHVAKLVVIGSY	14	28.6	nt	No
<b>UL107</b> <sub>27-41</sub>	QNSFFSFLSRKSMY	7	28.6	nt	Yes
<b>UL108</b> <sub>46-60</sub>	SSFFDVLSSRSCFV	7	28.6	nt	Yes
<b>US33</b> <sub>33-47</sub>	FDVVLTFVPSGFVMG	7	28.6	nt	yes
<b>PP65</b> <sub>347-361</sub>	ALFFFIDILLQRGP <sup>b</sup>	7	28.6	nt	No
<b>PP150</b> <sub>459-473</sub>	GGVSSIFSGLLSSGS	7	28.6	nt	Yes
<b>UL35</b> <sub>181-195</sub>	YPRLTYYNLLFHPPP	7	28.6	nt	No
<b>TRM3</b> <sub>222-236</sub>	IPIISFLKHMIGI	7	28.6	nt	No
<b>UL37</b> <sub>3-17</sub>	PVYVNLGSGVGLLAF	11	27.3	nt	Yes
<b>CEP3</b> <sub>18-32</sub>	GEPLKDALGRQVSLR	15	26.7	nt	No
<b>DNBI</b> <sub>844-858</sub>	LQFWQKVCNALPKN	16	25.0	nt	No
<b>HHLF1</b> <sub>306-320</sub>	MVLLGAWQELAQYEP	16	25.0	nt	Yes
<b>US15</b> <sub>191-205</sub>	FKIVLSFSLITCLA	8	25.0	nt	Yes
<b>CVC1</b> <sub>123-137</sub>	RMFYAVFTTLGLRCP	14	21.4	nt	Yes
<b>IRS1</b> <sub>168-182</sub>	RDWIVLVATVVHEV	19	21.1	nt	No
<b>UL22A</b> <sub>7-21</sub>	ILSLAVTLTVALAA	15	20.0	nt	No
<b>UL9</b> <sub>111-125</sub>	FDSLYTYGWVLRTP	15	20.0	nt	No
<b>UL36</b> <sub>42-56</sub>	ERCFIQLRSRSALGP	6	16.7	nt	Yes (UL36 <sub>41-55</sub> )
<b>UL67</b> <sub>76-90</sub>	FVYLHSVESYSLQFH	7	14.3	nt	Yes
<b>IR12</b> <sub>92-106</sub>	TTVYSTFNSTYANIS	7	14.3	nt	Yes (IR12 <sub>93-107</sub> )
<b>YHL4</b> <sub>111-125</sub>	WLLVLNLNVALPVTA	7	14.3	nt	No
<b>LTP</b> <sub>658-672</sub>	VLRLFYDLRDLKLCD	14	14.3	nt	Yes
<b>US36</b> <sub>46-60</sub>	RTALNLFLSMLCVP	14	14.3	nt	No
<b>UL88</b> <sub>406-420</sub>	LGYDRLVSADAGVSR	14	14.3	nt	No
<b>UL110</b> <sub>91-105</sub>	IMMIIIIHSPTIFIL	7	14.3	nt	No
<b>CEP3</b> <sub>31-45</sub>	LRSYDNIPPTSSSDE	15	13.3	nt	No
<b>IE2</b> <sub>501-515</sub>	VDLLGALNLCPLMQ	8	12.5	nt	Yes (IE2 <sub>502-516</sub> )
<b>UL29/28</b> <sub>430-444</sub>	MLGDTQYFGVVDRHK	8	12.5	nt	Yes
<b>DNBI</b> <sub>1115-1129</sub>	ASLMDKFAALQEQQV	8	12.5	nt	No
<b>UL8</b> <sub>231-245</sub>	SSDWVTLGTSASLLR	8	12.5	nt	Yes
<b>UL8</b> <sub>86-100</sub>	STPYVGLSLSCAANQ	8	12.5	nt	No
<b>UL9</b> <sub>105-119</sub>	YSGIYYFDSLYTYGW	8	12.5	nt	No
<b>RIR1</b> <sub>400-414</sub>	WAAMCKWMSTLSCGV	8	12.5	nt	No
<b>UL9</b> <sub>7-21</sub>	LLWWITILLRIQQFY	13	7.7	nt	Yes (UL9 <sub>8-22</sub> )
<b>US3</b> <sub>152-166</sub>	DDNWGLLFRLLVYL	16	6.3	nt	Yes (US3 <sub>153-167</sub> )



<b>GB</b> <sub>331-345</sub>	VISWDIQDEKNVTCQ	11	0.0	nt	Yes
<b>U7</b> <sub>23-37</sub>	YNKLLILALFTPVIL	8	0.0	nt	No
<b>UL97</b> <sub>82-96</sub>	VTTLTTLSSVSTTTV	8	0.0	nt	No
<b>UL97</b> <sub>559-573</sub>	VLGFCLMRLDRRGL	8	0.0	nt	Yes
<b>DPOL</b> <sub>1056-1070</sub>	LVLSSVLKDISLYR	8	0.0	nt	Yes
<b>DNBI</b> <sub>689-703</sub>	RSVFYVIQNVALITA	8	0.0	nt	Yes
<b>UL15A</b> <sub>85-99</sub>	MFLVFGLCSWLAMRY	8	0.0	nt	No
<b>LTP</b> <sub>830-844</sub>	NAVLSMFHTLVMRLA	7	0.0	nt	Yes
<b>PP150</b> <sub>59-73</sub>	WLGYYRELRFHNPDL	7	0.0	nt	Yes
<b>UL35</b> <sub>108-122</sub>	QLDVLVSDPLKTRLL	7	0.0	nt	Yes (UL35 <sub>110-124</sub> )
<b>UL35</b> <sub>462-476</sub>	KRFMELDRAPLGQE	7	0.0	nt	Yes
<b>EP84</b> <sub>471-485</sub>	LCDLPLVSSRLLPET	7	0.0	nt	No
<b>US9</b> <sub>196-210</sub>	YVVLVQFVKHVALFS	7	0.0	nt	No
<b>GH</b> <sub>108-122</sub>	YLTVFTVYLLSHLPS <sup>c</sup>	7	0.0	nt	No
<b>SCAF</b> <sub>118-132</sub>	DKVVEFLSGSYAGLS	7	0.0	nt	No
<b>PP71</b> <sub>282-296</sub>	GFQLLIPKSFTLTRI	7	0.0	nt	No
<b>RIR1</b> <sub>382-396</sub>	VPQYDFLISADPFSSR	7	0.0	nt	No
<b>VPAP</b> <sub>249-263</sub>	DTLLYVASRNGLFAV	6	0.0	nt	No
<b>EP84</b> <sub>298-312</sub>	MSLPLDTSEAVAFLN	6	0.0	nt	No
<b>UL35</b> <sub>439-453</sub>	TYHLQRIYSMMIEGA	6	0.0	nt	Yes (UL35 <sub>439-453</sub> )
<b>HEPA</b> <sub>264-278</sub>	WTHLYDVLFRGFAGQ	6	0.0	nt	No
<b>US6</b> <sub>134-148</sub>	WNAFRLIERHGFFAV	5	0.0	nt	No
<b>GM</b> <sub>57-71</sub>	MSAYNVMHLHTPMLF	5	0.0	nt	Yes
<b>UL101</b> <sub>88-102</sub>	LGAYRTMSVFGSGWR	7	0.0	nt	No
<b>US17</b> <sub>113-127</sub>	LTIYSVLTTLVIVA	8	0.0	nt	Yes
<b>UL42</b> <sub>100-114</sub>	FLAVVFTVVINRDSA	8	0.0	nt	Yes
<b>US5</b> <sub>21-35</sub>	TGVVYRDISSTIATE	6	0.0	nt	No
<b>IR04</b> <sub>57-71</sub>	FIIFFFLSSPFLNL	7	0.0	nt	Yes
<b>IR13</b> <sub>5-19</sub>	FTVMWUTILISALSES	7	0.0	nt	No

References: a – [210] (313-327), [185] (216-330); b – [211] (350-358)&(348-356), [212] (340-355), [213] (347-365); c – [184] (15-60). The position of the published peptide sequences in the proteins is given in brackets.

**Table 4: Tested peptides originating from the laboratory stock.** Positions of the published peptide sequences in the proteins are indicated in brackets if deviating from the position in column one. n<sub>td</sub>, number of tested PBMC cultures; rr, recognition rate; nt, not tested. Adapted from [188].

Protein <sub>position</sub>	Sequence	Elispot		ICS	Reference
		n <sub>td</sub>	rr		
PP65 <sub>109-123</sub>	MSIYVYALPLKMLNI	23	82.6	CD4 & CD8	[214]
VPAP <sub>253-267</sub>	YVASRNLFAVENFL	21	76.2	CD4	-
PP65 <sub>179-193</sub>	DVYYTSAFVFPTKDV	21	61.9	CD4	[129](177-191); [215](177-191); [214](180-194)
TEG7 <sub>37-51</sub>	LQAFLDENFKQLEIT	23	60.9	CD4	-
PP65 <sub>283-299</sub>	KPGKISHIMLDVAFTSH	20	60.0	CD4	[214];[129](285-299); [111](285-299); [215](281-295)
TEG7 <sub>36-50</sub>	ELQAFLDENFKQLEI	7	42.9	nt	-
PP65 <sub>366-382</sub>	HPTFTSQYRIQGKLEYR	5	40.0	CD4	[180](369-384. 361-376); [216](364-386); [111](365-379); [215](365-349); [214](366-380. 370-384)
PP65 <sub>510-425</sub>	YQEFFWDANDIYRIF	6	33.3	nt	[214]; [180](509-524); [129](509-523); [111](509-523); [215](509-523)
TEG7 <sub>34-48</sub>	LRELQAFLDENFKQL	6	33.3	nt	-
PP65 <sub>184-198</sub>	SAFVFPTKDVALRHV	14	28.6	nt	[129,215](177-191); [214](180-194)
PRIM <sub>508-522</sub>	RLPVFNFDVDFDLRL	13	23.1	nt	-
TEG7 <sub>39-53</sub>	AFLDENFKQLEITPA	5	20.0	nt	-
PP65 <sub>177-191</sub>	EPDVYYTSAFVFPTK	16	18.8	nt	[129, 215]; [214](180-194)
PP65 <sub>250-264</sub>	VEEDLTMTRNPQPFM	6	16.7	nt	[214]; [215](245-259)
PP65 <sub>496-503</sub>	LVPMVATV	6	16.7	nt	[180](485-500); [129](489-503); [111](493-507); [215](489-503)
PRIM <sub>498-512</sub>	YYTRHEVFNERLPVF	13	15.4	nt	-
PP65 <sub>39-53</sub>	TRLLQTGIHVRVSQP	7	14.3	nt	[214]; [111, 215](41-55)
TEG7 <sub>38-52</sub>	QAFLDENFKQLEITP	7	14.3	nt	-
PP65 <sub>497-503</sub>	VPMVATV	7	14.3	nt	[180](485-500); [129](489-503); [111](493-507); [215](489-503)

<b>PP65</b> <sub>174-188</sub>	QWKEPDVYYTSAFVF	14	7.1	nt	[129,215](177-191); [214](180-194)
<b>PP65</b> <sub>169-183</sub>	TRQQNQWKEPDVYYT	6	0.0	nt	[215]
<b>VPAP</b> <sub>263-276</sub>	VENFLTEEPFQRGD	6	0.0	nt	-
<b>PRIM</b> <sub>503-517</sub>	EVFNERLPVFNFVAD	5	0.0	nt	-
<b>VPAP</b> <sub>259-273</sub>	GLFAVENFLTEEPFQ	5	0.0	nt	-
<b>VPAP</b> <sub>256-270</sub>	SRNGLFAVENFLTEE	5	0.0	nt	-
<b>PRIM</b> <sub>493-507</sub>	PETQFYTRHEVFNE	4	0.0	nt	-

We defined epitopes with recognition rates  $\geq 50\%$  of the tested PBMC cultures as dominant epitopes, while epitopes which triggered IFN $\gamma$  responses in  $< 50\%$  of the PBMC cultures were categorized as subdominant. Figure 10 illustrates the proportion of dominant, subdominant, and non-recognized epitopes. Of all predicted peptides, 71.2% turned out to be either dominant or subdominant epitopes, 16.4% of which were dominant. No T-cell responses were detected for 28.9% of the peptides (Figure 10A) [188]. Among the peptides that reached the maximum score (top score) for one or two HLA allotypes, 18.6% were dominant epitopes, and only 23.7% were not recognized by T cells (Figure 10B). Among the epitope candidates not reaching a top score, there were less immunogenic peptides than among the top scorers.

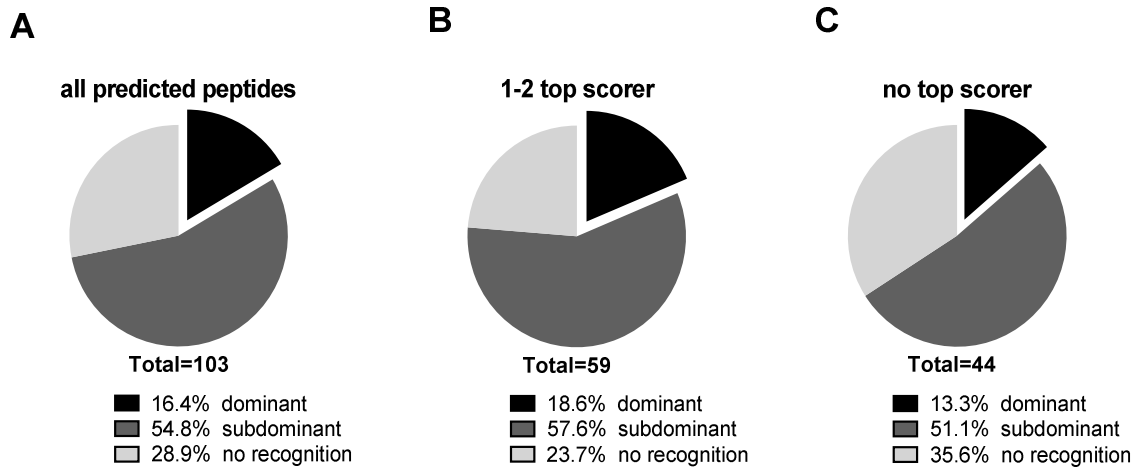


**Figure 10: Recognition rates of predicted peptides tested in ELISpot assays with a prior 12-day stimulation.** Depicted are all predicted peptides (**A**), the peptides reaching the maximum prediction score for one or two HLA allotypes (top scorer) (**B**), and all peptides not reaching the maximum prediction score (**C**). Dominant recognition rate (rr):  $\geq 50\%$ ; subdominant rr:  $< 50\%$ ; no recognition: no T-cell response detected. Adapted from [188].

Figure 11 shows the numbers of spot-forming cells (SFC) per 500,000 cells for each tested PBMC culture for the dominant epitopes. This number is highly variable between the PBMC cultures tested against the same peptide. However, the mean spot counts rise with higher recognition rates [188]. The epitope pp65<sub>109-123</sub>, for instance, induces spot counts of 1,000 or more in four assessed PBMC cultures. Nonetheless, high spot counts can also be seen with other epitopes that are not as frequently recognized.

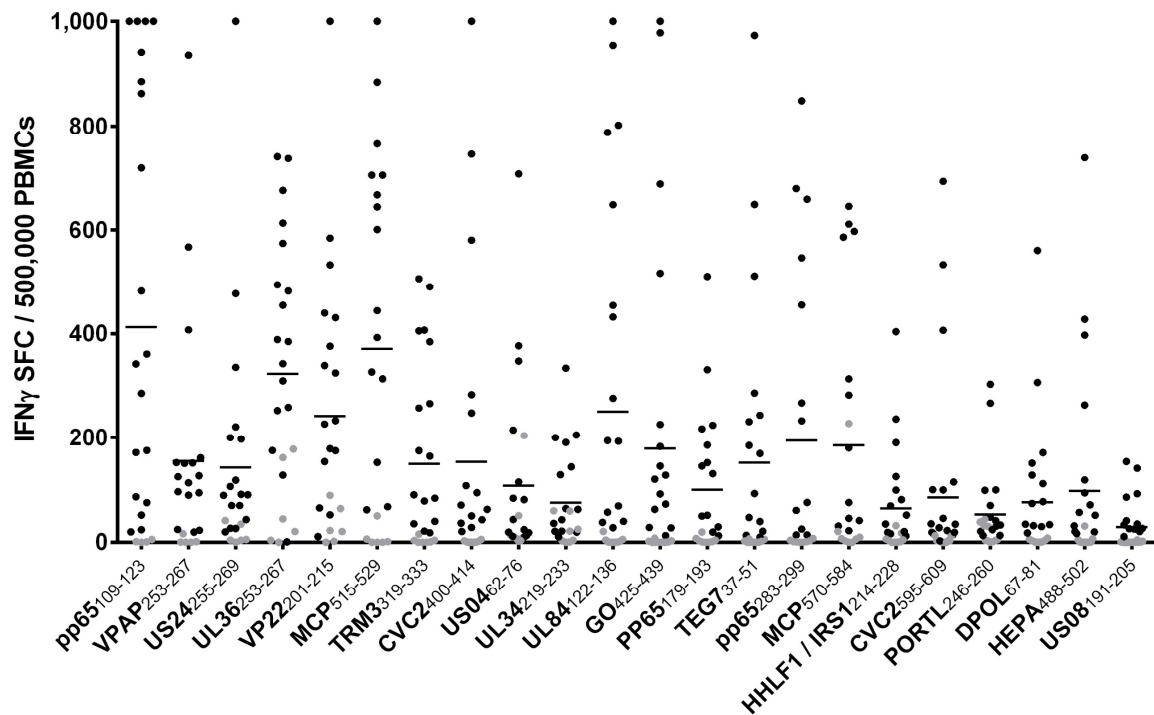


**Figure 11: ELISpot results of dominant epitopes.** The number of spot-forming cells (SFC) per 500,000 PBMCs are plotted for each dominant epitope (negative control subtracted, cut-off at 1,000 SFC). Each dot represents one tested PBMC culture. Negative results are indicated in grey. The horizontal lines show the mean spot counts of all tested PBMC cultures for each peptide. The peptides are sorted according to their recognition rates from highest (left) to lowest (right). Adapted from [188].

#### 4.2 Identified T-cell epitopes originate from a broad antigen spectrum

The predicted and identified 74 epitopes originate from 58 different proteins (Figure 12). The spectrum of source proteins covers all temporal stages of HCMV protein expression, as defined by Weekes et al. [44]. These proteins carry out various viral functions. UL 36 ( $n = 2$ ), DPOL ( $n = 2$ ), IRS1/HHLF1 ( $n = 2$ ), HEPA ( $n = 4$ ), MCP ( $n = 3$ ), TRM3 ( $n = 2$ ), CVC2 ( $n = 2$ ), RIR1 ( $n = 2$ ), DNBI ( $n = 3$ ), CEP3 ( $n = 2$ ), UL9 ( $n = 3$ ), UL8 ( $n = 2$ ) are represented with multiple epitopes. The majority of the source antigens we identified (34%) belong to temporal class five (Figure 12) [188].

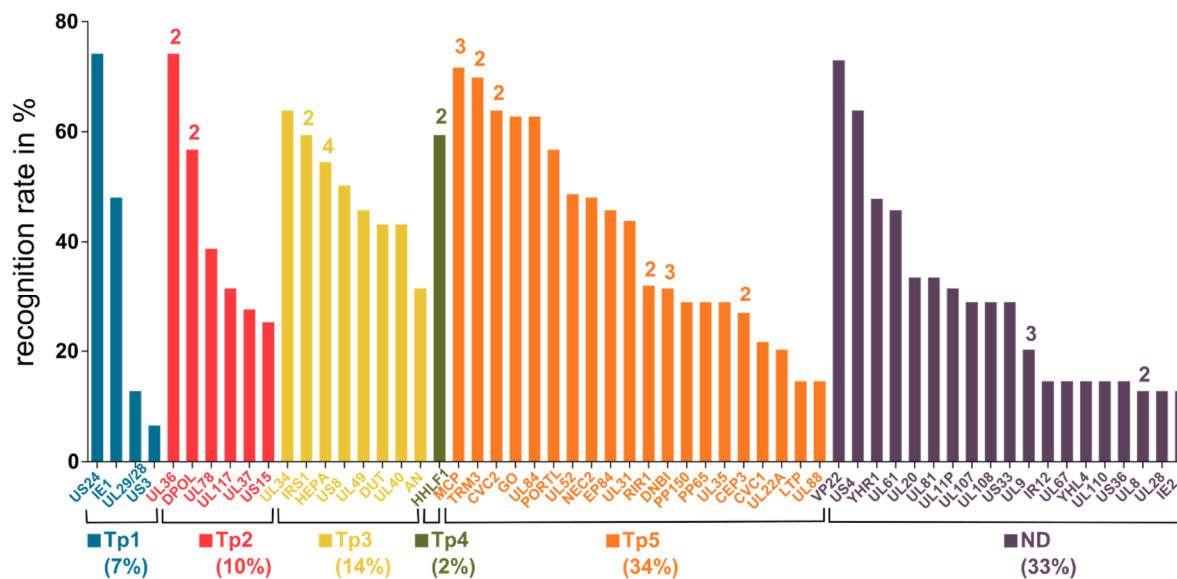


**Figure 12: Antigen spectrum of predicted dominant and subdominant peptides.** “For each source protein, the identified epitope with the highest recognition rate is shown (ELISpot recognition rate in percent). The numbers above the bars indicate the number of identified epitopes from the respective antigen. Abbreviations: Tp1-5, temporal classes of protein expression, defined by Weekes et al. [44]; ND, temporal class not determined” [188].

### 4.3 Validation of T-cell epitopes by intracellular cytokine staining

The T-cell epitopes that were identified by ELISpot screening assays had to be validated by ICS because IFN $\gamma$  release is not specific for CD4 $^{+}$  T cells. Hence, the donor-derived PBMC cultures that responded with high spot counts in ELISpot underwent a 12-day stimulation with the respective peptide again. Cytokine secretion (TNF, IFN $\gamma$ ) upon restimulation with the test peptide and CD4 or CD8 expression was then measured in flow cytometry.

Peptides are referred to as valid CD4 $^{+}$  T-cell epitopes if at least one CD4 $^{+}$  T-cell response was detected in ICS, and PBMC samples of not less than 20 donors were tested in ELISpot. The results of all tested peptides in ICS are summarized in Table 5. For each tested peptide, at least one PBMC culture with CD4 $^{+}$  cytokine-secreting T cells was detected [188]. Hence, all listed peptides in Table 5 are valid CD4 $^{+}$  T-cell epitopes.

Several epitopes triggered IFN $\gamma$  and TNF secretion in sizeable CD4<sup>+</sup> T-cell populations. CVC2<sub>400-414</sub>, for instance, activated 32.65% of the CD4<sup>+</sup> T cells in one PBMC culture (Figure 13A). Figure 13B illustrates the ICS results of one representative donor for each assessed peptide.

Only two peptides (pp65<sub>109-123</sub>, UL24<sub>201-215</sub>) showed detectable CD8<sup>+</sup> T-cell responses (Table 5) [188]. In case CD8<sup>+</sup> T-cell activating shorter variants of the peptide sequence were found in publications or our laboratory database, donors with the matching HLA-class I typing were chosen, if available.

**Table 5: Peptides tested in ICS.** The percentages of TNF and IFN $\gamma$  positive T cells in ICS are shown. The background, determined in the negative control, was subtracted. Positive results are indicated in green. For each peptide, PBMC samples of two to five donors were tested, of which at least one was positive. For only two peptides, CD8<sup>+</sup> T-cell responses could be detected. Negative percentages due to background subtraction were equated with zero.

Protein <sub>Position</sub>	Sequence	ELISpot rr	tested donors	CD4 <sup>+</sup> TNF <sup>+</sup> IFN $\gamma$ <sup>+</sup>	CD8 <sup>+</sup> TNF <sup>+</sup> IFN $\gamma$ <sup>+</sup>
PP65 <sub>109-123</sub>	MSIYVYALPLKMLNI	82.61	2985	0.24%	0.75%
			3094	0%	12.29%
			3105	21.64%	0.04%
VPAP <sub>253-267</sub>	YVASRNGLFAVENFL	76.19	2971	4.51%	0%
			3065	3.30%	0%
UL36 <sub>253-267</sub>	QYVLVDTFGVVYGVD	73.91	3196	0.49%	0.05%
			3231	1.35%	0%
US24 <sub>255-269</sub>	SRRWWWAVRANLATP	73.91	2962	4.31%	0.03%
			3160	0.08%	0%
UL24 <sub>201-215</sub>	KRYFRPLLRAWSLGL	72.73	3024	0.40%	0%
			3270	13.67%	10.39%
MCP <sub>515-529</sub>	DFVVTDFYKVGNITL	71.43	3168	24.41%	0%
			3255	3.30%	0%
TRM3 <sub>319-333</sub>	FNTILGFLAQNTTKI	69.57	2921	0.27%	0.01%
			2985	1.14%	0%
US4 <sub>62-76</sub>	PYFPMRFINVKSHVS	63.64	2897	0.09%	0%
			3168	0.00%	0%
UL34 <sub>219-233</sub>	NSFLHLLMNSGLDIA	63.64	3065	0.01%	0%
			3161	0.40%	0%
CVC2 <sub>400-414</sub>	RDDVLSLWSRLLVG	63.64	2921	0.31%	0.25%

			3105	32.64%	0.04%
<b>UL84</b> <sub>122-136</sub>	RDPFQILLSTPLQLG	62.50	3094	0.00%	0.41%
			3118	0.95%	0.04%
<b>GO</b> <sub>425-439</sub>	LLFLDEIRNFSLRSP	62.50	3105	9.91%	0%
			3155	1.57%	0%
<b>PP65</b> <sub>179-193</sub>	DVYYTSAFVFPTKDV	61.90	2507	0.03%	0%
			2863	0.02%	0.09%
			3170	0.03%	0.06%
			2473	0.10%	0.00%
			2567	36.98%	0%
<b>TEG7</b> <sub>37-51</sub>	LQAFLDENFKQLEIT	60.87	2971	14.26%	0%
			2986	4.79%	0%
<b>PP65</b> <sub>283-299</sub>	KPGKISHIMLDVAFTSH	60.00	2507	3.59%	0.07%
			2567	29.67%	0.27%
			2863	1.65%	0.50%
<b>MCP</b> <sub>570-584</sub>	FHELRTWEIMEHMRL	60.00	3270	0.18%	0%
			2915	0.62%	0.13%
			3164	0.88%	0.09%
<b>HHLF1 &amp; IRS1</b> <sub>214-228</sub>	FRVFVYDLANNTLIL	59.09	2986	0.07%	0%
			3155	0.05%	0%
			3174	0.03%	0.15%
			3184	0.32%	0%
			3154	0%	0.25%
<b>CVC2</b> <sub>595-609</sub>	EHGLGRLLSVTLPRH	57.69	3008	6.80%	0.42%
			3172	1.29%	0%
<b>PORTL</b> <sub>246-260</sub>	VRVFKKVRSERLEAQ	56.52	2813	1.70%	0%
			3115	8.39%	0%
<b>DPOL</b> <sub>67-81</sub>	LMFYREIKHLLSHDM	56.52	2971	1.89%	0%
			3105	0.09%	0%
<b>HEPA</b> <sub>488-502</sub>	FWQIQSLLGYISEHV	54.17	3930	0.12%	0.11%
			3172	4.10%	0%
<b>US8</b> <sub>191-205</sub>	MVLLLGYYVLARTVYR	50.00	2985	0.12%	0.22%
			3184	0.03%	0.07%
<b>IE1</b> <sub>313-327</sub>	CCVLEETSVMLAKR	47.83	2921	0.42%	0%
			2971	2.28%	0.12%
			2985	0%	0%
<b>YHR1</b> <sub>50-64</sub>	VLRFFT VVRD VDLPR	47.62	3024	2.69%	0.04%
			3221	0.13%	0%
<b>UL61</b> <sub>384-398</sub>	GFIGFQMPRLGGRSG	45.45	2962	0.19%	0.05%
			3160	0.09%	0.00%



<b>UL49</b> <sub>197-211</sub>	RFLFGVDLRLPVLHP	45.45	2915	0.38%	0.02%
			3168	7.27%	0%
<b>EP84</b> <sub>347-361</sub>	ALLLPIERGAVVSSP	45.45	2971	0.79%	0.07%
			2985	1.34%	0.46%
<b>UL31</b> <sub>203-217</sub>	GYKYDWSNVVTPKAA	43.48	3196	0.14%	0.03%
			3244	0.09%	0%
<b>PP65</b> <sub>366-382</sub>	HPTFTSQYRIQGKLEYR	40.00	2473	3.90%	0.00%
			2570	27.41%	0.29%
<b>UL81</b> <sub>73-87</sub>	LYLFLNNKNTETLII	33.33	2915	0.67%	0.01%
				0.21%	0%
<b>HEPA</b> <sub>438-452</sub>	VLIVDLVERVLAKCV	29.41	3008	1.04%	0%
			3172	0.96%	0.05%

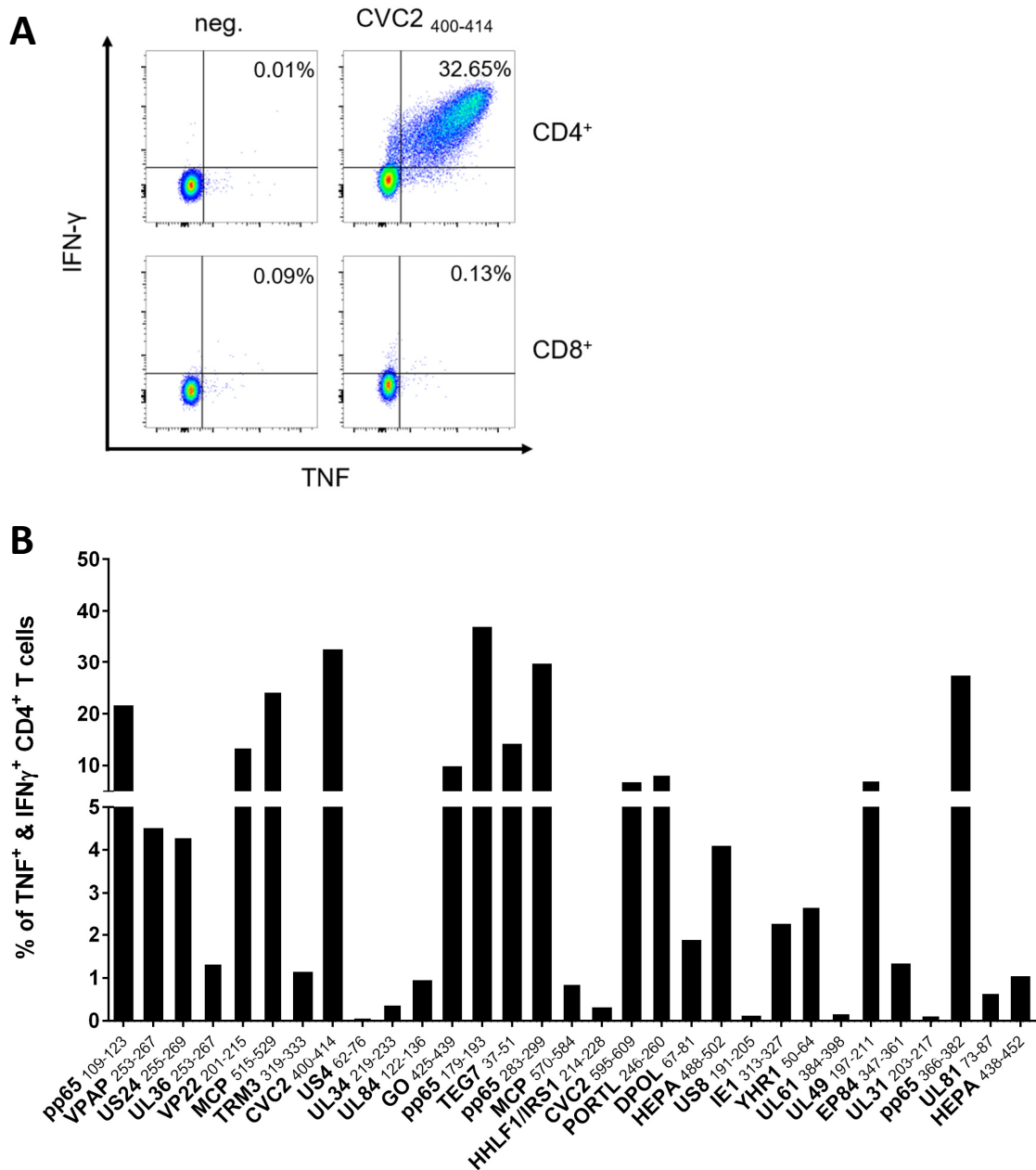


**Figure 13: Validation of CD4<sup>+</sup> T-cell epitopes by ICS. A:** Exemplary results of an ICS of the peptide CVC2<sub>400-414</sub>. The two plots on the left show the negative control (FLNA\_HUMAN<sub>1169-1683</sub>), the two plots on the right the peptide to be validated. The upper plots are gated on CD4<sup>+</sup> and the lower plots on CD8<sup>+</sup> lymphocytes. The horizontal axis indicates the signal intensity for the TNF antibody, the vertical axis the signal intensity for the IFN $\gamma$  antibody. **B:** Dominant epitopes identified in ELISpot were validated in ICS. The percentage of cytokine IFN $\gamma$ <sup>+</sup> and TNF<sup>+</sup> CD4<sup>+</sup> T cells of one representative PBMC culture per epitope is illustrated. Adapted from [188].

#### 4.4 Prediction of promiscuous CD4<sup>+</sup> T-cell epitopes from HCMV antigens

As described in 3.1, 193 proteins of HCMV strain AD169 were screened for potential T-cell epitopes. We predicted epitope candidates with the *in silico* prediction tool SYFPEITHI. Peptides that were predicted to bind to five or six different HLA class II allotypes were selected (n = 169; Table S1).

Further, we conducted a whole-proteome prediction, i.e., we took the 2% highest scored epitope candidates of the proteome into account instead of analyzing every single protein separately. We aimed to identify differences in the output lists of epitope candidates due to the methodology. In the single-protein prediction, 169 epitope candidates were predicted, while the whole-proteome prediction resulted in a list of 111 potential epitopes. 43.8% of the predicted epitopes in the single-protein prediction were identical or similar (shifted max. three positions either to the N- or C-terminus) to the ones predicted in the whole-proteome prediction. We predicted epitope candidates from 49 source antigens in the single-protein prediction that were not represented in the whole-proteome prediction.

Thirty-seven (33.3%) of the epitope candidates in the whole-proteome prediction did not appear in the single-protein prediction (Table S2). We found epitope candidates from 14 source proteins in the whole-proteome prediction that were not represented in the single-protein prediction.

Of the 56 predicted peptides that were immunogenic, 35 (62.5%) did not appear in the whole-proteome prediction (Table 3). Of the 17 dominant epitopes, 12 (70.6%) appeared on the whole-proteome prediction list, as well (nine identical, three similar).

We only synthesized epitope candidates for testing that were predicted with the single-protein prediction.

#### **4.5 Generation of peptide pools containing validated CD4<sup>+</sup> T-cell epitopes**

Dominant and validated CD4<sup>+</sup> T cell epitopes were pooled to trigger responses in PBMC cultures derived from numerous healthy, HCMV-seropositive blood donors, regardless of their HLA haplotypes. The Pool I contains 14 peptides, 11 of which were newly identified in this project (Table 6). It was tested in 48 PBMC cultures in ELISpot and elicited IFN $\gamma$  secretion in 95.8% (Table 7 and Figure 14). Two PBMC cultures could not be activated with the peptide pool [188].

Twenty percent (n = 9) of the tested donors have been assessed in single-peptide ELISpots before. This way, competition effects through parallel stimulation with multiple potent epitopes could be evaluated.

Pool II included the same peptides but without the three pp65-derived peptides. Pool II was tested in PBMC cultures of 30 donors and was positive in 100% (Table 7) [188].

The blood donors of the PBMC samples were selected randomly from a large stock in our laboratory to ensure the variability of the HLA polymorphisms.

**Table 6: Composition of peptide pool I.** Fourteen peptides that showed recognition rates in ELISpot screening of  $\geq 50\%$  and CD4<sup>+</sup> T-cell responses in ICS were pooled. rr, recognition rate. Adapted from [188].

Protein <sub>position</sub>	Sequence	ELISpot		ICS
		n <sub>td</sub>	rr	
PP65 <sub>109-123</sub>	MSIYVYALPLKMLNI	23	82.6	CD4 & CD8
VPAP <sub>253-267</sub>	YVASRNGLFAVENFL	21	76.2	CD4
TRM3 <sub>319-333</sub>	FNTILGFLAQNTTKI	23	69.6	CD4
CVC2 <sub>400-414</sub>	RDDVLSLWSRLLVG	22	63.6	CD4
UL84 <sub>122-136</sub>	RDPFQILLSTPLQLG	24	62.5	CD4
GO <sub>425-439</sub>	LLFLDEIRNFSLRSP	24	62.5	CD4
PP65 <sub>179-193</sub>	DVYYTSAFVFPTKDV	21	61.9	CD4
TEG7 <sub>37-51</sub>	LQAFLDENFKQLEIT	23	60.9	CD4
PP65 <sub>283-299</sub>	KPGKISHIMLDVAFTSH	20	60.0	CD4
HHLF1 & IRS1 <sub>214-228</sub>	FRVFVYDLANNTLIL	22	59.1	CD4
CVC2 <sub>595-609</sub>	EHGLGRLLSVTLPRH	26	57.7	CD4
DPOL <sub>67-81</sub>	LMFYREIKHLLSHDM	23	56.5	CD4
HEPA <sub>488-502</sub>	FWQIQSLLGYISEHV	24	54.2	CD4
US8 <sub>191-205</sub>	MVLLLGYYVLARTVYR	24	50.0	CD4

**Table 7: ELISpot results of the peptide pools.** 12d, ELISpot with a prior 12-day stimulation; *ex vivo*, without a 12-day stimulation; rr, recognition rate; n<sub>tested PBMC cultures</sub>, number of tested donors. Adapted from [188].

	n <sub>tested PBMC cultures</sub>	rr <sub>ELISpot</sub>
Pool I, 12d	48	95.8%
Pool II, 12d	30	100.0%
Pool I, <i>ex vivo</i>	20	40.0%
Pool II, <i>ex vivo</i>	9	11.1%

In Figure 15, the spot counts are plotted for the PBMC cultures of 29 donors that were tested against peptide pool I and II (in different experiments). There is a tendency of higher spot counts after stimulation with Pool I. However, eight PBMC cultures (28%) responded with higher spot counts when stimulated with Pool II.

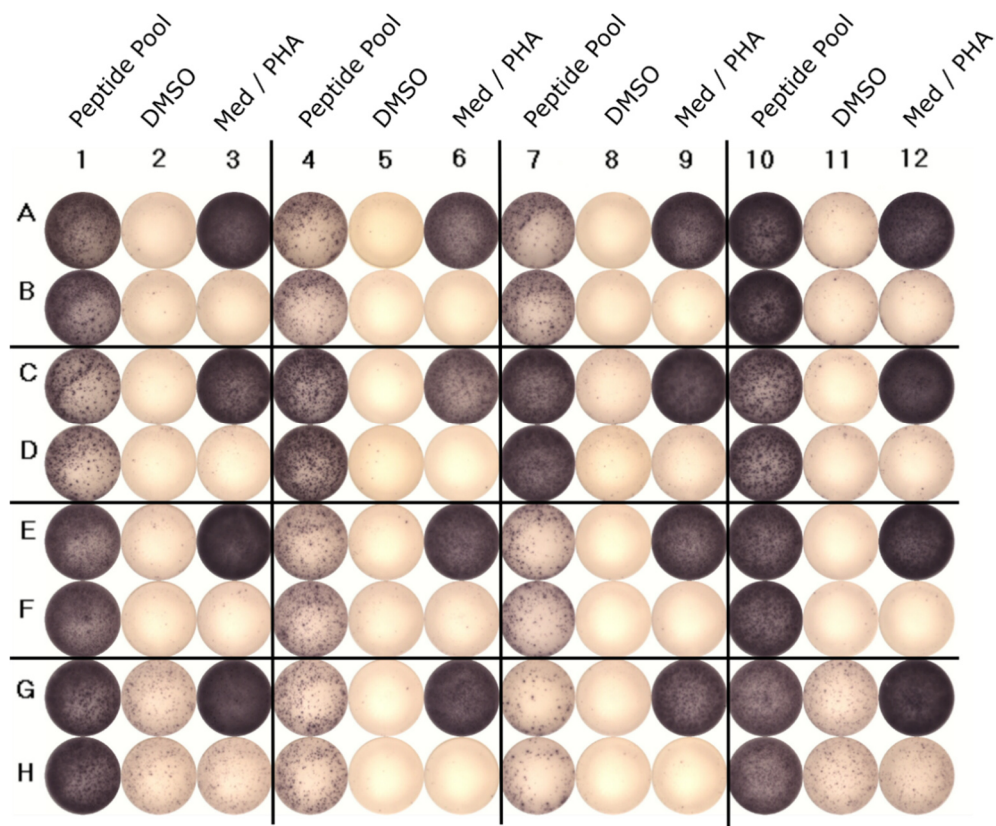


**Figure 14: Peptide pools activate the vast majority of tested PBMC cultures.**

Eleven dominant epitopes were pooled with three previously published epitopes (Pool I) to activate T cells of many donors regardless of their HLA haplotype. This peptide pool activated 46 out of 48 PBMC cultures [188]. Here, a representative ELISpot plate of the Pool I is shown. PBMCs of one donor were added into six wells. The peptide pool and DMSO (negative control) were tested in duplicates. Med, medium control; PHA is the positive control.

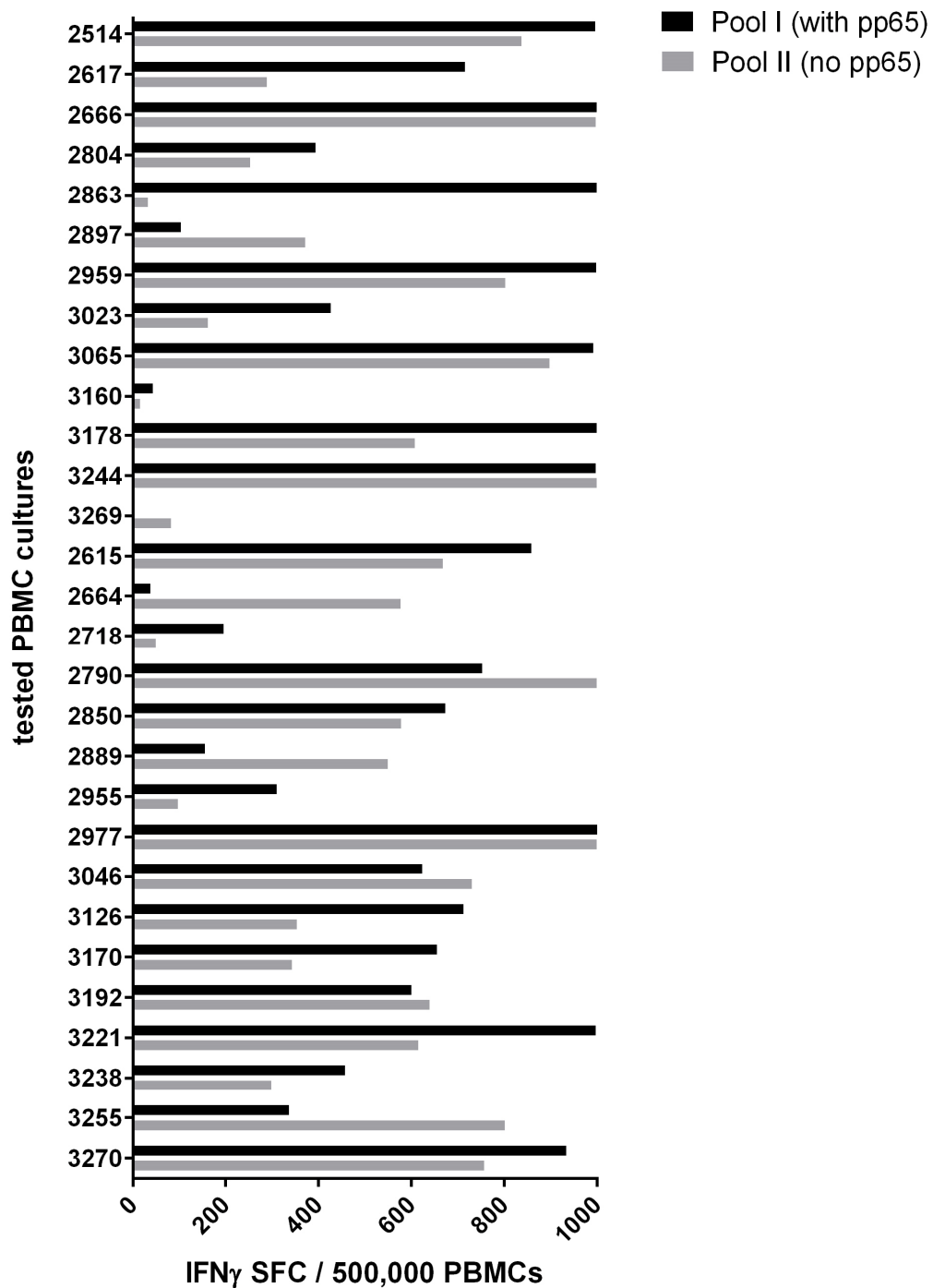


**Figure 15: Comparison of the recognition rates of peptide pool I and II.** 29 PBMC cultures were separately stimulated with both peptide pools (different experiments). The ELISpot results for each PBMC sample (encoded by a four-digit number) are depicted as SFC/500,000 PBMCs (negative control subtracted, SFC cut-off at 1,000).

#### 4.6 Epitopes and peptide pools tested in *ex vivo* ELISpot assays

*Ex vivo* ELISpot assays were conducted to investigate how the 12-day pre-stimulation affects the magnitude of the T-cell responses. PBMC cultures were stimulated with the single peptides or the peptide pool one day after thawing.

In Figure 16, the results of two exemplary peptides are shown. *Ex vivo* responses, i.e., without the pre-stimulatory period, were generally sporadic and low. Table 8 lists the results of all tested peptides. Four of fourteen peptides elicited detectable T-cell responses in *ex vivo* assays.

The peptide pools were assessed in *ex vivo* ELISpot assays, as well. PBMC cultures of twenty-one donors were stimulated with the peptide pool I. In eight PBMC cultures (40%), IFN $\gamma$  release was evaluated as positive. Pool II activated one out of nine assessed PBMC cultures (Table 7). PBMC cultures of seven donors were stimulated *ex vivo* with both peptide pools in separate experiments. Four of these PBMC cultures responded to Pool I but only one to pool II (Figure 18).

Figure 18 reveals the effect of the 12-day stimulation for Pool I and Pool II separately. The spot counts are higher with a pre-stimulation, and the majority of the T-cell responses cannot be detected without it. By comparing the spot counts of PBMC samples that were evaluated as positive in *ex vivo* assays and assays with a pre-stimulation, we calculated a mean amplification factor of 21.2 (SD = 29.4). The peptide pool I activates more PBMC cultures *ex vivo* than the pool II (Figure 18 and Table 7).





**Table 8: Peptides tested in *ex vivo* ELISpot assays.** The listed peptides were tested in *ex vivo* ELISpot assays. The PBMC samples of donors with the highest number of SFC/500,000 PBMCs in ELISpot assays after 12-day stimulation were selected. In 4 out of 14 peptides, an *ex vivo* response was detected. rr, recognition rate; n<sub>td</sub>, number of tested PBMC cultures in *ex vivo* ELISpot assays.

<b>Protein</b> <sub>position</sub>	<b>Sequence</b>	<b>rr</b> ELISpot 12-d	<b>rr</b> <i>ex vivo</i>	<b>n</b> <sub>td</sub>
<b>PP65</b> <sub>109-123</sub>	MSIYVYALPLKMLNI	82.61	0	4
<b>VPAP</b> <sub>253-267</sub>	YVASRNGLFAVENFL	76.19	0	3
<b>TRM3</b> <sub>319-333</sub>	FNTILGFLAQNTTKI	69.57	0	6
<b>CVC2</b> <sub>400-414</sub>	RDDVLSLWSRRLLVG	63.64	25	4
<b>UL84</b> <sub>122-136</sub>	RDPFQILLSTPLQLG	62.50	20	5
<b>GO</b> <sub>425-439</sub>	LLFLDEIRNFSLRSP	62.50	25	4
<b>PP65</b> <sub>179-193</sub>	DVYYTSAFVFPTKDV	61.90	25	4
<b>TEG7</b> <sub>37-51</sub>	LQAFLDENFKQLEIT	60.87	0	4
<b>PP65</b> <sub>283-299</sub>	KPGKISHIMLDVAFTSH	60.00	0	3
<b>HHLF1 &amp; IRS1</b> <sub>214-228</sub>	FRVFVYDLANNTLIL	59.09	0	4
<b>CVC2</b> <sub>595-609</sub>	EHGLGRLLSVTLPRH	57.69	0	1
<b>DPOL</b> <sub>67-81</sub>	LMFYREIKHLLSHDM	56.52	0	4
<b>HEPA</b> <sub>488-502</sub>	FWQIQSLLGYISEHV	54.17	0	2
<b>US8</b> <sub>191-205</sub>	MVLLLGYYVLARTVYR	50.00	0	3

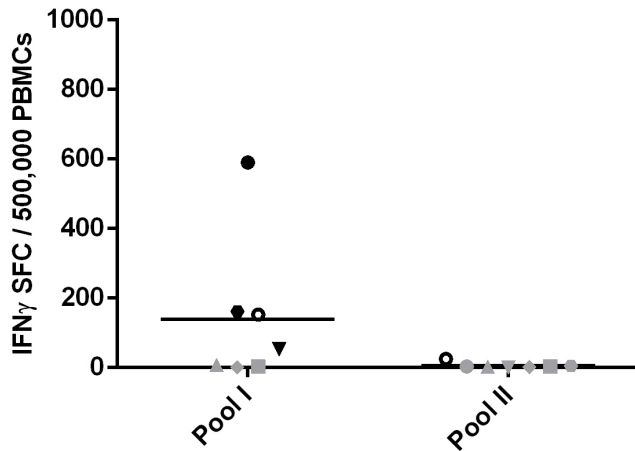


**Figure 17: *Ex vivo* T-cell responses to the peptide pools.** Here, the spot counts of PBMC cultures of seven donors tested separately against Pool I and Pool II are plotted. Each symbol type represents one PBMC culture. The horizontal line indicates the mean spot count of all tested PBMC cultures.

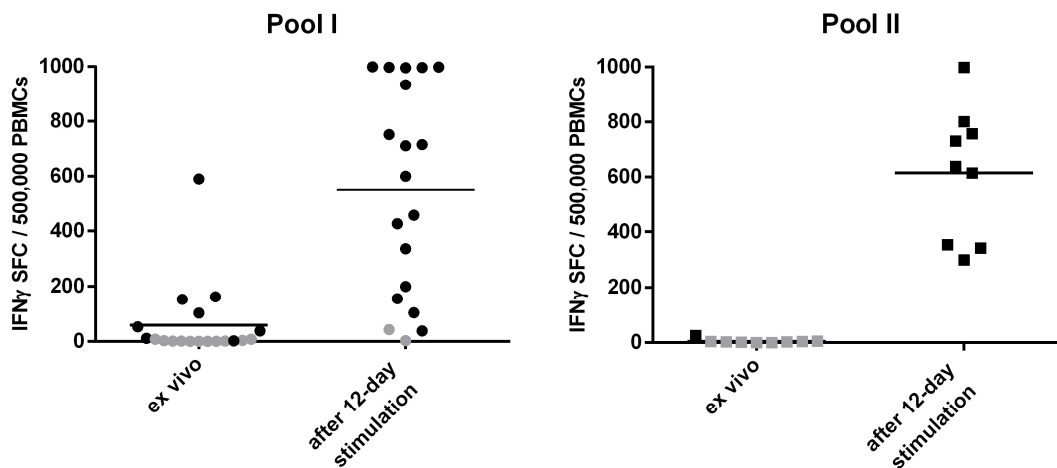


**Figure 18: Amplification of T-cell populations by 12-day stimulation with Pool I and II.** This figure illustrates T-cell responses in *ex vivo* ELISpot assays and after 12-day stimulation. Each dot represents a PBMC culture that was tested in both assays. The horizontal line indicates the mean spot count of all tested PBMC cultures.

#### 4.7 Dominant epitopes tested in PBMC cultures of HCMV-seronegative blood donors

Dominant epitopes (n = 18) were tested against PBMCs of eight HCMV-seronegative blood donors in ELISpot (with a 12-day stimulation). The serostatus of the blood donors was determined by the Institute of Clinical and Experimental Transfusion Medicine at the University Hospital Tübingen. Figure 19 shows exemplary ELISpot results. PBMC cultures of seven out of eight tested donors responded with IFN $\gamma$  secretion to dominant HCMV epitopes.

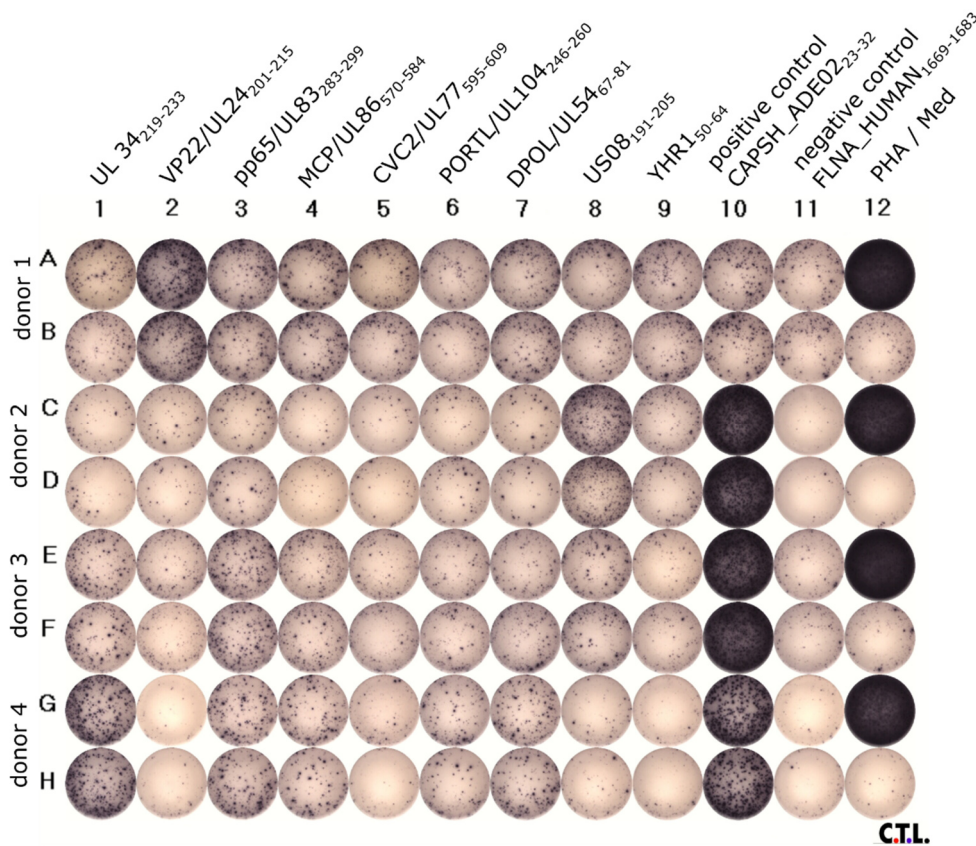


**Figure 19: Dominant epitopes were tested in PBMC cultures of HCMV-seronegative donors.**

In one assay, nine different peptides (column 1-9) were tested in PBMC cultures of eight different donors in duplicates (rows) on two 96-well plates (only one plate shown). The adenovirus-derived peptide CAPSH\_ADE02<sub>23-32</sub> served as a positive control; human Filamin-A derived FLNA<sub>1669-1683</sub> as a negative control. Additionally, PHA, as an unspecific positive control, and a medium control was applied.

#### 4.8 Alignment of the source protein sequences of dominant epitopes with correspondent protein sequences of the HCMV strain Merlin

We aligned the aa sequences of the source proteins of all dominant epitopes with the correspondent proteins of the HCMV low-passage, wild-type prototype strain Merlin (HCMVM) (Figure 20). Besides GO<sub>425-439</sub> and US4<sub>62-67</sub>, all epitopes can be found identically in both strains. GO<sub>425-439</sub> is altered at positions 6, 13, and 14. US4 has no protein entry in Swiss-Prot for HCMVM (Figure S2) [188].

UL84<sub>122-136</sub>

```

sp|P16727|UL84_HCMVA      IRDPFQILLSTPLQLGEANDESQTAPATLQEEETAASHEPEKKKEKQEKK-EEDEDDRND 179
sp|F5HB40|UL84_HCMVM     IRDPFQILLSTPLQLGEANGESQTAPATSQEEETAASHEPEKKKEKKEEKKEEEDDDRND 180
*****_*****_*****_*****_*****_*****_*****_*****_*****

```

GO<sub>425-439</sub>

```

sp|P16750|GO_HCMVA      IDPLWDYLDSELLFLDEIRNFSLSRSPFYVNLTPPEHRRAVNLSTLNSLWWLQ 466
sp|F5HGP1|GO_HCMVM     IDPLWDYLDSELLFLDKIRNFSLQLPAYGNLTPPEHRRANLSTLNSLWWWSQ 472
*****_*****_*****_*****_*****_*****_*****_*****_*****

```

**Figure 20: Exemplary alignment of two source protein sequences from HCMV strain AD169 (HCMVA) and Merlin (HCMVM).** \*, identical residues; :, highly conserved; ., weakly conserved; The amino acids: A, V, F, P, M, I, L, W are red, D, E are blue, R, H, K are magenta, S, T, Y, H, C, N, G, Q are green, and all other residues are depicted in grey [209].

## 5 Discussion

Immunotherapy, like the adoptive transfer of autologous T cells, is a potent treatment for HCMV disease and is based on comprehensive knowledge on T-cell target antigens and epitopes. The role of CD4<sup>+</sup> T cells in establishing a durable antiviral immune response has been emphasized recently [122]. However, CD4<sup>+</sup> T-cell epitopes have been identified only for a few immunodominant antigens. Hence, we aimed to contribute novel, frequently recognized promiscuous CD4<sup>+</sup> T-cell epitopes from numerous HCMV antigens [188].

### 5.1 Identification of T-cell epitopes by the IFN $\gamma$ ELISpot assay

We screened 103 predicted epitopes and 26 published or previously tested epitopes for T-cell responses in PBMC cultures of healthy, HCMV-seropositive blood donors in IFN $\gamma$  ELISpot assays. In advance, the PBMCs were pre-stimulated with peptides and IL-2 [188].

Nastke et al. suggested to define epitopes that are recognized by a large cohort as dominant [214]. Here, we defined epitopes that activated memory T cells in PBMC cultures of 50% or more of the tested blood donors as dominant, and epitopes recognized by less than 50% as subdominant [188].

Our results showed that promiscuous T-cell epitope prediction is an efficient method to identify novel dominant and subdominant T-cell epitopes from a high number of antigens while screening a limited number of peptides. Of all tested epitopes, 71.2% were immunogenic, and 16.4% were dominant. Among the top-scored epitopes, only 24% were not recognized by T cells in ELISpot assays [188].

We also tested peptides from earlier experiments in our laboratory that have already elicited CD4<sup>+</sup> T-cell responses. We confirmed the results of several previously published epitopes from the immunodominant pp65 (Table 4). Among the epitopes that were not selected by our prediction approach, five were immunodominant, and 15 were subdominant. However, all the dominant epitopes, except TEG7<sub>37-51</sub> can be

found among the top two percent highest-predicted peptides [188]. pp65<sub>109-123</sub> was predicted to cover four HLA allotypes. A shifted version of VPAP<sub>253-267</sub> (VPAP<sub>249-263</sub>) was predicted to bind to five allotypes. It was tested in six PBMC cultures but was not recognized. A shifted version of pp65<sub>179-193</sub> (pp65<sub>182-196</sub>) was predicted to bind to four allotypes. pp65<sub>283-299</sub> is represented as a shifted version (pp65<sub>283-300</sub>) and covers three HLA allotypes. TEG7<sub>37-51</sub> or a similar version cannot be found among the top two percent.

In order to find more FREPs, the ELISpot screening could be extended to all epitope candidates that are predicted to bind to five HLA allotypes but are not top scored. Additionally, all epitope candidates that were predicted to bind to four or fewer HLA allotypes could be included. We expect numerous FREPS among these peptides since many of the tested dominant epitopes that were not predicted to cover five or six HLA allotypes were among the 2% highest-scored epitope candidates covering four or fewer HLA allotypes [188].

However, our selection criteria for this project are convenient to identify frequently recognized promiscuous epitopes from numerous different antigens by screening a limited number of peptides for immunogenicity.

In total, we contributed 80 novel T-cell epitopes identified in ELISpot assays (72 predicted, eight not predicted) that have not been published before.

## **5.2 Identified T-cell epitopes originate from a broad antigen spectrum**

CD4<sup>+</sup> T-cell epitopes have been identified only for a few immunodominant antigens, so far. However, several studies revealed that the HCMV-specific CD8<sup>+</sup> and CD4<sup>+</sup> T-cell compartment is comprised of clonotypes directed against a broad spectrum of different antigens [110, 123, 179]. Numerous CD8<sup>+</sup> T-cell epitopes derived from various source proteins have been identified ever since [110, 210, 214, 217].

The repertoire of CD4<sup>+</sup> epitopes is still restricted to a small number of proteins. Numerous epitopes have been identified from pp65 [180] and IE1 [181]. gB [183], gH [184], and IE-2 [185] have been investigated as targets for CD4<sup>+</sup> T cells, and several epitopes have been found. Few T-cell epitopes have been published for DNBI [182], MCP [186], pp50 [187], and pp150 [187].

In this project, we identified 74 epitopes from 58 different proteins. Thus, we confirmed the findings of several previous studies that T cells against HCMV target various antigens [110, 123]. These proteins represent each temporal stage of viral gene expression, suggesting that T cells are primed at each moment of the viral life cycle. The PBMCs we used in our experiments are from healthy HCMV-seropositive blood donors. Hence, we assume that they carry the virus in a status of latency with reduced transcription of protein-coding genes. However, recent studies revealed that lytic gene expression can be detected in latently infected myeloid cells, as well [57, 58]. The observation that T cells specific for a broad range of lytic proteins are present in healthy, latently infected individuals indicates that lytic gene expression takes place to a certain extent. This is supported by Shnayder et al., who stated that the changes in viral gene expression from lytic to latent infection are rather quantitative than qualitative [58, 59].

Weekes et al. defined five subsequent temporal classes of protein expression (Tp1-5) [44]. Most of our identified source proteins cluster in Tp5 (34%), followed by Tp3 (14%) and Tp2 (10%). In Tp1 gather only 7% of the source proteins, while in Tp4, there are 2%. Tp5 includes all capsid proteins and half of all tegument proteins [44]. Lübke et al. analyzed the clustering of naturally presented CD8<sup>+</sup> T-cell epitopes of HCMV [217]. They showed a similar distribution of the source proteins to the different temporal classes. However, compared to Weekes et al. and Lübke et al., we found fewer proteins in Tp3. For 33% of our identified source proteins, no temporal class could be assigned.

Further, the identified source proteins are part of different viral structures, like the tegument (e.g. pp150, CEP3, US24) [8], the capsid (e.g. MCP [8], CVC2 [218]), or



the envelope (e.g. GO) [8] and carry out various functions ,e.g., DNA encapsidation (CVC2 [218], PORTL [6]), DNA replication (HEPA [219], DNBI [220]), virion egress (pp150) [221] and immune evasion (IE1) [222].

Sylwester et al. demonstrated that CD4<sup>+</sup> T cells recognize antigens from 125 different open reading frames (ORFs). Immune evasion proteins, tegument- and glycoproteins were primary targets of these CD4<sup>+</sup> T cells. The most immunogenic ones were gB, pp65, MCP, CEP3, pp150, and UL153 [123]. We identified one subdominant epitope of pp65, two dominant and one subdominant epitope of MCP, two subdominant epitopes of CEP3, and one subdominant epitope of pp150. We could not detect any reactive T cells upon stimulation with gB-derived peptides. UL153 is not included in the referenced protein database (SwissProt) of the HCMV strain AD169, and was, therefore, not part of the prediction.

Other important target antigens detected in this project were the source proteins of the dominant epitopes: US24, UL36, UL24, TRM3, CVC2, US4, UL84, GO, HHLF1/IRS1, CVC2, PORTL, DPOL, HEPA, and US8. Several proteins were the source of two epitopes. HEPA was represented with four epitopes and DNBI with three epitopes.

In conclusion, we found novel frequently targeted antigens and verified antigens that were identified with a different method by Sylwester et al. [123] as well.

It has been repeatedly shown that a T-cell response targeting a broad spectrum of antigens can clear viral infections more effectively [223]. Lilleri et al. showed that SOT patients who cleared an HCMV infection had T cells against multiple viral antigens and not only against pp65 and IE1 [224]. Besides, the possibility of emerging resistance can be reduced when more than one or two antigens are targeted.

### 5.3 Validation of T-cell epitopes by ICS

We analyzed the CD4<sup>+</sup> T-cell activation for each of the dominant epitopes in flow cytometry by ICS of IFN $\gamma$  and TNF. We also stained CD4 and CD8 to differentiate between reactive T-cell subsets.

We could confirm that every dominant epitope triggers cytokine release in at least one tested PBMC culture. Further, most of the activated T cells are multifunctional, secreting IFN $\gamma$  and TNF. As outlined by Seder et al., these multifunctional CD4<sup>+</sup> T cells contribute to better virus control, which could be shown for HIV [188, 225].

The ELISpot assay is highly sensitive and allows testing of numerous epitopes in a cost- and time-efficient manner. Hence, it is ideal for screening large numbers of peptides for T-cell activating epitopes. However, we only validated the dominant epitopes and several subdominant ones in ICS, so we confirmed CD4<sup>+</sup> T-cell activation only in a small number of PBMC cultures. CD8<sup>+</sup> T-cell responses among the positive test results in ELISpot can, therefore, not be excluded. Since in the PBMC cultures that were tested in ICS, cytokine-secreting CD8<sup>+</sup> T-cell populations were rarely found, the vast majority of the activated cells are likely CD4<sup>+</sup> [188].

In a therapeutic setting, parallel activation of both CD8<sup>+</sup> and CD4<sup>+</sup> T cells is beneficial, aiming for a stable immune reconstitution against viral infections [116, 165]. Concealed CD8<sup>+</sup> T-cell responses would augment the desired effects of our therapeutic peptides [188].

We detected activation of CD8<sup>+</sup> T cells with two peptides: pp65<sub>109-123</sub>, UL24<sub>201-215</sub>. Different substrings of pp65<sub>109-123</sub>, i.e., shorter aa sequences, have been published as CD8<sup>+</sup> T-cell epitopes before [226]. In the ELISpot assay, the HLA class II molecules are loaded exogenously with the peptides. Hence, it is likely that the 15-aa-long peptides that we added to the PBMCs broke during solution or were cleaved by peptidases during incubation with the cells. The resulting shorter peptides could have bound to HLA class I molecules and been recognized by CD8<sup>+</sup> T cells. Alternatively, 15-mers could have bound directly to an HLA class I molecule since it

is known that binding of longer peptides can occur and they are recognized by CD8<sup>+</sup> T cells [73, 74].

Due to the high recognition rates, we can assume that we identified promiscuous T-cell epitopes that bind to several different HLA allotypes [188]. However, HLA specificity was not verified in this project. Peptide binding assays, e.g., with recombinant HLA class II molecules, can reveal HLA specificity of the epitopes [227]. These assays could be conducted in subsequent experiments to reveal the degree of promiscuity of the identified epitopes.

In our experiments, we analyzed the IFN $\gamma$  and TNF response. IFN $\gamma$  is the most prevalent cytokine produced by HCMV-specific CD4<sup>+</sup> T cells, predominantly by Th1 cells [228]. However, cytotoxic CD4<sup>+</sup> T cells play an essential role in the immune response against HCMV, as well. Analysis of CD107a, macrophage inflammatory protein 1 $\beta$ , and granzyme A and B expression could give further insights into the polyfunctionality and the cytotoxic potential of CD4<sup>+</sup> T effector cells [228]. Acquiring polyfunctional CD4<sup>+</sup> T cells for adoptive T-cell transfer is crucial to improve the efficacy of the therapy [229].

#### **5.4 Prediction of promiscuous CD4<sup>+</sup> T-cell epitopes from HCMV antigens**

We used reverse immunology to predict CD4<sup>+</sup> T-cell epitopes that bind promiscuously to multiple HLA allotypes covering the majority of the German population [190]. We selected 169 epitope candidates with our promiscuous epitope prediction. Throughout the project, we noticed that top-scored (maximum prediction score for one HLA allotype) epitope candidates trigger IFN $\gamma$  release in PBMC cultures of more blood donors than not top-scored peptides. That means they are more frequently recognized in ELISpot assays. The large protein-coding capacity of HCMV affords assessment of an exceptionally high number of epitopes compared to other viruses. Hence, the high number of peptides to be synthesized in-house exceeded our capacities. Therefore, we narrowed testing to top scorers since our

primary goal was to identify FREPs from as many different antigens as possible. In addition, we included all epitope candidates predicted to bind to six different HLA allotypes because we assumed higher recognition chances among these peptides. In total, 103 peptides were synthesized and tested in ELISpot assays [188]. The better recognition of top-scored epitope candidates compared to not top-scored peptides was confirmed by analyzing the final dataset. The epitope candidates predicted for six HLA allotypes did not show better recognition rates than the ones predicted for five (data not shown). Most of the top-scored epitopes were predicted for HLA-DRB1\*04. The prediction matrices for this allotype assign a maximum absolute score of 28. Peptides predicted for other allotypes, like HLA-DRB1\*03, can be assigned scores up to 40. In consequence, more peptides predicted for HLA-DRB1\*04 reach a maximum score and are selected for testing by our method. Hence, our epitope selection is biased. However, this selection method increases the recognition rate of the promiscuous epitope candidates, even though HLA-DRB1\*04 is the least frequent allele in a representative German population.

We conducted a whole-proteome prediction and compared the results with the prediction results on a single-protein level. Predicting the whole proteome sequence at once instead of each protein separately is more time-efficient. In a single-protein prediction, we potentially miss epitope candidates with high scores, especially in short proteins, because we only select few peptides (top 2%). A whole-proteome prediction bears the advantage that epitope candidates of all proteins are ranked together independently of the source proteins (see 3.1).

However, 62.5% of all immunogenic peptides, which were predicted in the single-protein prediction, did not appear in the whole-proteome prediction. Five of 17 dominant predicted epitopes dropped out in the whole-proteome prediction. Despite the intersection of over 40% of both predictions, we would have missed immunogenic and dominant epitopes by analyzing just the whole proteome. Therefore, our single-protein approach remains indispensable for this project. Still, the fourteen additional antigens and their epitopes, which were exclusively predicted

with the whole-proteome approach, could include important T-cell targets and dominant epitopes.

There are three main strategies for the identification of T-cell epitopes: First, the application of pools of overlapping peptides spanning whole protein sequences [123]. Second, the direct isolation of naturally presented HLA ligands [217, 230]. Third, the *in silico* prediction of epitope candidates, as it was employed in this project [188].

We aimed to identify promiscuous T-cell epitopes that bind at different positions of the peptide chain to different HLA molecules, presumably. Therefore, the aa sequences of the epitopes must contain multiple binding cores. To avoid missing these precise sequences, only minimal overlap of synthesized peptides for the pools could be accepted. Hence, we would have had to synthesize an immense number of peptides, which was not feasible.

The direct isolation of naturally presented HLA ligands is valuable because it reveals the ligands associated with the HLA molecules *in vivo*. Hence, immunogenicity screening includes relevant, naturally presented HLA ligands only. However, it is hampered by the down-regulation of HLA molecules from the surface of infected cells by HCMV [104, 105, 117]. Lübke et al. successfully circumvented this encounter using viral deletion models, which lack immune-evasive genes [217]. Nevertheless, these cell lines do not express HLA class II molecules, and to our knowledge, there has not been an alternative approach for the direct isolation of HLA class II ligands [188]. Therefore, reverse immunology is still crucial for the identification of CD4<sup>+</sup> T-cell epitopes. IFN $\gamma$  can induce HLA-class II expression in fibroblasts, which could enable the direct isolation of HLA-class II ligands in the future. Nonetheless, direct isolation and prediction should be used complementary to achieve optimal results [231].

The *in silico* prediction of CD4<sup>+</sup> T-cell epitopes is less accurate compared to the CD8<sup>+</sup> T-cell epitope prediction. Anchors and interaction sites of HLA class II

molecules allow greater variability among the epitopes compared to HLA class I [70, 91]. Further, these epitopes bind to several different HLA class II allotypes promiscuously [83]. Consequently, more epitope candidates must be tested for immunogenicity to find the actual epitopes that are recognized by T cells.

### **5.5 Generation of peptide pools containing validated CD4<sup>+</sup> T-cell epitopes**

pp65 is the major immunodominant antigen of HCMV. It has been in the spotlight of the research on T-cell responses against this virus. The adoptive T-cell transfer has been conducted using mainly pp65-derived epitopes or pp65 antigen lysate, so far [116, 165, 176].

Here, we pooled newly identified epitopes with previously published epitopes from many different antigens to activate T cells in PBMC cultures from any donor. Our peptide pool I activated all tested PBMC cultures in ELISpot, except two: one had not been tested before in single-peptide ELISpots, and the other one had been tested against 18 other single peptides and had negative results only [188].

We showed that the high recognition rates do not depend on pp65, since we activated 30 out of 30 PBMC cultures with peptide pool II that contained all peptides of pool I, except for the pp65-derived peptides [188]. However, the spot counts tend to be higher after stimulation with peptide pool I in most PBMC cultures that we tested against both pools. The higher spot counts could be explained by an additive effect of multiple epitopes being recognized in parallel by one PBMC culture. Since pool I includes three more epitopes, it should induce higher spot counts than pool II. It must be considered, though, that there can be a certain variability in the spot counts due to the experimental conditions since the PBMC cultures were stimulated with peptide pool I and II in different assays.

Our peptide pool is an effective activator of HCMV-specific CD4<sup>+</sup> T cells independent of the individual HLA haplotype. There are several options for a clinical translation of these results: Adoptive T-cell therapy is a promising treatment for patients

suffering under chemo refractory HCMV-disease after SOT or HSCT [116, 163-165, 174-176]. CD4<sup>+</sup> T-cell epitopes derived from multiple HCMV antigens or peptide pools can be used for the T-cell stimulation and isolation.

Further, the status of the CD4<sup>+</sup> T-cell-dependent immunity can be evaluated using these epitopes as a diagnostic tool. Assessing the frequency of epitope-specific T cells could help to personalize antiviral chemotherapy for patients after SOT [177, 188].

T-cell epitopes against HCMV are not equally significant for the T-cell response. Here, we used the term immunodominance to describe that PBMCs of many donors recognize the same epitope. Another definition of immunodominance refers to the concept that an individual has a small number of T-cell clonotypes directed against one antigen [232]. Hence, a few dominant epitopes trigger strong reactions in memory T cells, while subdominant epitopes play a subordinate role. However, the domination of single T-cell clonotypes seems to be more explicit with CD8<sup>+</sup> T cells than with CD4<sup>+</sup> T cells. Nastke et al. suggested a codominance of several HLA class II-restricted epitopes [214]. Hence, by stimulation with a peptide pool, responses of one donor-derived PBMC culture to different peptides can add up. This codominance possibly explains the tendency of higher spot counts after stimulation with the pool I.

Another phenomenon called immunodomination has been described for CD8<sup>+</sup> T cells. It says that different T-cell subsets compete in response to an antigen. Reasons for immunodomination can lie in functional differences of T-cell subsets or higher affinity of one T-cell clonotype to the HLA-peptide complex [233-235]. Immunodomination has been barely analyzed for CD4<sup>+</sup> T cells, so far. In our experiments, we could not detect immunodomination. We observed distinct responses to dominant epitopes even if we conducted the pre-stimulation with peptide pools of multiple potent epitopes. Besides, we tested PBMC samples of nine donors against single peptides and against the peptide pool I that included these peptides, too, to discover competition effects. Each PBMC culture with an IFN $\gamma$  response against single peptides responded strongly to the pool, as well. However,

stimulation with pool II triggered higher T-cell activation than pool I in some PBMC cultures. Since pool II contains fewer peptides, the spot counts should be lower. The higher spot counts with pool II could be due to immunodomination. However, the comparability is limited because the pools were tested in different assays.

### **5.6 Epitopes and peptide pools tested in *ex vivo* ELISpot assays**

We tested 14 dominant epitopes in *ex vivo* ELISpot assays to measure the T-cell responses without a 12-day *in vitro* pre-stimulation. Only four epitopes elicited IFN $\gamma$  responses in the tested PBMC cultures, which clearly shows that antigen-specific T cells undergo extensive amplification after pre-stimulation. Previous studies compared the results of *ex vivo* ELISpot assays and assays after *in vitro* pre-stimulation and developed harmonized protocols for cultured ELISpot assays [195, 236].

The peptide pools were tested in *ex vivo* ELISpot assays, as well. Peptide pool I (with pp65) elicited *ex vivo* responses in 36.7% and pool II (without pp65) in 11.1% of the tested PBMC cultures. Hence, pp65-derived epitopes enhance *ex vivo* recognition. These results are in line with previous studies that demonstrated the high frequency of pp65-specific T cells in the peripheral blood of HCMV-seropositive donors [111, 178].

*Ex vivo* assays show the number of effector T cells or T<sub>EM</sub> cells. The cultured ELISpot enables the assessment of T<sub>CM</sub> cells that perpetuate a more durable immune response [237]. Godkin et al. showed that memory T cells against Hepatitis C Virus detected in *ex vivo* assays gradually declined after infection. CD4<sup>+</sup> T cells that were detected after *in vitro* stimulation, however, formed durable populations [238]. T<sub>CM</sub> cells express CCR7 and CD45R0, while T<sub>EM</sub> cells are CCR7<sup>-</sup> and CD45R0<sup>+</sup> [126]. Staining of these surface molecules could give insight into the functional profile of the amplified T-cell populations in this project.



From a therapeutic point of view, it is reasonable to activate T<sub>CM</sub> cells that build a sustained response. Hence, T-cell populations detected after pre-stimulation should be effective when transferred to the recipient. However, it is crucial to establish short protocols for the generation of HCMV-specific T cells for adoptive transfer in a clinical setting. In a protocol by Rauser et al., HCMV-specific T cells are expanded for 7-11 days and are shown to lyse HCMV-infected fibroblasts efficiently [47].

Feuchtinger et al. showed that even low amounts of antigen-specific T cells could be sufficient for reestablishing antiviral immunity. Further, circumventing *ex vivo* expansion can sustain the differentiation potential and antiviral efficacy *in vivo* [165]. Stemberger and coworkers could show that low-dose adoptive T-cell transfer leads to a strong pathogen-specific T-cell response. T-cell populations derived from a single cell were protective against a bacterium in a murine model [239]. Further investigations on how the variation of the pre-stimulatory protocol affects the quantity and function of the epitope-specific T cells could help to optimize the cell preparation before transfer.

### **5.7 Dominant epitopes tested in PBMC cultures of HCMV-seronegative blood donors**

We tested PBMC samples of eight HCMV-seronegative blood donors against the dominant epitopes. Seven of them responded with IFN $\gamma$  release upon stimulation with the epitopes.

Several studies have previously questioned the serostatus as an indicator of HCMV naivety. Litjens et al. showed that 39% of HCMV-seronegative patients had memory T cells and were at lower risk for viremia after kidney transplantation [240]. Terlutter et al. investigated the T-cell response to an HCMV peptide pool in PBMC cultures of 82 donors, 82% of which showing memory T-cell activation [241]. Our results are in line with these findings suggesting an assessment of cellular immunity as an indicator for latent HCMV infection in the transplantation setting.

Furthermore, the HCMV-serostatus of many blood donors was assessed years ago by the Institute for Clinical and Experimental Transfusion Medicine. In the meantime, these donors could have encountered HCMV.

### **5.8 Alignment of the source protein sequences of dominant epitopes with correspondent protein sequences of the HCMV strain Merlin**

When propagated in cells, e.g., fibroblasts, HCMV mutates and undergoes substantial genome alterations [242]. We investigated the standard laboratory strain AD169, which lacks several genes at the end of its unique long region [243], and differs in various ways from a wild-type prototype virus [188, 244].

Low-passage HCMV strain Merlin is a wild-type prototype [245]. Hence, we aligned the aa sequences of the source proteins from our identified dominant epitopes of strain AD169 with the correspondent proteins of strain Merlin. Besides GO<sub>425-439</sub> and US<sub>462-67</sub>, all epitopes can be found in proteins of both strains. The alterations of GO<sub>425-439</sub> do not affect the anchor positions for HLA-class II epitopes (1, 4, 6, 9) [70, 84], which possibly explains that it is still frequently recognized in ELISpot (rr = 62.5%). The gene product of ORF US4 from HCMV AD169 is not listed for HCMV Merlin in Swiss-Prot [188].

Dolan et al. demonstrated that there are conserved proteins between strain Merlin and strain AD169, as well as several proteins with high divergence in the aa sequence. These different proteins represent predominantly membrane-associated and secreted proteins that play a role in cell tropism and pathogenicity [245].

Analysis of the proteome of virions and dense bodies of different HCMV strains indicated mainly strain-independent morphogenesis. Hence, proteins involved in tegument assembly seem to be rather conserved [246].

However, all the mentioned strains are cultured in fibroblasts. Hence, they comprise a proteome that probably differs from virus propagated in other cell types like

endothelial or epithelial cells. Viral strains from different cell types have to be analyzed in the future to detect target antigens that, for instance, mediate viral entry into these cells [246].

In summary, the identified epitopes seem to be conserved between different strains of HCMV, which can enable immunotherapy in a strain-independent manner. Nonetheless, we analyzed T-cell epitopes from a laboratory strain cultured in fibroblasts, which lacks some genes that could be relevant T-cell targets *in vivo*.

## 5.9 Conclusion and outlook

This work confirmed that the CD4<sup>+</sup> T-cell response against HCMV targets a broad spectrum of antigens. We successfully applied an *in silico* prediction method to identify a set of novel dominant and subdominant CD4<sup>+</sup> T-cell epitopes. We showed that a peptide pool, including dominant epitopes, induced strong T-cell responses in PBMC cultures of almost every donor with different HLA polymorphisms.

Further, we could demonstrate that the CD4<sup>+</sup> T-cell immune response against pp65 is dispensable in a peptide pool with other dominant epitopes from different antigens. Hence, it is beneficial to focus on alternative target antigens that are perhaps equally important for viral clearance. We validated that the T cells responding to dominant epitopes express CD4 and are multifunctional, secreting IFN $\gamma$  and TNF. The promiscuous epitope prediction is a powerful instrument to identify FREPs from a large number of different antigens. However, complementary approaches are necessary to investigate the complete T-cell response against HCMV.

Further research on the HLA class II restriction of the identified epitopes would reveal the degree of promiscuity of the epitopes. An extended characterization of the cytokine profile of the activated CD4<sup>+</sup> T cells could give insight into the functional spectrum of the cells. Also, the variation in the pre-stimulatory protocols can help to find optimal conditions for the therapeutic application of the epitopes.

The set of novel dominant epitopes and our peptide pool can be directly translated into the clinic. It can be used to stimulate and isolate HCMV-specific CD4<sup>+</sup> T cells or determine the status of the CD4<sup>+</sup> T cell-mediated immune response against HCMV.

Also, our method can be transferred to other viruses, bacteria, or cancers and can help to map the CD4<sup>+</sup> T-cell response against these pathogens or cancer cells.

## 6 Summary

Sixty percent of our population encountered Human Cytomegalovirus (HCMV), followed by a life-long persistence of the virus in the host. Immunotherapies, like the adoptive transfer of HCMV-specific T cells, have been shown to cure HCMV disease in patients susceptible to viral infection or reactivation due to immunosuppression. The adoptive T-cell transfer depends on comprehensive knowledge about target antigens and T-cell epitopes presented on HLA molecules. HCMV-specific CD4<sup>+</sup> T cells efficiently control viral infection. However, CD4<sup>+</sup> T-cell epitopes have only been identified for a few immunodominant antigens of HCMV so far.

In this project, we screened the entire proteome of HCMV for frequently recognized promiscuous CD4<sup>+</sup> T-cell epitopes using *in silico* epitope prediction. We tested 103 predicted epitope candidates for immunogenicity in PBMCs of HCMV-seropositive donors in ELISpot assays after a 12-day stimulation with peptide and IL-2. This way, we identified 74 T-cell epitopes from 58 different source proteins. The spectrum of source proteins covers all temporal stages of gene expression and comprises various functional profiles. Seventeen of the 74 epitopes were immunodominant (recognized by > 50% of the tested PBMC samples) and have not been published before. We validated the dominant T-cell epitopes by intracellular cytokine staining, i.e., we confirmed IFN $\gamma$  and TNF release of CD4<sup>+</sup> T cells after stimulation with the epitopes. Subsequently, we generated a peptide pool containing 14 dominant epitopes, including three previously published epitopes. The peptide pool triggered T-cell activation in 46 of 48 randomly selected PBMC samples. Another peptide pool, lacking the pp65-derived peptides, achieved an analogous recognition rate of 30 out of 30. Our pool of promiscuous dominant epitopes stimulates HCMV-specific T cells of blood donors with different HLA polymorphisms, circumventing the elaborate design of individualized therapy. The novel T-cell epitopes can be directly translated into the clinic to improve T-cell therapy.

## 7 Zusammenfassung

Sechzig Prozent der Bevölkerung sind mit dem Humanen Zytomegalievirus (HCMV) infiziert, welches nach der Primärinfektion lebenslang im Wirtsorganismus persistiert. Immuntherapien, wie der adoptive T-Zell-Transfer, heilen nachweislich HCMV-assoziierte Erkrankungen, die vor allem bei immunsupprimierten Patienten auftreten. Der adoptive T-Zell-Transfer basiert auf genauen Kenntnissen über T-Zell-Zielantigene und -Epitope. CD4<sup>+</sup> T-Zell-Epitope sind jedoch bisher nur für einige wenige immundominante Antigene des HCMV identifiziert worden.

In diesem Projekt durchsuchten wir das Proteom des HCMV nach häufig erkannten promiskuitiven CD4<sup>+</sup>-T-Zell-Epitopen mithilfe der *in silico* Epitop-Vorhersage. Wir testeten 103 vorhergesagte Epitop-Kandidaten auf ihre Immunogenität an PBMCs von HCMV-seropositiven Spendern in ELISpot Tests nach einer 12-Tages-Stimulation mit Peptid und Interleukin-2. Dadurch identifizierten wir 74 T-Zell-Epitope aus 58 verschiedenen Ursprungproteinen, welche aus allen zeitlichen Stadien der viralen Genexpression stammen und verschiedene Funktionen erfüllen. Siebzehn der 74 Epitope wurden als immundominant klassifiziert (von > 50% der getesteten PBMC-Proben erkannt) und wurden bisher noch nicht publiziert. Wir validierten die IFN $\gamma$ - und TNF-Freisetzung von CD4<sup>+</sup> T-Zellen nach der Stimulation mit den dominanten Epitopen durch eine intrazelluläre Zytokinfärbung. Anschließend generierten wir einen Peptidpool aus 11 vorhergesagten und drei bereits publizierten dominanten Epitopen. Dieser Peptidpool löste in 46 aus 48 zufällig ausgewählten PBMC-Proben eine T-Zell-Aktivierung aus. Ein zweiter Peptidpool, ohne die von pp65 abgeleiteten Epitope, erreichte eine analoge Erkennungsrate von 30 aus 30. Unser Pool aus promiskuitiven dominanten Epitopen stimuliert HCMV-spezifische T-Zellen von Blutspendern mit unterschiedlichen HLA-Polymorphismen und umgeht so das aufwendige Erstellen einer individualisierten Therapie. Die hier identifizierten T-Zell-Epitope können direkt in die klinische Anwendung übertragen werden, um T-Zell-Therapien zu verbessern.

## 8 Appendix

```
In [1]: import numpy as np
import pandas

In [2]: xl = pandas.ExcelFile('results whole proteome ad169_Edit5.2.xlsx')
df = xl.parse("Tabelle1", header=None, names=['A', 'B', 'C', 'D', 'E', 'F', 'G', 'H', 'I', 'J', 'K', 'L', 'M', 'N', 'O', 'P', 'Q', 'R', 'S', 'T', 'U', 'V', 'W', 'X', 'Y', 'Z'],
Sequenzen=df.E
Liste=Sequenzen.astype(str)
print(Liste)

0          Ligand
1  RCRWYLLGAVGSYRA
2  QVCFEILPCTELITF

In [3]: seq_parts={}
for str15 in Liste:
    for i in np.arange(7):
        str9=str15[i:i+9]
        if not seq_parts.get(str9):
            seq_parts.update({str9:1})
        else:
            seq_parts[str9]+=1

In [4]: for item in seq_parts.items():
        if item[1] >= 5:
            print(item)
print('kein Epitop')

('IILIGTLVP', 6)
('IILIGTLVPT', 6)
```

**Figure S1: Algorithm for the detection of identical core sequences among predicted peptides.** The algorithm shown here was coded in python 3. It was used in this project to detect identical nine aa-long core sequences among the two percent highest scored peptides for the six HLA allotypes of interest. The algorithm lists all core sequences that appear more than five times. The promiscuity of the epitope candidates containing the listed cores was assessed manually.

**Table S1: Predicted promiscuous epitope candidates from the single-protein prediction.** All epitope candidates that were predicted binders to five or six HLA allotypes are listed here. The peptide sequences that were identically predicted in the whole-proteome prediction are highlighted in green. Peptide sequences that occurred in the whole-proteome prediction as a shifted version (max. 3 aa to the N- or C-terminus) are highlighted in blue. Abbreviations: pos, position in the protein sequence;  $n_{HLA}$ , number of covered HLA-DR allotypes (six are highlighted in yellow);  $n_{ts}$ , number of top-scored epitope candidates (one and two are highlighted in yellow); no., laboratory batch number;  $HLA_{nc}$ , not covered HLA allotypes; ns, not synthesized; sf, synthesis failed. Adapted from [188].

Protein	Pos	Sequence	$n_{HLA}$	$n_{ts}$	no.	$HLA_{nc}$
EP84	347	ALLLPIERGAVVSSP	6	0	184428	-
EP84	298	MSLPLDTSEAVAFLN	5	0	184429	11
EP84	471	LCDLPLVSSRLLPET	5	0	184430	11
VPAP	249	DTLLYVASRNGLFAV	5	0	154219	1
US9	196	YVVLVQFVKHVALFS	5	1	184431	7
GH	8	YLTVFTVYLLSHLPS	5	1	184432	3
LTP	658	VLRLFYDLRDLKLCD	5	0	184433	11
LTP	830	NAVLSMFHTLVMRLA	5	1	184434	3
HHLF1	214	FRVFVYDLANNTLIL	5	1	184468	1
HHLF1	306	MVLLGAWQELAQYEP	5	0	184469	7
UL7	23	YNKLLILALFTPVIL	5	1	184470	11
UL8	23	YNKLLILALFTPVIL	5	1	duplicate, see 184470	11
PRIM	198	MGEFARLLLGSFRQ	5	0	sf	7
PRIM	254	VHYVYLAYRTALARA	5	0	sf	7
PRIM	378	ESVFSPLERSLSGLL	6	1	sf	-
PRIM	893	VQVFIDLRTEHSYAL	6	1	sf	-
US8	191	MVLLLGIVLARTVYR	5	0	184475	11
IE1	313	CCYVLEETSVMLAKR	5	1	184476	11
IE2	501	VDLLGALNLCPLMQ	5	0	184477	11
UL97	82	VTTLTTLSSVSTTTV	5	0	184478	3
UL97	559	VLGFCLMRLLDRRGL	5	0	184479	7
TRM3	222	IPIISFLLKHMIGI	5	0	194315	3
TRM3	319	FNTILGFLAQNTTKI	5	0	184481	3
UL119	252	LREFVYFLNGTYTVV	5	0	sf	11
AN	238	LGLLIDPTSGLLGAS	5	1	184483	11
UL29/28	430	MLGDTQYFGVVRDHK	5	1	184484	1
DPOL	67	LMFYREIKHLLSHDM	5	1	184485	3
DPOL	988	CEFVKGVTRDVLSLL	5	0	184486	
DPOL	1056	LVLSSVLSKDISLYR	5	0	184487	3
UL11	133	CYYVYVTQNGTLPTT	6	2	184488	-
UL117	330	VATFKFFHQDPNRVL	5	1	184514	11



GO	425	LLFLDEIRNFSLRSP	5	1	184515	1
UL84	122	RDPFQILLSTPLQLG	5	1	184516, 194122	11
UL84	474	WLELTVLVSDENGAT	5	0	sf	
DNBI	689	RSVfyVIQNVALITA	6	1	184518	-
DNBI	844	LQFWQKVC SNALPKN	5	1	184519	3
DNBI	871	VKFLVAVTADYQEHD	5	0	184520	4
DNBI	1115	ASLMDKFAALQE QGV	5	0	184521	4
CVC2	400	RDDVLSLWSRRLVVG	5	0	184522	11
CVC2	595	EHGLGRLLSVTLPRH	5	0	184523	3
HEPA	23	LSWYGLLEASVPIVQ	5	0	sf	3
HEPA	150	LSLFHVAKLVVIGSY	5	0	194001	3
HEPA	264	WTHLYDVLFRGFAGQ	5	1	194002	3
HEPA	438	VLIVDLVERVLAKCV	5	0	194003	
HEPA	488	FWQIQSLLGYISEHV	5	0	194004	3
HEPA	706	YREILFRFVARRNDV	5	0	194005	3
UL20	190	FMDYVILTPLAVLTC	5	0	194006	11
HHLF1	170	AWIVLVATVVHEVDP	5	0	ns	3
UL52	240	LIIMSEFTHLLQQHF	5	0	194008	11
RIR1	341	IYRFHLDARFEGEVL	5	0	194009	1
RIR1	382	VPQYDFLISADPF SR	5	0	194010	3
RIR1	400	WAAMCKWMSTLSCGV	5	1	194386	3
RIR1	454	FVDMWDVAAIRVIN F	5	0	ns	3
RIR1	658	WWVESALEKLRPLHI	5	0	ns	3
RIR1	689	FASWDLIERIFEHMY	5	0	ns	1
NEC2	103	FNVLKVNESLIVTLK	6	0	194064	-
HELI	167	IYRVFGFVSKHVPLA	5	0	ns	3
HELI	877	RTAMTIAKSQGLSLE	5	0	ns	11
DUT	311	RFTYLPVGSHP LQGM	5	1	194068	3
NEC1	175	FQIYYLLHAANHDIV	5	0	ns	3
TRX1	141	GITSL LTCVMRGYLY	5	0	ns	15
UL8	86	STPYVGLSLSCAANQ	5	1	194069	3
UL8	231	SSDWVTLGTSASLLR	6	2	194062	-
MCP	515	DFVVTDfyKVG NITL	5	1	195033	11
MCP	570	FHELRTWEIMEHMRL	5	1	194120	3
MCP	621	VDAFL LIRTFV ARCI	5	1	194080	3
MCP	1321	ALPILSTTTLALMET	5	0	ns	11
PORTL	246	VRVFKKVRSERLEAQ	5	1	194081	3
UL15A	85	MFLVFGLC SWLAMRY	6	0	194066	-
PP85	352	TEVYQTLRDYNVLFY	5	0	ns	11
CVC1	123	RMFYAVFTTLGLRCP	5	1	194121	3
UL95	284	HVEAVLRQVYTPG LL	5	0	ns	15
UL132	83	AILFYIVTGTSIFSF	5	0	ns	3
UL9	7	LLWWITILLRIQQFY	5	1	194221	1
UL9	105	YSGIYYFDSLTYGW	5	1	194222	3

UL9	111	FDSLYTYGWVLRTP	5	1	194317	3
US29	363	LRHATSLVTVPTLL	5	0	ns	11
UL34	219	NSFLHLLMNSGLDIA	6	0	194065	-
UL34	248	LFQIGHTDSVSAALE	5	0	ns	3
US22	292	LVLLDKFGVVYLH	5	0	ns	7
US22	360	LRWHGALGTITRSQL	5	0	ns	1
US17	113	LTIVSVLTTLSVIVA	5	1	194224	3
US15	191	FKIVLSFSVLITCLA	5	2	194067	3
UL27	227	FLEPEERELIGRCLP	5	0	ns	15
UL27	423	VQRLIRLFKGEAALL	5	0	ns	3
UL116	117	VSILTTVTPAATSTI	5	0	ns	3
TR14	99	LIGDSSLTGTCPV	5	0	ns	11
UL42	100	FLAVVFTVVINRDSA	5	1	194225	3
UL24	201	KRYFRPLLRASLGL	5	1	194226	3
US24	255	SRRWWAVRANLATP	5	1	194316	3
US19	192	TLMLIHDSLITCQS	5	0	ns	1
UL96	3	SVNKQLLKDVMRVDL	5	0	ns	7
UL88	406	LGYDRLVSADAGVSR	5	1	195118	3
UL36	42	ERCFIQLRSRSGALP	5	1	194318	7
UL36	253	QYVLVDTFGVVGYD	6	1	194387 *1	-
US31	103	FTWWKRLRHSTRRWL	5	0	ns	1
US34	39	FYGYLQLDLLGPVVA	5	0	ns	7
UL87	190	MACLPRDLSHLDDY	5	0	ns	1
UL87	458	VRRYVCIISRLMYAR	5	1	sf	11
UL87	760	AKQLVFLRACLK	5	0	ns	11
UL19	4	NALYELFRRRLPRAP	5	0	ns	7
UL14	138	YTCVLGNETHSLATE	5	0	ns	15
UL14	265	KIGLLAAGSVALTSL	5	0	ns	11
UL28	108	MLGDTQYFGVVRD	5	1	duplicate, see 184484	1
UL28	279	FVVIGWMEPVNKAVF	5	0	ns	4
UL49	197	RFLFGVDLRLPVLHP	5	1	194319	1
UL40	185	MYTVGILALGSFSSF	5	0	ns	7
UL40	196	FSSFYSQIARSLGVL	5	1	194304	3
UL31	202	CGYKYDWSNVVTPKA	5	1	194389 *2	3
US26	33	IRHLVRSYADMNISL	5	0	ns	7
UL78	272	IMDYVELATRTLLTM	5	1	194282	11
J1I	240	RLLFAVRAARRFYSP	5	0	ns	7
YHR1	50	VLRFFTVVRDVLPR	6	1	194283	-
UL107	27	QNSFFSFLSRKKS	5	2	194284	7
UL108	46	SSFFDVLLSSRSCFV	5	1	194285	15
US33	33	FDVVLTFFVPSGFVMG	6	0	194286	-
UL101	88	LGAYRTMSVFGSGWR	5	1	194287	3
UL110	91	IMMIIIIHSPTIFIL	6	0	194288	-
US4	62	PYFPMRFINVKSHVS	5	1	194289	3

US25	50	LRTDLAFGPVRRNSR	5	0	ns	7
UL39	40	HRSIFFILSVMIGKG	5	0	ns	3
US5	21	TGVVYRDISSTIATE	5	1	194290	15
US36	46	RTALNLFSLMSLCVP	5	1	195146	1
UL81	47	LPAPHAVDPASRERL	5	0	ns	7
UL81	73	LYFLNKNKTETLII	5	1	194320	1
UL90	23	VSADWFRFSGRSPVG	5	0	ns	11
UL60	4	VEKYWRMRTTHTVEF	5	0	ns	11
UL61	69	VRAEFFWGAAGEGSV	5	0	ns	3
UL61	138	TPLPELLTGPPAPNL	5	0	ns	7
UL61	384	GFIGFQMPRLGGRSG	6	0	194321	-
UL65	64	SIVLYEHLDARVTDD	5	0	ns	3
UL66	55	MMWVVLTVSFSYYR	5	0	ns	4
UL67	8	IYYIYSDDSVVNIS	5	0	ns	11
UL67	76	FVYLHSVESYSLQFH	5	1	194293	7
IR04	57	FIIFYLSSPFLNL	5	1	194294	11
IR04	63	FLSSPFLNLGLSFPS	5	0	ns	4
IR12	17	AYTIIFYILHRVTC	5	0	ns	3
IR12	92	TTVYSTFNNTSYANIS	5	1	194295	11
IR12	99	NTSYANISNTAATTE	5	0	ns	3
IR02	15	IASFAATLLHRYPIN	5	0	ns	1
IR09	103	YRQGGFLEKQHVVG	5	0	ns	15
IR14	93	RWPVDRFLRVPLQRA	5	0	ns	7
IR07	48	IFTQSFLRFRNQVQV	5	0	ns	1
IR13	5	FTVMWTLISALSES	5	1	194296	15
YHL4	111	WLLVLNLNVALPVTA	6	1	194297	-
PP65	347	ALFFFDIDLLLQRGP	6	0	194305	-
PP71	204	AIPLTLVDALEQLAC	5	0	ns	1
PP71	488	WHVFASLDDLVPPLTV	5	0	ns	3
PP150	459	GGVSSIFSGLLSSGS	5	1	194306	3
IRS1	214	FRVYVYDLANNTLIL	5	1	duplicate, see 184468	1
US6	152	LCCGITLLVVILALL	5	0	ns	1
ICP27	512	YRFMIAYCPFDEQSL	5	0	ns	3
SCAF	376	KDAFFSLLGASRSVAV	5	0	ns	3
UL35	181	YPRLTYYNLLFHPPP	5	1	194307	3
US6	155	GITLLVVILALLCSI	5	0	sf	7
US6	134	WNAFRLIERHGFFAV	5	0	184414	7
GB	331	VISWDIQDEKNVTCQ	5	0	184415	11
GM	57	MSAYNVMHLHTPMLF	5	0	184416	3
IRS1	168	RDWIVLVATVVHEV	5	0	184417	3
VGLI	3	PVYVNLGSGVGLLAF	5	0	184435	3
UL22A	7	ILSLLAVTLTVALAA	5	0	184436	4
PP150	59	WLGYYRELRFHNPDL	5	1	184437	
UL35	108	QLDVLVSDPLKTRLL	6	0	184438	-

UL35	439	TYHLQRIYSMMIEGA	5	0	184439	3
UL35	462	KRFMELLDRAPLGQE	5	0	184440	7
SCAF	118	DKVVEFLSGSYAGLS	5	0	184441	4
PP71	282	GFQLLIPKSFTLTRI	5	0	184442	11
CEP3	18	GEPLKDALGRQVSLR	5	0	184444	3
CEP3	31	LRSYDNIPPTSSSDE	6	1	184445	-
US2	178	LFIVYVTVDCNLSMM	5	0	sf	1
US3	152	DDNWGLLFRLLVYL	5	1	184447	3
UL31	203	GKYDWSNVVTPKAA	5	1	194389	3

\*1 predicted from Pos. 254, synthesized from Pos. 253 because of C-terminal Prolin \*2 from Pos.

203; 202 not producible due to N-terminal cysteine

**Table S2: Predicted promiscuous epitope candidates from the whole-proteome prediction.**

This table lists all peptides that were exclusively predicted in the whole-proteome prediction. Abbreviations: pos, position in the protein sequence; n<sub>HLA</sub>, number of covered HLA-DR allotypes (six are highlighted in yellow); n<sub>ts</sub>, number of top-scored epitope candidates (one and two are highlighted in yellow); HLA<sub>nc</sub>, not covered HLA allotypes

Protein	Pos	Sequence	nHLA	nts	HLAnc
HVLF1	243	LILFTTEDSLDKLIA	5	1	1
HVLF4	68	VYGLLTLETAFSVLI	5	0	3
HVLF4	131	FALYVALLSFTTAGL	5	1	11
HVLF5	120	AILIDYTLVLTWIA	5	1	11
HVLF6	214	VLIRDTLTVLYRSPS	5	0	1
US7	174	LYVFMWTYLVTLQY	5	1	3
TRM1	46	AAIVLYRKIYPEVV	5	0	4
TRM1	368	NRIIDLITSLSIQAF	5	0	11
TRM3	197	QTSIDIFKQKATVFL	5	0	3
TRM3	574	QPFYLMGRDKALAVE	5	0	4
gM	66	HTPMLFLDSVQLVCY	5	0	11
PORTL	368	VESFLQDLTPSLVDQ	5	1	11
UL121	162	LWKVDYDRSVAVGPK	5	0	11
UL78	83	LSQFFSILATMLSKG	5	2	3
UL78	126	FFLFILDRLSAISY	5	1	7
UL78	161	AFAWVLSIVAAPTA	5	1	3
UL78	227	DHVWSYVGRVCTFYV	5	1	3
UL24	266	GMRVLGLGTVSLKGE	5	0	11
UL27	215	ELYLRLDGTLCLFLE	5	0	11

<b>UL5</b>	12	GLAVYRVSRSLKLV	5	0	1
<b>UL92</b>	92	LSGVYSYLMTHAGRY	5	0	3
<b>IR11</b>	170	IISDLKRQWSGLSLH	5	0	7
<b>IRL12</b>	78	IGNITNVTSDLSTFT	5	0	7
<b>IRL12</b>	246	WYWLRILTSHTVCHS	5	1	3
<b>HEPA</b>	101	ARVLLEGALIRVLA	5	0	3
<b>HEPA</b>	108	SALIRVLARTFTPVQ	5	0	3
<b>gL</b>	22	CLLLPIVSSVAVSVA	5	0	3
<b>UL31</b>	4	KPTLVTLTVAVSSP	5	0	3
<b>UL33</b>	147	YMILLTWLAGLIFS	5	0	11
<b>UL33</b>	248	VLLISFVALQTPYVS	5	2	11
<b>UL33</b>	260	YVSLMIFNSYATTAW	5	0	3
<b>PRIM</b>	198	MGEFARLLLGSPFRQ	5	0	7
<b>PRIM</b>	254	VHYVYLAYRTALARA	5	0	7
<b>US28</b>	80	LLFVCTLPLWMQYLL	5	0	11
<b>US18</b>	31	QQLFQWLKRFKLLME	5	1	7
<b>US18</b>	195	GLYVLVVTAAASAVLI	5	1	3

pp65 109-123

```

sp|P06725|PP65_HCMVA      YTPDSTPCHRGDNQLQVQHTYFTGSEVENVSVNVHNPTRGRSICPSQEFMSIYVYALPLKM 120
sp|Q6SW59|PP65_HCMVM      YTPDSTPCHRGDNQLQVQHTYFTGSEVENVSVNVHNPTRGRSICPSQEFMSIYVYALPLKM 120
*****

```

```

sp|P06725|PP65_HCMVA      LNIPSINVHHYPSAAERKHRHLPVADAVIHASGKQMWQARLTVSGLAWTRQQNQWKEPDV 180
sp|Q6SW59|PP65_HCMVM      LNIPSINVHHYPSAAERKHRHLPVADAVIHASGKQMWQARLTVSGLAWTRQQNQWKEPDV 180
*****

```

VPAP 253-267

```

sp|P16790|VPAP_HCMVA      TLRIVTEHDTLLYVASRNGLFAVENFLEEEPFQRGDPFDKNYVGNSGKSRGGGGGGGSL 300
sp|F5HC97|VPAP_HCMVM      TLRIVTEHDTLLYVASRNGLFAVENFLEEEPFQRGDPFDKNYVGNSGKSRGGGGGGGSL 300
*****

```

US24 255-269

```

sp|P09700|US24_HCMVA      LHRIWPFCALTEVSRRRWWAVRANLATPNYVLGVTGRPRPGRSFVAEVLVLLDWFGAVY 300
sp|F5H8S6|US24_HCMVM      LHRIWPFCALTEVSRRRWWAVRANLATPNYVLGVTGRPRPGRSFVAEVLVLLDWFGAVY 300
*****

```

UL36 253-267

```

sp|P16767|UL36_HCMVA      HEVPERKEFLVHQYVLVDTFGVVYGYDPAMDAVYRLAEDVVMFTCVMGKKGHRNHRFSGR 300
sp|F5HAY6|VICA_HCMVM      HEVPERKEFLVHQYVLVDTFGVVYGYDPAMDAVYRLAEDVVMFTCVMGKKGHRNHRFSGR 300
*****

```

VP22 201-215

```

sp|P16760|VP22_HCMVA      VGLRAVETLHCMRYLTSSLVKRYFRPLLRAWSLGLDTMARFIIRHHGQFMPLTYPPGTEL 240
sp|F5H9N4|VP22_HCMVM      VGLRAVETLHCMRYLTSSLVKRYFRPLLRAWSLGLDTMARFIIRHHGQFMPLTYPPGTEL 240
*****

```

MCP 515-529

```

sp|P16729|MCP_HCMVA      CRFQQEPMGGAARRIPHFYRVRREVPRVTNEMKQDFVVDDFYKVGNITLYTELHPPFDFT 540
sp|F5HGT1|MCP_HCMVM      CRFQQEPMGGAARRIPHFYRVRREVPRVTNEMKQDFVVDDFYKVGNITLYTELHPPFDFT 540
*****

```

TRM3 319-333

```

sp|P16732|TRM3_HCMVA      QNFHLLLVDEAHFIKKEAFNTILGFLAQNTTKIIFISTNTTSDSTCFLTRLNNAPFDM 360
sp|F5HCU8|TRM3_HCMVM      QNFHLLLVDEAHFIKKEAFNTILGFLAQNTTKIIFISTNTTSDATCFLTRLNNAPFDM 360
*****

```

CVC2 400-414

```

sp|P16726|CVC2_HCMVA      TFDRHVLVRLFHKRGVIQHLPGYGITEELVQERLSGQVRDDVLSLWSRRLVGKLRDV 420
sp|Q6SW65|CVC2_HCMVM      TFDRHVLVRLFHKRGVIQHLPGYGITEELVQERLSGQVRDDVLSLWSRRLVGKLRDV 414
*****

```

US04 62-67

no UniProt entry for HCMVM

UL34 219-233

```

sp|P16812|UL34_HCMVA      PHERHRELCHVLIGLLHQTPHMWARSIRLIHLRHYLQNSFLHLLMNSGLDIAQVFDGCY 240
sp|F5HC16|UL34_HCMVM      PHERHRELCHVLIGLLHQTPHMWARSIRLIHLRHYLQNSFLHLLMNSGLDIAQVFDGCY 240
*****

```

UL84 122-136

```

sp|P16727|UL84_HCMVA      IRDPFQILLSTPLQLGEANDESQTAPATLQEEETAASHEPEKKKEKQEKK-EEDEDDRND 179
sp|F5HB40|UL84_HCMVM      IRDPFQILLSTPLQLGEANGESQTAPATSQEEETAASHEPEKKKEKQEKK-EEDEDDRND 180
*****

```

GO 425-439

```

sp|P16750|GO_HCMVA      IDPLWDYLDSLLFLDEIRNFSLRSPTVNLTPPEHRRAVNLSTLNSLLWWWLQ 466
sp|F5HGP1|GO_HCMVM      IDPLWDYLDSLLFLDKIRNFSLQLPAYGNLTPPEHRRAANLSTLNSLLWWWSQ 472
*****

```



pp65 179-193

```

sp|P06725|PP65_HCMVA LNIPSLNVHHYPSAAERKRRHLPVADAVIHASGKQMWQARLTVSGLAWTRQQNQWKEFDV 180
sp|Q6SW59|PP65_HCMVM LNIPSLNVHHYPSAAERKRRHLPVADAVIHASGKQMWQARLTVSGLAWTRQQNQWKEFDV 180
*****

sp|P06725|PP65_HCMVA YYTSAFVFPTKDVLRHVVCACHELVCSMENTRATKMQVIGDQYVKVYLESFCEDVPSGKL 240
sp|Q6SW59|PP65_HCMVM YYTSAFVFPTKDVLRHVVCACHELVCSMENTRATKMQVIGDQYVKVYLESFCEDVPSGKL 240
*****

```

TEG7 37-51

```

sp|P16823|TEG7_HCMVA MQLAQRLCELLMCRKKAAPVADYVLLQPSSEDELRELQAFLDENFKQLEITPADLRTFSR 60
sp|F5HEA3|TEG7_HCMVM MQLAQRLCELLMCRKKAAPVADYVLLQPSSEDELRELQAFLDENFKQLEITPADLRTFSR 60
*****

```

pp65 283-299

```

sp|P06725|PP65_HCMVA FMHVTLGS DVEEDLTMRNPQPFMRPHERNGFTVLCPKNMIKPGKISHIMLDVAFTSHE 300
sp|Q6SW59|PP65_HCMVM FMHVTLGS DVEEDLTMRNPQPFMRPHERNGFTVLCPKNMIKPGKISHIMLDVAFTSHE 300
*****

```

MCP 570-584

```

sp|P16729|MCP_HCMVA HCQENSETVALCTPRIVIGNLDPGLAPGFHELRWEIMEHMLRPPPDYEETLRLFKTT 600
sp|F5HGT1|MCP_HCMVM HCQENSETVALCTPRIVIGNLDPGLAPGFHELRWEIMEHMLRPPPDYEETLRLFKTT 600
*****

```

TRS1 & IRS1 214-228

```

sp|P09695|TRS1_HCMVA EVDPAADPTLGDKAGHPGLCAQDGLYLALGAGFRVVFYDLANNTLILAAARDADEWFRHG 240
sp|Q6SVX2|TRS1_HCMVM EVDPAADPTVGDKAGHPGLCAQDGLYLALGAGFRVVFYDLANNTLILAAARDADEWFRHG 240
*****

```

```

sp|P09715|IRS1_HCMVA EVDPAADPTVGDKAGHPGLCAQDGLYLALGAGFRVVFYDLANNTLILAAARDADEWFRHG 240
sp|Q6SW04|IRS1_HCMVM EVDPAADPTVGDKAGHPGLCAQDGLYLALGAGFRVVFYDLANNTLILAAARDADEWFRHG 240
*****

```

CVC2 595-609

```

sp|P16726|CVC2_HCMVA SRREDSAGGGDGGGAVLMQLSKSNPVADYMFQSSKQYGDRLRLEVHDALLFHYEHGLGR 600
sp|Q6SW65|CVC2_HCMVM SRREDSAGGGDGGGAVLMQLSKSNPVADYMFQSSKQYGDRLRLEVHDALLFHYEHGLGR 594
*****

```

```

sp|P16726|CVC2_HCMVA LLSVTLPRHRVSTLGSSLFNVNDIYELLYFLVLGFLPSVAVL 642
sp|Q6SW65|CVC2_HCMVM LLSVTLPRHRVSTLGSSLFNVNDIYELLYFLVLGFLPSVAVL 636
*****

```

PORTL 246-260

```

sp|P16735|PORTL_HCMVA ANAPEVRFVKVRSERLEAQLRGKHIRLYVAAEPLAYERDKLLFTTPVAHLHEEILRYDG 300
sp|F5HBR4|PORTL_HCMVM ANAPEVRFVKVRSERLEAQLRGKHIRLYVAAEPLAYERDKLLFTTPVAHLHEEILRYDG 300
*****

```

DPOL 67-81

```

sp|P08546|DPOL_HCMVA KTGRLELMFYREIKHLLSHDMWPCPWRETLVGRVVGPIRFHTYDQTDVAVLFFDSPENV 120
sp|Q6SW77|DPOL_HCMVM KTGRLELMFYREIKHLLSHDMWPCPWRETLVGRVVGPIRFHTYDQTDVAVLFFDSPENV 120
*****

```

HEPA 488-502

```

sp|P16827|HEPA_HCMVA RFRSRRFWQIQSLLGYISEHVTSACASAGLLWVLSRGHREFYVYDGYSGHGVPVSAEVCV 540
sp|F5HIG1|HEPA_HCMVM RFRSRRFWQIQSLLGYISEHVTSACASAGLLWVLSRGHREFYVYDGYSGHGVPVSAEVCV 540
*****

```

US08 191-205

```

sp|P09730|US08_HCMVA LGVVIAICMAMVLLLGTVLARTVYRVSAYYLRWHACVPQKCKSLC 227
sp|F5HB52|US08_HCMVM LGVVIAIQMAMVLLLGTVLARTVYRVSAYYLRWHACVPQKCKSLC 227
*****

```

**Figure S2: Sequence alignment of dominant epitopes with the HCMV strain Merlin.** We aligned the aa sequences of the source proteins of all dominant epitopes with the correspondent proteins of the HCMV low-passage, wild type prototype strain Merlin (HCMVM). Adapted from [188].



## 9 References

1. Mocarski, E.S., T. Shenk, P. Griffiths, and R.F. Pass, *Cytomegaloviruses*, in *Fields Virology, 6th edition*, D.M. Knipe and P.M. Howley, Editors. 2013, Lippincott Williams & Wilkins: Philadelphia, PA, USA. p. 1960-2014.
2. Steven, A.C., C.R. Roberts, J. Hay, M.E. Bisher, T. Pun, and B.L. Trus, *Hexavalent capsomers of herpes simplex virus type 2: symmetry, shape, dimensions, and oligomeric status*. J Virol, 1986. **57**(2): p. 578-84.
3. Wildy, P., W.C. Russell, and R.W. Horne, *The morphology of herpes virus*. Virology, 1960. **12**(2): p. 204-22.
4. Schrag, J.D., B.V. Prasad, F.J. Rixon, and W. Chiu, *Three-dimensional structure of the HSV1 nucleocapsid*. Cell, 1989. **56**(4): p. 651-60.
5. Landolfo, S., M. Gariglio, G. Gribaudo, and D. Lembo, *The human cytomegalovirus*. Pharmacol Ther, 2003. **98**(3): p. 269-97.
6. Dittmer, A., J.C. Drach, L.B. Townsend, A. Fischer, and E. Bogner, *Interaction of the putative human cytomegalovirus portal protein pUL104 with the large terminase subunit pUL56 and its inhibition by benzimidazole-D-ribonucleosides*. J Virol, 2005. **79**(23): p. 14660-7.
7. Chen, D.H., H. Jiang, M. Lee, F. Liu, and Z.H. Zhou, *Three-dimensional visualization of tegument/capsid interactions in the intact human cytomegalovirus*. Virology, 1999. **260**(1): p. 10-6.
8. Varnum, S.M., D.N. Streblow, M.E. Monroe, P. Smith, K.J. Auberry, L. Pasa-Tolic, D. Wang, D.G. Camp, 2nd, K. Rodland, S. Wiley, W. Britt, T. Shenk, R.D. Smith, and J.A. Nelson, *Identification of proteins in human cytomegalovirus (HCMV) particles: the HCMV proteome*. J Virol, 2004. **78**(20): p. 10960-6.
9. McLaughlin-Taylor, E., H. Pande, S.J. Forman, B. Tanamachi, C.R. Li, J.A. Zaia, P.D. Greenberg, and S.R. Riddell, *Identification of the major late human cytomegalovirus matrix protein pp65 as a target antigen for CD8+ virus-specific cytotoxic T lymphocytes*. J Med Virol, 1994. **43**(1): p. 103-110.
10. Jahn, G., B.-C. Scholl, B. Traupe, and B. Fleckenstein, *The two major structural phosphoproteins (pp65 and pp150) of human cytomegalovirus and their antigenic properties*. J Gen Virol, 1987. **68**(5): p. 1327-1337.
11. Kalejta, R.F., *Tegument proteins of human cytomegalovirus*. Microbiol Mol Biol Rev, 2008. **72**(2): p. 249-65.
12. Yu, X., S. Shah, M. Lee, W. Dai, P. Lo, W. Britt, H. Zhu, F. Liu, and Z.H. Zhou, *Biochemical and structural characterization of the capsid-bound tegument proteins of human cytomegalovirus*. J Struct Biol, 2011. **174**(3): p. 451-60.
13. Petrik, D.T., K.P. Schmitt, and M.F. Stinski, *The autoregulatory and transactivating functions of the human cytomegalovirus IE86 protein use independent mechanisms for promoter binding*. J Virol, 2007. **81**(11): p. 5807-5818.

14. Tooze, J., M. Hollinshead, B. Reis, K. Radsak, and H. Kern, *Progeny vaccinia and human cytomegalovirus particles utilize early endosomal cisternae for their envelopes*. Eur J Cell Biol, 1993. **60**(1): p. 163-178.
15. Das, S., A. Vasanji, and P.E. Pellett, *Three-dimensional structure of the human cytomegalovirus cytoplasmic virion assembly complex includes a reoriented secretory apparatus*. J Virol, 2007. **81**(21): p. 11861-9.
16. Tandon, R., D.P. AuCoin, and E.S. Mocarski, *Human cytomegalovirus exploits ESCRT machinery in the process of virion maturation*. J Virol, 2009. **83**(20): p. 10797-10807.
17. Isaacson, M.K. and T. Compton, *Human cytomegalovirus glycoprotein B is required for virus entry and cell-to-cell spread but not for virion attachment, assembly, or egress*. J Virol, 2009. **83**(8): p. 3891-3903.
18. Compton, T., D.M. Nowlin, and N.R. Cooper, *Initiation of human cytomegalovirus infection requires initial interaction with cell surface heparan sulfate*. Virology, 1993. **193**(2): p. 834-41.
19. Wang, X., S.-M. Huong, M.L. Chiu, N. Raab-Traub, and E.-S. Huang, *Epidermal growth factor receptor is a cellular receptor for human cytomegalovirus*. Nature, 2003. **424**(6947): p. 456.
20. Soroceanu, L., A. Akhavan, and C.S. Cobbs, *Platelet-derived growth factor- $\alpha$  receptor activation is required for human cytomegalovirus infection*. Nature, 2008. **455**(7211): p. 391.
21. Viswanathan, K., M.S. Smith, D. Malouli, M. Mansouri, J.A. Nelson, and K. Fruh, *BST2/Tetherin enhances entry of human cytomegalovirus*. PLoS Pathog, 2011. **7**(11): p. e1002332.
22. Ryckman, B.J., B.L. Rainish, M.C. Chase, J.A. Borton, J.A. Nelson, M.A. Jarvis, and D.C. Johnson, *Characterization of the human cytomegalovirus gH/gL/UL128-131 complex that mediates entry into epithelial and endothelial cells*. J Virol, 2008. **82**(1): p. 60-70.
23. *Swiss Institute for Bioinformatics, Viral Zone, Access Date: 08.09.2020*. Available from: [https://viralzone.expasy.org/180?outline=all\\_by\\_species](https://viralzone.expasy.org/180?outline=all_by_species).
24. Sijmons, S., M. Van Ranst, and P. Maes, *Genomic and functional characteristics of human cytomegalovirus revealed by next-generation sequencing*. Viruses, 2014. **6**(3): p. 1049-72.
25. Delius, H. and J.B. Clements, *A partial denaturation map of herpes simplex virus type 1 DNA: evidence for inversions of the unique DNA regions*. J Gen Virol, 1976. **33**(1): p. 125-33.
26. Sauer, A., J.B. Wang, G. Hahn, and M.A. McVoy, *A human cytomegalovirus deleted of internal repeats replicates with near wild type efficiency but fails to undergo genome isomerization*. Virology, 2010. **401**(1): p. 90-5.
27. Murphy, E., I. Rigoutsos, T. Shibuya, and T.E. Shenk, *Reevaluation of human cytomegalovirus coding potential*. Proc Natl Acad Sci U S A, 2003. **100**(23): p. 13585-90.

28. Stern-Ginossar, N., B. Weisburd, A. Michalski, V.T. Le, M.Y. Hein, S.X. Huang, M. Ma, B. Shen, S.B. Qian, H. Hengel, M. Mann, N.T. Ingolia, and J.S. Weissman, *Decoding human cytomegalovirus*. *Science*, 2012. **338**(6110): p. 1088-93.
29. Gatherer, D., S. Seirafian, C. Cunningham, M. Holton, D.J. Dargan, K. Baluchova, R.D. Hector, J. Galbraith, P. Herzyk, G.W. Wilkinson, and A.J. Davison, *High-resolution human cytomegalovirus transcriptome*. *Proc Natl Acad Sci U S A*, 2011. **108**(49): p. 19755-60.
30. Sinzger, C., B. Plachter, A. Grefte, T.H. The, and G. Jahn, *Tissue macrophages are infected by human cytomegalovirus in vivo*. *J Infect Dis*, 1996. **173**(1): p. 240-5.
31. Bissinger, A., C. Sinzger, E. Kaiserling, and G. Jahn, *Human cytomegalovirus as a direct pathogen: correlation of multiorgan involvement and cell distribution with clinical and pathological findings in a case of congenital inclusion disease*. *J Med Virol*, 2002. **67**(2): p. 200-206.
32. Percivalle, E., M.G. Revello, L. Vago, F. Morini, and G. Gerna, *Circulating endothelial giant cells permissive for human cytomegalovirus (HCMV) are detected in disseminated HCMV infections with organ involvement*. *J Clin Invest*, 1993. **92**(2): p. 663-70.
33. Grefte, A., M. van der Giessen, W. van Son, and T.H. The, *Circulating cytomegalovirus (CMV)-infected endothelial cells in patients with an active CMV infection*. *J Infect Dis*, 1993. **167**(2): p. 270-7.
34. Ogawa-Goto, K., K. Tanaka, W. Gibson, E. Moriishi, Y. Miura, T. Kurata, S. Irie, and T. Sata, *Microtubule network facilitates nuclear targeting of human cytomegalovirus capsid*. *J Virol*, 2003. **77**(15): p. 8541-7.
35. Lischka, P., G. Sorg, M. Kann, M. Winkler, and T. Stamminger, *A nonconventional nuclear localization signal within the UL84 protein of human cytomegalovirus mediates nuclear import via the importin  $\alpha/\beta$  pathway*. *J Virol*, 2003. **77**(6): p. 3734-3748.
36. Poole, E. and J. Sinclair, *Sleepless latency of human cytomegalovirus*. *Med Microbiol Immunol*, 2015. **204**(3): p. 421-9.
37. Stinski, M.F., *Sequence of protein synthesis in cells infected by human cytomegalovirus: early and late virus-induced polypeptides*. *J Virol*, 1978. **26**(3): p. 686-701.
38. Wathen, M.W. and M.F. Stinski, *Temporal patterns of human cytomegalovirus transcription: mapping the viral RNAs synthesized at immediate early, early, and late times after infection*. *J Virol*, 1982. **41**(2): p. 462-477.
39. Ghazal, P., H. Lubon, C. Reynolds-Kohler, L. Hennighausen, and J.A. Nelson, *Interactions between cellular regulatory proteins and a unique sequence region in the human cytomegalovirus major immediate-early promoter*. *Virology*, 1990. **174**(1): p. 18-25.
40. Shamu, C.E., C.M. Story, T.A. Rapoport, and H.L. Ploegh, *The pathway of US11-dependent degradation of MHC class I heavy chains involves a ubiquitin-conjugated intermediate*. *J Cell Biol*, 1999. **147**(1): p. 45-58.
41. Skaletskaya, A., L.M. Bartle, T. Chittenden, A.L. McCormick, E.S. Mocarski, and V.S. Goldmacher, *A cytomegalovirus-encoded inhibitor of apoptosis that suppresses caspase-8 activation*. *Proc Natl Acad Sci U S A*, 2001. **98**(14): p. 7829-7834.

42. Fehr, A.R. and D. Yu, *Human cytomegalovirus early protein pUL21a promotes efficient viral DNA synthesis and the late accumulation of immediate-early transcripts*. J Virol, 2011. **85**(2): p. 663-74.
43. Phillips, S.L. and W.A. Bresnahan, *The human cytomegalovirus (HCMV) tegument protein UL94 is essential for secondary envelopment of HCMV virions*. J Virol, 2012. **86**(5): p. 2523-2532.
44. Weekes, M.P., P. Tomasec, E.L. Huttlin, C.A. Fielding, D. Nusinow, R.J. Stanton, E.C.Y. Wang, R. Aichele, I. Murrell, G.W.G. Wilkinson, P.J. Lehner, and S.P. Gygi, *Quantitative temporal viromics: an approach to investigate host-pathogen interaction*. Cell, 2014. **157**(6): p. 1460-1472.
45. Forte, E., Z. Zhang, E.B. Thorp, and M. Hummel, *Cytomegalovirus Latency and Reactivation: An Intricate Interplay With the Host Immune Response*. Front Cell Infect Microbiol, 2020. **10**(130): p. 130.
46. Sinclair, J. and P. Sissons, *Latent and persistent infections of monocytes and macrophages*. Intervirology, 1996. **39**(5-6): p. 293-301.
47. Mendelson, M., S. Monard, P. Sissons, and J. Sinclair, *Detection of endogenous human cytomegalovirus in CD34+ bone marrow progenitors*. J Gen Virol, 1996. **77** ( Pt 12)(12): p. 3099-102.
48. Hahn, G., R. Jores, and E.S. Mocarski, *Cytomegalovirus remains latent in a common precursor of dendritic and myeloid cells*. Proc Natl Acad Sci U S A, 1998. **95**(7): p. 3937-42.
49. Taylor-Wiedeman, J., J.G. Sissons, L.K. Borysiewicz, and J.H. Sinclair, *Monocytes are a major site of persistence of human cytomegalovirus in peripheral blood mononuclear cells*. J Gen Virol, 1991. **72** ( Pt 9)(9): p. 2059-64.
50. Sissons, J.G., M. Bain, and M.R. Wills, *Latency and reactivation of human cytomegalovirus*. J Infect, 2002. **44**(2): p. 73-7.
51. Soderberg-Naucler, C., D.N. Streblow, K.N. Fish, J. Allan-Yorke, P.P. Smith, and J.A. Nelson, *Reactivation of latent human cytomegalovirus in CD14(+) monocytes is differentiation dependent*. J Virol, 2001. **75**(16): p. 7543-54.
52. Reeves, M.B., P.J. Lehner, J.G.P. Sissons, and J.H. Sinclair, *An in vitro model for the regulation of human cytomegalovirus latency and reactivation in dendritic cells by chromatin remodelling*. J Gen Virol, 2005. **86**(Pt 11): p. 2949-2954.
53. Reeves, M.B., *Chromatin-mediated regulation of cytomegalovirus gene expression*. Virus Res, 2011. **157**(2): p. 134-43.
54. Goodrum, F., M. Reeves, J. Sinclair, K. High, and T. Shenk, *Human cytomegalovirus sequences expressed in latently infected individuals promote a latent infection in vitro*. Blood, 2007. **110**(3): p. 937-45.
55. Reeves, M.B. and J.H. Sinclair, *Analysis of latent viral gene expression in natural and experimental latency models of human cytomegalovirus and its correlation with histone modifications at a latent promoter*. J Gen Virol, 2010. **91**(Pt 3): p. 599-604.

56. Cheung, A.K., D.J. Gottlieb, B. Plachter, S. Pepperl-Klindworth, S. Avdic, A.L. Cunningham, A. Abendroth, and B. Slobedman, *The role of the human cytomegalovirus UL111A gene in down-regulating CD4+ T-cell recognition of latently infected cells: implications for virus elimination during latency*. *Blood*, 2009. **114**(19): p. 4128-37.
57. Cheng, S., K. Caviness, J. Buehler, M. Smithey, J. Nikolich-Zugich, and F. Goodrum, *Transcriptome-wide characterization of human cytomegalovirus in natural infection and experimental latency*. *Proc Natl Acad Sci U S A*, 2017. **114**(49): p. E10586-E10595.
58. Shnayder, M., A. Nachshon, B. Krishna, E. Poole, A. Boshkov, A. Binyamin, I. Maza, J. Sinclair, M. Schwartz, and N. Stern-Ginossar, *Defining the Transcriptional Landscape during Cytomegalovirus Latency with Single-Cell RNA Sequencing*. *mBio*, 2018. **9**(2): p. e00013-18.
59. Schwartz, M. and N. Stern-Ginossar, *The Transcriptome of Latent Human Cytomegalovirus*. *J Virol*, 2019. **93**(11): p. e00047-19.
60. Artyomov, M.N., M. Lis, S. Devadas, M.M. Davis, and A.K. Chakraborty, *CD4 and CD8 binding to MHC molecules primarily acts to enhance Lck delivery*. *Proc Natl Acad Sci U S A*, 2010. **107**(39): p. 16916-21.
61. Marrack, P. and J. Kappler, *The T cell receptor*. *Science*, 1987. **238**(4830): p. 1073-9.
62. Beck, S. and J. Trowsdale, *The human major histocompatibility complex: lessons from the DNA sequence*. *Annu Rev Genomics Hum Genet*, 2000. **1**(1): p. 117-37.
63. Beck, S., D. Geraghty, H. Inoko, L. Rowen, B. Aguado, S. Bahram, R.D. Campbell, S.A. Forbes, T. Guillaudoux, L. Hood, R. Horton, M. Janer, C. Jasoni, A. Madan, S. Milne, M. Neville, A. Oka, S. Qin, G. Ribas-Despuig, J. Rogers, T. Shiina, T. Spies, G. Tamiya, H. Tashiro, J. Trowsdale, Q. Vu, L. Williams, M. Yamazaki, and M.H.C.S. Consortium, *Complete sequence and gene map of a human major histocompatibility complex. The MHC sequencing consortium*. *Nature*, 1999. **401**(6756): p. 921-3.
64. Goldberg, A.C. and L.V. Rizzo, *MHC structure and function - antigen presentation. Part 1*. Einstein (Sao Paulo), 2015. **13**(1): p. 153-6.
65. Carroll, M.C., P. Katzman, E.M. Alicot, B.H. Koller, D.E. Geraghty, H.T. Orr, J.L. Strominger, and T. Spies, *Linkage map of the human major histocompatibility complex including the tumor necrosis factor genes*. *Proc Natl Acad Sci U S A*, 1987. **84**(23): p. 8535-9.
66. Sargent, C.A., I. Dunham, and R.D. Campbell, *Identification of multiple HTF-island associated genes in the human major histocompatibility complex class III region*. *EMBO J*, 1989. **8**(8): p. 2305-12.
67. Germain, R.N., *MHC-dependent antigen processing and peptide presentation: providing ligands for T lymphocyte activation*. *Cell*, 1994. **76**(2): p. 287-99.
68. Kloetzel, P.M., *Antigen processing by the proteasome*. *Nat Rev Mol Cell Biol*, 2001. **2**(3): p. 179-87.
69. Gromme, M. and J. Neefjes, *Antigen degradation or presentation by MHC class I molecules via classical and non-classical pathways*. *Mol Immunol*, 2002. **39**(3-4): p. 181-202.

70. Rammensee, H.G., *Chemistry of peptides associated with MHC class I and class II molecules*. *Curr Opin Immunol*, 1995. **7**(1): p. 85-96.
71. Kern, F., I.P. Surel, C. Brock, B. Freistedt, H. Radtke, A. Scheffold, R. Blasczyk, P. Reinke, J. Schneider-Mergener, A. Radbruch, P. Walden, and H.D. Volk, *T-cell epitope mapping by flow cytometry*. *Nat Med*, 1998. **4**(8): p. 975-8.
72. Kiecker, F., M. Streitz, B. Ay, G. Cherepnev, H.-D. Volk, R. Volkmer-Engert, and F. Kern, *Analysis of antigen-specific T-cell responses with synthetic peptides—what kind of peptide for which purpose?* *Hum Immunol*, 2004. **65**(5): p. 523-536.
73. Ebert, L.M., Y.C. Liu, C.S. Clements, N.C. Robson, H.M. Jackson, J.L. Markby, N. Dimopoulos, B.S. Tan, I.F. Luescher, I.D. Davis, J. Rossjohn, J. Cebon, A.W. Purcell, and W. Chen, *A long, naturally presented immunodominant epitope from NY-ESO-1 tumor antigen: implications for cancer vaccine design*. *Cancer Res*, 2009. **69**(3): p. 1046-54.
74. Hassan, C., E. Chabrol, L. Jahn, M.G. Kester, A.H. de Ru, J.W. Drijfhout, J. Rossjohn, J.H. Falkenburg, M.H. Heemskerk, S. Gras, and P.A. van Veelen, *Naturally processed non-canonical HLA-A\*02:01 presented peptides*. *J Biol Chem*, 2015. **290**(5): p. 2593-603.
75. Ruppert, J., J. Sidney, E. Celis, R.T. Kubo, H.M. Grey, and A. Sette, *Prominent role of secondary anchor residues in peptide binding to HLA-A2.1 molecules*. *Cell*, 1993. **74**(5): p. 929-37.
76. Falk, K., O. Rotzschke, S. Stevanovic, G. Jung, and H.G. Rammensee, *Allele-specific motifs revealed by sequencing of self-peptides eluted from MHC molecules*. *Nature*, 1991. **351**(6324): p. 290-6.
77. Neefjes, J., M.L. Jongsma, P. Paul, and O. Bakke, *Towards a systems understanding of MHC class I and MHC class II antigen presentation*. *Nat Rev Immunol*, 2011. **11**(12): p. 823-36.
78. Holling, T.M., N. van der Stoep, E. Quinten, and P.J. van den Elsen, *Activated human T cells accomplish MHC class II expression through T cell-specific occupation of class II transactivator promoter III*. *J Immunol*, 2002. **168**(2): p. 763-70.
79. Denzin, L.K. and P. Cresswell, *HLA-DM induces CLIP dissociation from MHC class II  $\alpha\beta$  dimers and facilitates peptide loading*. *Cell*, 1995. **82**(1): p. 155-165.
80. Hartman, I.Z., A. Kim, R.J. Cotter, K. Walter, S.K. Dalai, T. Boronina, W. Griffith, D.E. Lanar, R. Schwenk, U. Krzych, R.N. Cole, and S. Sadegh-Nasseri, *A reductionist cell-free major histocompatibility complex class II antigen processing system identifies immunodominant epitopes*. *Nat Med*, 2010. **16**(11): p. 1333-40.
81. Denzin, L.K., D.B. Sant'Angelo, C. Hammond, M.J. Surman, and P. Cresswell, *Negative regulation by HLA-DO of MHC class II-restricted antigen processing*. *Science*, 1997. **278**(5335): p. 106-9.
82. Vignali, D.A., R.G. Urban, R.M. Chicz, and J.L. Strominger, *Minute quantities of a single immunodominant foreign epitope are presented as large nested sets by major histocompatibility complex class II molecules*. *Eur J Immunol*, 1993. **23**(7): p. 1602-1607.

83. Chicz, R.M., R.G. Urban, J.C. Gorga, D. Vignali, W.S. Lane, and J.L. Strominger, *Specificity and promiscuity among naturally processed peptides bound to HLA-DR alleles*. J Exp Med, 1993. **178**(1): p. 27-47.
84. Jones, E.Y., L. Fugger, J.L. Strominger, and C. Siebold, *MHC class II proteins and disease: a structural perspective*. Nat Rev Immunol, 2006. **6**(4): p. 271-82.
85. Rammensee, H.G., K. Falk, and O. Rotzschke, *Peptides naturally presented by MHC class I molecules*. Annu Rev Immunol, 1993. **11**(1): p. 213-44.
86. Bevan, M.J., *Minor H antigens introduced on H-2 different stimulating cells cross-react at the cytotoxic T cell level during in vivo priming*. J Immunol, 1976. **117**(6): p. 2233-2238.
87. Joffre, O.P., E. Segura, A. Savina, and S. Amigorena, *Cross-presentation by dendritic cells*. Nat Rev Immunol, 2012. **12**(8): p. 557-69.
88. Schmid, D., M. Pypaert, and C. Münz, *MHC class II antigen loading compartments continuously receive input from autophagosomes*. Immunity, 2007. **26**(1): p. 79.
89. Rammensee, H., J. Bachmann, N.P. Emmerich, O.A. Bachor, and S. Stevanovic, *SYFPEITHI: database for MHC ligands and peptide motifs*. Immunogenetics, 1999. **50**(3-4): p. 213-9.
90. Rammensee, H.G., T. Friede, and S. Stevanovic, *MHC ligands and peptide motifs: first listing*. Immunogenetics, 1995. **41**(4): p. 178-228.
91. Falk, K., O. Rotzschke, S. Stevanovic, G. Jung, and H.G. Rammensee, *Pool sequencing of natural HLA-DR, DQ, and DP ligands reveals detailed peptide motifs, constraints of processing, and general rules*. Immunogenetics, 1994. **39**(4): p. 230-42.
92. Boehme, K.W., M. Guerrero, and T. Compton, *Human cytomegalovirus envelope glycoproteins B and H are necessary for TLR2 activation in permissive cells*. J Immunol, 2006. **177**(10): p. 7094-102.
93. Orange, J.S., B. Wang, C. Terhorst, and C.A. Biron, *Requirement for natural killer cell-produced interferon gamma in defense against murine cytomegalovirus infection and enhancement of this defense pathway by interleukin 12 administration*. J Exp Med, 1995. **182**(4): p. 1045-56.
94. Ulbrecht, M., S. Martinozzi, M. Grzeschik, H. Hengel, J.W. Ellwart, M. Pla, and E.H. Weiss, *Cutting edge: the human cytomegalovirus UL40 gene product contains a ligand for HLA-E and prevents NK cell-mediated lysis*. J Immunol, 2000. **164**(10): p. 5019-22.
95. Cosman, D., N. Fanger, L. Borges, M. Kubin, W. Chin, L. Peterson, and M.L. Hsu, *A novel immunoglobulin superfamily receptor for cellular and viral MHC class I molecules*. Immunity, 1997. **7**(2): p. 273-82.
96. Arnon, T.I., H. Achdout, O. Levi, G. Markel, N. Saleh, G. Katz, R. Gazit, T. Gonen-Gross, J. Hanna, E. Nahari, A. Porgador, A. Honigman, B. Plachter, D. Mevorach, D.G. Wolf, and O. Mandelboim, *Inhibition of the NKp30 activating receptor by pp65 of human cytomegalovirus*. Nat Immunol, 2005. **6**(5): p. 515-23.

97. Fowler, K.B., S. Stagno, R.F. Pass, W.J. Britt, T.J. Boll, and C.A. Alford, *The outcome of congenital cytomegalovirus infection in relation to maternal antibody status*. N Engl J Med, 1992. **326**(10): p. 663-7.
98. Snyderman, D.R., B.G. Werner, B. Heinze-Lacey, V.P. Berardi, N.L. Tilney, R.L. Kirkman, E.L. Milford, S.I. Cho, H.L. Bush Jr, and A.S. Levey, *Use of cytomegalovirus immune globulin to prevent cytomegalovirus disease in renal-transplant recipients*. N Engl J Med, 1987. **317**(17): p. 1049-1054.
99. Urban, M., M. Klein, W. Britt, E. Hassfurth, and M. Mach, *Glycoprotein H of human cytomegalovirus is a major antigen for the neutralizing humoral immune response*. J Gen Virol, 1996. **77**(7): p. 1537-1547.
100. Macagno, A., N.L. Bernasconi, F. Vanzetta, E. Dander, A. Sarasini, M.G. Revello, G. Gerna, F. Sallusto, and A. Lanzavecchia, *Isolation of human monoclonal antibodies that potently neutralize human cytomegalovirus infection by targeting different epitopes on the gH/gL/UL128-131A complex*. J Virol, 2010. **84**(2): p. 1005-1013.
101. Polic, B., H. Hengel, A. Krmpotic, J. Trgovcich, I. Pavic, P. Luccaronin, S. Jonjic, and U.H. Koszinowski, *Hierarchical and redundant lymphocyte subset control precludes cytomegalovirus replication during latent infection*. J Exp Med, 1998. **188**(6): p. 1047-54.
102. Cwynarski, K., J. Ainsworth, M. Cobbold, S. Wagner, P. Mahendra, J. Apperley, J. Goldman, C. Craddock, and P.A. Moss, *Direct visualization of cytomegalovirus-specific T-cell reconstitution after allogeneic stem cell transplantation*. Blood, 2001. **97**(5): p. 1232-40.
103. Jacobson, M.A., H.T. Maecker, P.L. Orr, R. D'Amico, M. Van Natta, X.D. Li, R.B. Pollard, B.M. Bredt, A.C.T.G. Adult, and A.R.G. the Studies of Ocular Complications of, *Results of a cytomegalovirus (CMV)-specific CD8+/interferon-gamma+ cytokine flow cytometry assay correlate with clinical evidence of protective immunity in patients with AIDS with CMV retinitis*. J Infect Dis, 2004. **189**(8): p. 1362-73.
104. Wiertz, E.J., T.R. Jones, L. Sun, M. Bogoy, H.J. Geuze, and H.L. Ploegh, *The human cytomegalovirus US11 gene product dislocates MHC class I heavy chains from the endoplasmic reticulum to the cytosol*. Cell, 1996. **84**(5): p. 769-79.
105. Jones, T.R., L.K. Hanson, L. Sun, J.S. Slater, R.M. Stenberg, and A.E. Campbell, *Multiple independent loci within the human cytomegalovirus unique short region down-regulate expression of major histocompatibility complex class I heavy chains*. J Virol, 1995. **69**(8): p. 4830-4841.
106. Jones, T.R., E.J. Wiertz, L. Sun, K.N. Fish, J.A. Nelson, and H.L. Ploegh, *Human cytomegalovirus US3 impairs transport and maturation of major histocompatibility complex class I heavy chains*. Proc Natl Acad Sci U S A, 1996. **93**(21): p. 11327-33.
107. Ahn, K., A. Gruhler, B. Galocha, T.R. Jones, E.J. Wiertz, H.L. Ploegh, P.A. Peterson, Y. Yang, and K. Fruh, *The ER-luminal domain of the HCMV glycoprotein US6 inhibits peptide translocation by TAP*. Immunity, 1997. **6**(5): p. 613-21.
108. Besold, K., M. Wills, and B. Plachter, *Immune evasion proteins gpUS2 and gpUS11 of human cytomegalovirus incompletely protect infected cells from CD8 T cell recognition*. Virology, 2009. **391**(1): p. 5-19.



109. Gilbert, M.J., S.R. Riddell, B. Plachter, and P.D. Greenberg, *Cytomegalovirus selectively blocks antigen processing and presentation of its immediate-early gene product*. *Nature*, 1996. **383**(6602): p. 720-2.
110. Elkington, R., S. Walker, T. Crough, M. Menzies, J. Tellam, M. Bharadwaj, and R. Khanna, *Ex vivo profiling of CD8+-T-cell responses to human cytomegalovirus reveals broad and multispecific reactivities in healthy virus carriers*. *J Virol*, 2003. **77**(9): p. 5226-40.
111. Kern, F., T. Bunde, N. Faulhaber, F. Kiecker, E. Khatamzas, I.M. Rudawski, A. Pruss, J.W. Gratama, R. Volkmer-Engert, R. Ewert, P. Reinke, H.D. Volk, and L.J. Picker, *Cytomegalovirus (CMV) phosphoprotein 65 makes a large contribution to shaping the T cell repertoire in CMV-exposed individuals*. *J Infect Dis*, 2002. **185**(12): p. 1709-16.
112. Kern, F., I.P. Surel, N. Faulhaber, C. Frommel, J. Schneider-Mergener, C. Schonemann, P. Reinke, and H.D. Volk, *Target structures of the CD8(+)-T-cell response to human cytomegalovirus: the 72-kilodalton major immediate-early protein revisited*. *J Virol*, 1999. **73**(10): p. 8179-84.
113. Crough, T. and R. Khanna, *Immunobiology of human cytomegalovirus: from bench to bedside*. *Clin Microbiol Rev*, 2009. **22**(1): p. 76-98.
114. Hegde, N.R., C. Dunn, D.M. Lewinsohn, M.A. Jarvis, J.A. Nelson, and D.C. Johnson, *Endogenous human cytomegalovirus gB is presented efficiently by MHC class II molecules to CD4+ CTL*. *J Exp Med*, 2005. **202**(8): p. 1109-1119.
115. Jonjic, S., I. Pavic, P. Lucin, D. Rukavina, and U.H. Koszinowski, *Efficacious control of cytomegalovirus infection after long-term depletion of CD8+ T lymphocytes*. *J Virol*, 1990. **64**(11): p. 5457-64.
116. Einsele, H., E. Roosnek, N. Rufer, C. Sinzger, S. Riegler, J. Loffler, U. Grigoleit, A. Moris, H.G. Rammensee, L. Kanz, A. Kleihauer, F. Frank, G. Jahn, and H. Hebart, *Infusion of cytomegalovirus (CMV)-specific T cells for the treatment of CMV infection not responding to antiviral chemotherapy*. *Blood*, 2002. **99**(11): p. 3916-22.
117. Odeberg, J., B. Plachter, L. Branden, and C. Soderberg-Naucler, *Human cytomegalovirus protein pp65 mediates accumulation of HLA-DR in lysosomes and destruction of the HLA-DR alpha-chain*. *Blood*, 2003. **101**(12): p. 4870-7.
118. Tomazin, R., J. Boname, N.R. Hegde, D.M. Lewinsohn, Y. Altschuler, T.R. Jones, P. Cresswell, J.A. Nelson, S.R. Riddell, and D.C. Johnson, *Cytomegalovirus US2 destroys two components of the MHC class II pathway, preventing recognition by CD4+ T cells*. *Nat Med*, 1999. **5**(9): p. 1039-43.
119. Hegde, N.R., R.A. Tomazin, T.W. Wisner, C. Dunn, J.M. Boname, D.M. Lewinsohn, and D.C. Johnson, *Inhibition of HLA-DR assembly, transport, and loading by human cytomegalovirus glycoprotein US3: a novel mechanism for evading major histocompatibility complex class II antigen presentation*. *J Virol*, 2002. **76**(21): p. 10929-41.
120. Swain, S.L., K.K. McKinstry, and T.M. Strutt, *Expanding roles for CD4(+) T cells in immunity to viruses*. *Nat Rev Immunol*, 2012. **12**(2): p. 136-48.

121. van Leeuwen, E.M., E.B. Remmerswaal, M.H. Heemskerk, I.J. ten Berge, and R.A. van Lier, *Strong selection of virus-specific cytotoxic CD4+ T-cell clones during primary human cytomegalovirus infection*. *Blood*, 2006. **108**(9): p. 3121-7.
122. Lim, E.Y., S.E. Jackson, and M.R. Wills, *The CD4+ T Cell Response to Human Cytomegalovirus in Healthy and Immunocompromised People*. *Front Cell Infect Microbiol*, 2020. **10**: p. 202.
123. Sylwester, A.W., B.L. Mitchell, J.B. Edgar, C. Taormina, C. Pelte, F. Ruchti, P.R. Sleath, K.H. Grabstein, N.A. Hosken, F. Kern, J.A. Nelson, and L.J. Picker, *Broadly targeted human cytomegalovirus-specific CD4+ and CD8+ T cells dominate the memory compartments of exposed subjects*. *J Exp Med*, 2005. **202**(5): p. 673-85.
124. Sester, M., U. Sester, B. Gartner, B. Kubuschok, M. Girndt, A. Meyerhans, and H. Kohler, *Sustained high frequencies of specific CD4 T cells restricted to a single persistent virus*. *J Virol*, 2002. **76**(8): p. 3748-55.
125. Dutton, R.W., L.M. Bradley, and S.L. Swain, *T cell memory*. *Annu Rev Immunol*, 1998. **16**(1): p. 201-23.
126. Sallusto, F., D. Lenig, R. Forster, M. Lipp, and A. Lanzavecchia, *Two subsets of memory T lymphocytes with distinct homing potentials and effector functions*. *Nature*, 1999. **401**(6754): p. 708-12.
127. Bitmansour, A.D., D.C. Douek, V.C. Maino, and L.J. Picker, *Direct ex vivo analysis of human CD4(+) memory T cell activation requirements at the single clonotype level*. *J Immunol*, 2002. **169**(3): p. 1207-18.
128. Rentenaar, R.J., L.E. Gamadia, N. van DerHoek, F.N. van Diepen, R. Boom, J.F. Weel, P.M. Wertheim-van Dillen, R.A. van Lier, and I.J. ten Berge, *Development of virus-specific CD4(+) T cells during primary cytomegalovirus infection*. *J Clin Invest*, 2000. **105**(4): p. 541-8.
129. Bitmansour, A.D., S.L. Waldrop, C.J. Pitcher, E. Khatamzas, F. Kern, V.C. Maino, and L.J. Picker, *Clonotypic structure of the human CD4+ memory T cell response to cytomegalovirus*. *J Immunol*, 2001. **167**(3): p. 1151-63.
130. Price, D.A., A.D. Bitmansour, J.B. Edgar, J.M. Walker, M.K. Axthelm, D.C. Douek, and L.J. Picker, *Induction and evolution of cytomegalovirus-specific CD4+ T cell clonotypes in rhesus macaques*. *J Immunol*, 2008. **180**(1): p. 269-80.
131. Klenerman, P. and A. Oxenius, *T cell responses to cytomegalovirus*. *Nat Rev Immunol*, 2016. **16**(6): p. 367-77.
132. Vescovini, R., C. Biasini, F.F. Fagnoni, A.R. Telera, L. Zanlari, M. Pedrazzoni, L. Bucci, D. Monti, M.C. Medici, C. Chezzi, C. Franceschi, and P. Sansoni, *Massive load of functional effector CD4+ and CD8+ T cells against cytomegalovirus in very old subjects*. *J Immunol*, 2007. **179**(6): p. 4283-91.
133. Pourgheysari, B., N. Khan, D. Best, R. Bruton, L. Nayak, and P.A. Moss, *The cytomegalovirus-specific CD4+ T-cell response expands with age and markedly alters the CD4+ T-cell repertoire*. *J Virol*, 2007. **81**(14): p. 7759-65.

134. Fletcher, J.M., M. Vukmanovic-Stejic, P.J. Dunne, K.E. Birch, J.E. Cook, S.E. Jackson, M. Salmon, M.H. Rustin, and A.N. Akbar, *Cytomegalovirus-specific CD4+ T cells in healthy carriers are continuously driven to replicative exhaustion*. J Immunol, 2005. **175**(12): p. 8218-25.
135. Jackson, S.E., G.X. Sedikides, G. Okecha, and M.R. Wills, *Generation, maintenance and tissue distribution of T cell responses to human cytomegalovirus in lytic and latent infection*. Med Microbiol Immunol, 2019. **208**(3-4): p. 375-389.
136. Griffiths, P., I. Baraniak, and M. Reeves, *The pathogenesis of human cytomegalovirus*. J Pathol, 2015. **235**(2): p. 288-97.
137. Fowler, K.B. and R.F. Pass, *Risk factors for congenital cytomegalovirus infection in the offspring of young women: exposure to young children and recent onset of sexual activity*. Pediatrics, 2006. **118**(2): p. e286-92.
138. Kenneson, A. and M.J. Cannon, *Review and meta-analysis of the epidemiology of congenital cytomegalovirus (CMV) infection*. Rev Med Virol, 2007. **17**(4): p. 253-76.
139. Ross, S.A., N. Arora, Z. Novak, K.B. Fowler, W.J. Britt, and S.B. Boppana, *Cytomegalovirus reinfections in healthy seroimmune women*. J Infect Dis, 2010. **201**(3): p. 386-9.
140. Ljungman, P., D. Engelhard, H. Link, P. Biron, L. Brandt, S. Brunet, C. Cordonnier, L. Debusscher, A. de Laurenzi, H.J. Kolb, and et al., *Treatment of interstitial pneumonitis due to cytomegalovirus with ganciclovir and intravenous immune globulin: experience of European Bone Marrow Transplant Group*. Clin Infect Dis, 1992. **14**(4): p. 831-5.
141. Bowen, E.F., *Cytomegalovirus reactivation in patients infected with HIV: the use of polymerase chain reaction in prediction and management*. Drugs, 1999. **57**(5): p. 735-41.
142. Gkrania-Klotsas, E., C. Langenberg, S.J. Sharp, R. Luben, K.T. Khaw, and N.J. Wareham, *Higher immunoglobulin G antibody levels against cytomegalovirus are associated with incident ischemic heart disease in the population-based EPIC-Norfolk cohort*. J Infect Dis, 2012. **206**(12): p. 1897-903.
143. Gkrania-Klotsas, E., C. Langenberg, S.J. Sharp, R. Luben, K.T. Khaw, and N.J. Wareham, *Seropositivity and higher immunoglobulin g antibody levels against cytomegalovirus are associated with mortality in the population-based European prospective investigation of Cancer-Norfolk cohort*. Clin Infect Dis, 2013. **56**(10): p. 1421-7.
144. Stagno, S., D.W. Reynolds, A. Tsiantos, D.A. Fuccillo, W. Long, and C.A. Alford, *Comparative serial virologic and serologic studies of symptomatic and subclinical congenitally and natally acquired cytomegalovirus infections*. J Infect Dis, 1975. **132**(5): p. 568-77.
145. Boppana, S.B., L.B. Rivera, K.B. Fowler, M. Mach, and W.J. Britt, *Intrauterine transmission of cytomegalovirus to infants of women with preconceptional immunity*. N Engl J Med, 2001. **344**(18): p. 1366-71.
146. Erard, V., K.A. Guthrie, S. Seo, J. Smith, M. Huang, J. Chien, M.E. Flowers, L. Corey, and M. Boeckh, *Reduced mortality of cytomegalovirus pneumonia after hematopoietic cell transplantation due to antiviral therapy and changes in transplantation practices*. Clin Infect Dis, 2015. **61**(1): p. 31-39.

147. Machado, C.M., F.L. Dulley, L.S. Boas, J.B. Castelli, M.C. Macedo, R.L. Silva, R. Pallota, R.S. Saboya, and C.S. Pannuti, *CMV pneumonia in allogeneic BMT recipients undergoing early treatment of pre-emptive ganciclovir therapy*. Bone Marrow Transplant, 2000. **26**(4): p. 413-7.
148. Deayton, J.R., C.A. Prof Sabin, M.A. Johnson, V.C. Emery, P. Wilson, and P.D. Griffiths, *Importance of cytomegalovirus viraemia in risk of disease progression and death in HIV-infected patients receiving highly active antiretroviral therapy*. Lancet, 2004. **363**(9427): p. 2116-21.
149. Boeckh, M., T.A. Gooley, D. Myerson, T. Cunningham, G. Schoch, and R.A. Bowden, *Cytomegalovirus pp65 antigenemia-guided early treatment with ganciclovir versus ganciclovir at engraftment after allogeneic marrow transplantation: a randomized double-blind study*. Blood, 1996. **88**(10): p. 4063-4071.
150. Crumpacker, C.S., *Ganciclovir*. N Engl J Med, 1996. **335**(10): p. 721-9.
151. Singh, N., *Antiviral drugs for cytomegalovirus in transplant recipients: advantages of preemptive therapy*. Rev Med Virol, 2006. **16**(5): p. 281-7.
152. Marty, F.M., P. Ljungman, R.F. Chemaly, J. Maertens, S.S. Dadwal, R.F. Duarte, S. Haider, A.J. Ullmann, Y. Katayama, J. Brown, K.M. Mullane, M. Boeckh, E.A. Blumberg, H. Einsele, D.R. Snyderman, Y. Kanda, M.J. DiNubile, V.L. Teal, H. Wan, Y. Murata, N.A. Kartsonis, R.Y. Leavitt, and C. Badshah, *Letermovir Prophylaxis for Cytomegalovirus in Hematopoietic-Cell Transplantation*. N Engl J Med, 2017. **377**(25): p. 2433-2444.
153. Marty, F.M., P. Ljungman, G.A. Papanicolaou, D.J. Winston, R.F. Chemaly, L. Strasfeld, J.A. Young, T. Rodriguez, J. Maertens, M. Schmitt, H. Einsele, A. Ferrant, J.H. Lipton, S.A. Villano, H. Chen, M. Boeckh, and G. Maribavir -300 Clinical Study, *Maribavir prophylaxis for prevention of cytomegalovirus disease in recipients of allogeneic stem-cell transplants: a phase 3, double-blind, placebo-controlled, randomised trial*. Lancet Infect Dis, 2011. **11**(4): p. 284-92.
154. El Chaer, F., D.P. Shah, and R.F. Chemaly, *How I treat resistant cytomegalovirus infection in hematopoietic cell transplantation recipients*. Blood, 2016. **128**(23): p. 2624-2636.
155. Meyers, J.D., J. Leszczynski, J.A. Zaia, N. Flournoy, B. Newton, D.R. Snyderman, G.G. Wright, M.J. Levin, and E.D. Thomas, *Prevention of cytomegalovirus infection by cytomegalovirus immune globulin after marrow transplantation*. Ann Intern Med, 1983. **98**(4): p. 442-6.
156. Ruutu, T., P. Ljungman, L. Brinch, S. Lenhoff, B. Lonnqvist, O. Ringden, P. Ruutu, L. Volin, D. Albrechtsen, B. Sallerfors, F. Ebeling, and G. Myllyla, *No prevention of cytomegalovirus infection by anti-cytomegalovirus hyperimmune globulin in seronegative bone marrow transplant recipients. The Nordic BMT Group*. Bone Marrow Transplant, 1997. **19**(3): p. 233-6.
157. Raanani, P., A. Gafter-Gvili, M. Paul, I. Ben-Bassat, L. Leibovici, and O. Shpilberg, *Immunoglobulin prophylaxis in hematopoietic stem cell transplantation: systematic review and meta-analysis*. J Clin Oncol, 2009. **27**(5): p. 770-81.
158. Snyderman, D.R., B.G. Werner, B. Heinze-Lacey, V.P. Berardi, N.L. Tilney, R.L. Kirkman, E.L. Milford, S.I. Cho, H.L. Bush, Jr., A.S. Levey, and et al., *Use of cytomegalovirus*

- immune globulin to prevent cytomegalovirus disease in renal-transplant recipients.* N Engl J Med, 1987. **317**(17): p. 1049-54.
159. Razonable, R.R. and A. Humar, *Cytomegalovirus in solid organ transplant recipients- Guidelines of the American Society of Transplantation Infectious Diseases Community of Practice.* Clin Transplant, 2019. **33**(9): p. e13512.
160. Pass, R.F., C. Zhang, A. Evans, T. Simpson, W. Andrews, M.L. Huang, L. Corey, J. Hill, E. Davis, C. Flanigan, and G. Cloud, *Vaccine prevention of maternal cytomegalovirus infection.* N Engl J Med, 2009. **360**(12): p. 1191-9.
161. Bernstein, D.I., F.M. Munoz, S.T. Callahan, R. Rupp, S.H. Wootton, K.M. Edwards, C.B. Turley, L.R. Stanberry, S.M. Patel, M.M. McNeal, S. Pichon, C. Amegashie, and A.R. Bellamy, *Safety and efficacy of a cytomegalovirus glycoprotein B (gB) vaccine in adolescent girls: A randomized clinical trial.* Vaccine, 2016. **34**(3): p. 313-9.
162. Anderholm, K.M., C.J. Bierle, and M.R. Schleiss, *Cytomegalovirus Vaccines: Current Status and Future Prospects.* Drugs, 2016. **76**(17): p. 1625-1645.
163. Riddell, S.R., K.S. Watanabe, J.M. Goodrich, C.R. Li, M.E. Agha, and P.D. Greenberg, *Restoration of viral immunity in immunodeficient humans by the adoptive transfer of T cell clones.* Science, 1992. **257**(5067): p. 238-41.
164. Walter, E.A., P.D. Greenberg, M.J. Gilbert, R.J. Finch, K.S. Watanabe, E.D. Thomas, and S.R. Riddell, *Reconstitution of cellular immunity against cytomegalovirus in recipients of allogeneic bone marrow by transfer of T-cell clones from the donor.* N Engl J Med, 1995. **333**(16): p. 1038-44.
165. Feuchtinger, T., K. Opherk, W.A. Bethge, M.S. Topp, F.R. Schuster, E.M. Weissinger, M. Mohty, R. Or, M. Maschan, M. Schumm, K. Hamprecht, R. Handgretinger, P. Lang, and H. Einsele, *Adoptive transfer of pp65-specific T cells for the treatment of chemorefractory cytomegalovirus disease or reactivation after haploidentical and matched unrelated stem cell transplantation.* Blood, 2010. **116**(20): p. 4360-7.
166. Fuji, S., H. Einsele, and M. Kapp, *Cytomegalovirus disease in hematopoietic stem cell transplant patients: current and future therapeutic options.* Curr Opin Infect Dis, 2017. **30**(4): p. 372-376.
167. Rauser, G., H. Einsele, C. Sinzger, D. Wernet, G. Kuntz, M. Assenmacher, J.D. Campbell, and M.S. Topp, *Rapid generation of combined CMV-specific CD4+ and CD8+ T-cell lines for adoptive transfer into recipients of allogeneic stem cell transplants.* Blood, 2004. **103**(9): p. 3565-72.
168. Odendahl, M., G.U. Grigoleit, H. Bonig, M. Neuenhahn, J. Albrecht, F. Anderl, L. Germeroth, M. Schmitz, M. Bornhauser, H. Einsele, E. Seifried, D.H. Busch, and T. Tonn, *Clinical-scale isolation of 'minimally manipulated' cytomegalovirus-specific donor lymphocytes for the treatment of refractory cytomegalovirus disease.* Cytotherapy, 2014. **16**(9): p. 1245-56.
169. Neuenhahn, M., J. Albrecht, M. Odendahl, F. Schlott, G. Dossinger, M. Schiemann, S. Lakshmiipathi, K. Martin, D. Bunjes, S. Harsdorf, E.M. Weissinger, H. Menzel, M. Verbeek, L. Uharek, N. Kroger, E. Wagner, G. Kobbe, T. Schroeder, M. Schmitt, G. Held, W. Herr, L. Germeroth, H. Bonig, T. Tonn, H. Einsele, D.H. Busch, and G.U. Grigoleit, *Transfer of*

- minimally manipulated CMV-specific T cells from stem cell or third-party donors to treat CMV infection after allo-HSCT. Leukemia, 2017. 31(10): p. 2161-2171.*
170. Leen, A.M., C.M. Bollard, A.M. Mendizabal, E.J. Shpall, P. Szabolcs, J.H. Antin, N. Kapoor, S.Y. Pai, S.D. Rowley, P. Kebriaei, B.R. Dey, B.J. Grilley, A.P. Gee, M.K. Brenner, C.M. Rooney, and H.E. Heslop, *Multicenter study of banked third-party virus-specific T cells to treat severe viral infections after hematopoietic stem cell transplantation. Blood, 2013. 121(26): p. 5113-23.*
171. Koehne, G., A. Hasan, E. Doubrovina, S. Prockop, E. Tyler, G. Wasilewski, and R.J. O'Reilly, *Immunotherapy with Donor T Cells Sensitized with Overlapping Pentadecapeptides for Treatment of Persistent Cytomegalovirus Infection or Viremia. Biol Blood Marrow Transplant, 2015. 21(9): p. 1663-78.*
172. O'Reilly, R.J., S. Prockop, A.N. Hasan, G. Koehne, and E. Doubrovina, *Virus-specific T-cell banks for 'off the shelf' adoptive therapy of refractory infections. Bone Marrow Transplant, 2016. 51(9): p. 1163-72.*
173. Eiz-Vesper, B., B. Maecker-Kolhoff, and R. Blasczyk, *Adoptive T-cell immunotherapy from third-party donors: characterization of donors and set up of a T-cell donor registry. Front Immunol, 2012. 3: p. 410.*
174. Holmes-Liew, C.L., M. Holmes, L. Beagley, P. Hopkins, D. Chambers, C. Smith, and R. Khanna, *Adoptive T-cell immunotherapy for ganciclovir-resistant CMV disease after lung transplantation. Clin Transl Immunology, 2015. 4(3): p. e35.*
175. Macesic, N., D. Langsford, K. Nicholls, P. Hughes, D.J. Gottlieb, L. Clancy, E. Blyth, K. Micklethwaite, B. Withers, S. Majumdar, S. Fleming, and J. Sasadeusz, *Adoptive T cell immunotherapy for treatment of ganciclovir-resistant cytomegalovirus disease in a renal transplant recipient. Am J Transplant, 2015. 15(3): p. 827-32.*
176. Smith, C., L. Beagley, S. Rehan, M.A. Neller, P. Crooks, M. Solomon, C.L. Holmes-Liew, M. Holmes, S.C. McKenzie, P. Hopkins, S. Campbell, R.S. Francis, D.C. Chambers, and R. Khanna, *Autologous Adoptive T-cell Therapy for Recurrent or Drug-resistant Cytomegalovirus Complications in Solid Organ Transplant Recipients: A Single-arm Open-label Phase I Clinical Trial. Clin Infect Dis, 2019. 68(4): p. 632-640.*
177. Kumar, D., M. Mian, L. Singer, and A. Humar, *An Interventional Study Using Cell-Mediated Immunity to Personalize Therapy for Cytomegalovirus Infection After Transplantation. Am J Transplant, 2017. 17(9): p. 2468-2473.*
178. Wills, M.R., A.J. Carmichael, K. Mynard, X. Jin, M.P. Weekes, B. Plachter, and J.G. Sissons, *The human cytotoxic T-lymphocyte (CTL) response to cytomegalovirus is dominated by structural protein pp65: frequency, specificity, and T-cell receptor usage of pp65-specific CTL. J Virol, 1996. 70(11): p. 7569-79.*
179. Manley, T.J., L. Luy, T. Jones, M. Boeckh, H. Mutimer, and S.R. Riddell, *Immune evasion proteins of human cytomegalovirus do not prevent a diverse CD8+ cytotoxic T-cell response in natural infection. Blood, 2004. 104(4): p. 1075-1082.*
180. Khattab, B.A.M., W. Lindenmaier, R. Frank, and H. Link, *Three T-cell epitopes within the C-terminal 265 amino acids of the matrix protein pp65 of human cytomegalovirus recognized by human lymphocytes. J Med Virol, 1997. 52(1): p. 68-76.*

181. Alp, N.J., T.D. Allport, J. Van Zanten, B. Rodgers, J.G. Sissons, and L.K. Borysiewicz, *Fine specificity of cellular immune responses in humans to human cytomegalovirus immediate-early 1 protein*. J Virol, 1991. **65**(9): p. 4812-20.
182. Hiemstra, H.S., N.C. Schloot, P.A. van Veelen, S.J. Willemsen, K.L. Franken, J.J. van Rood, R.R. de Vries, A. Chaudhuri, P.O. Behan, J.W. Drijfhout, and B.O. Roep, *Cytomegalovirus in autoimmunity: T cell crossreactivity to viral antigen and autoantigen glutamic acid decarboxylase*. Proc Natl Acad Sci U S A, 2001. **98**(7): p. 3988-91.
183. Liu, Y.-N., J. Curtsinger, P. Donahue, A. Klaus, G. Opitz, J. Cooper, R. Karr, F. Bach, and R. Gehrz, *Molecular analysis of the immune response to human cytomegalovirus glycoprotein B1 Mapping of HLA-restricted helper T cell epitopes on gp93*. J Gen Virol, 1993. **74**(10): p. 2207-2214.
184. Beninga, J., H. Kalbacher, and M. Mach, *Analysis of T helper cell response to glycoprotein H (gpUL75) of human cytomegalovirus: evidence for strain-specific T cell determinants*. J Infect Dis, 1996. **173**(5): p. 1051-61.
185. Braendstrup, P., B.K. Mortensen, S. Justesen, T. Osterby, M. Rasmussen, A.M. Hansen, C.B. Christiansen, M.B. Hansen, M. Nielsen, L. Vindelov, S. Buus, and A. Stryhn, *Identification and HLA-tetramer-validation of human CD4+ and CD8+ T cell responses against HCMV proteins IE1 and IE2*. PLoS One, 2014. **9**(4): p. e94892.
186. Fuhrmann, S., M. Streitz, P. Reinke, H.-D. Volk, and F. Kern, *T cell response to the cytomegalovirus major capsid protein (UL86) is dominated by helper cells with a large polyfunctional component and diverse epitope recognition*. J Infect Dis, 2008. **197**(10): p. 1455-1458.
187. Zhong, J., M. Rist, L. Cooper, C. Smith, and R. Khanna, *Induction of pluripotent protective immunity following immunisation with a chimeric vaccine against human cytomegalovirus*. PLoS One, 2008. **3**(9): p. e3256.
188. Höttler, A., L. März, M. Lübke, H.-G. Rammensee, and S. Stevanović, *Broad and Efficient Activation of Memory CD4+ T Cells by Novel HAdV- and HCMV-Derived Peptide Pools*. Front Immunol, 2021. **12**(2691).
189. UniProt, C., *UniProt: a worldwide hub of protein knowledge*. Nucleic Acids Res, 2019. **47**(D1): p. D506-D515.
190. Gonzalez-Galarza, F.F., L.Y. Takeshita, E.J. Santos, F. Kempson, M.H. Maia, A.L. da Silva, A.L. Teles e Silva, G.S. Ghataoraya, A. Alfievic, A.R. Jones, and D. Middleton, *Allele frequency net 2015 update: new features for HLA epitopes, KIR and disease and HLA adverse drug reaction associations*. Nucleic Acids Res, 2015. **43**(Database issue): p. D784-8.
191. Merrifield, R.B., *Solid phase peptide synthesis. I. The synthesis of a tetrapeptide*. J Am Chem Soc, 1963. **85**(14): p. 2149-2154.
192. Atherton, E., H. Fox, D. Harkiss, and R. Sheppard, *Application of polyamide resins to polypeptide synthesis: an improved synthesis of  $\beta$ -endorphin using fluorenylmethoxycarbonylamino-acids*. J Chem Soc Chem Commun, 1978(13): p. 539-540.

193. English, D. and B.R. Andersen, *Single-step separation of red blood cells. Granulocytes and mononuclear leukocytes on discontinuous density gradients of Ficoll-Hypaque*. J Immunol Methods, 1974. **5**(3): p. 249-52.
194. Rall, W.F. and G.M. Fahy, *Ice-free cryopreservation of mouse embryos at -196 degrees C by vitrification*. Nature, 1985. **313**(6003): p. 573-5.
195. Chudley, L., K.J. McCann, A. Coleman, A.M. Cazaly, N. Bidmon, C.M. Britten, S.H. van der Burg, C. Gouttefangeas, C. Jandus, K. Laske, D. Maurer, P. Romero, H. Schroder, L.F. Stynenbosch, S. Walter, M.J. Welters, and C.H. Ottensmeier, *Harmonisation of short-term in vitro culture for the expansion of antigen-specific CD8(+) T cells with detection by ELISPOT and HLA-multimer staining*. Cancer Immunol Immunother, 2014. **63**(11): p. 1199-211.
196. Bachmann, M.F. and A. Oxenius, *Interleukin 2: from immunostimulation to immunoregulation and back again*. EMBO Rep, 2007. **8**(12): p. 1142-8.
197. Czerkinsky, C.C., L.A. Nilsson, H. Nygren, O. Ouchterlony, and A. Tarkowski, *A solid-phase enzyme-linked immunospot (ELISPOT) assay for enumeration of specific antibody-secreting cells*. J Immunol Methods, 1983. **65**(1-2): p. 109-21.
198. Herr, W., J. Schneider, A.W. Lohse, K.H. Meyer zum Buschenfelde, and T. Wolfel, *Detection and quantification of blood-derived CD8+ T lymphocytes secreting tumor necrosis factor alpha in response to HLA-A2.1-binding melanoma and viral peptide antigens*. J Immunol Methods, 1996. **191**(2): p. 131-42.
199. Scheibenbogen, C., K.H. Lee, S. Mayer, S. Stevanovic, U. Moebius, W. Herr, H.G. Rammensee, and U. Keilholz, *A sensitive ELISPOT assay for detection of CD8+ T lymphocytes specific for HLA class I-binding peptide epitopes derived from influenza proteins in the blood of healthy donors and melanoma patients*. Clin Cancer Res, 1997. **3**(2): p. 221-6.
200. Yang, J., V.M. Lemas, I.W. Flinn, C. Krone, and R.F. Ambinder, *Application of the ELISPOT assay to the characterization of CD8(+) responses to Epstein-Barr virus antigens*. Blood, 2000. **95**(1): p. 241-8.
201. Nowell, P.C., *Phytohemagglutinin: an initiator of mitosis in cultures of normal human leukocytes*. Cancer Res, 1960. **20**(4): p. 462-6.
202. Green, J.A., S.R. Cooperband, and S. Kibrick, *Immune specific induction of interferon production in cultures of human blood lymphocytes*. Science, 1969. **164**(3886): p. 1415-7.
203. McGadey, J., *A tetrazolium method for non-specific alkaline phosphatase*. Histochemie, 1970. **23**(2): p. 180-4.
204. Hesse, M.D., A.Y. Karulin, B.O. Boehm, P.V. Lehmann, and M. Tary-Lehmann, *A T cell clone's avidity is a function of its activation state*. J Immunol, 2001. **167**(3): p. 1353-61.
205. Dubey, S., J. Clair, T.-M. Fu, L. Guan, R. Long, R. Mogg, K. Anderson, K.B. Collins, C. Gaunt, and V.R. Fernandez, *Detection of HIV vaccine-induced cell-mediated immunity in HIV-seronegative clinical trial participants using an optimized and validated enzyme-linked immunospot assay*. J Acquir Immune Defic Syndr, 2007. **45**(1): p. 20-27.



206. Tobery, T.W., S.A. Dubey, K. Anderson, D.C. Freed, K.S. Cox, J. Lin, M.T. Prokop, K.J. Sykes, R. Mogg, D.V. Mehrotra, T.M. Fu, D.R. Casimiro, and J.W. Shiver, *A comparison of standard immunogenicity assays for monitoring HIV type 1 gag-specific T cell responses in Ad5 HIV Type 1 gag vaccinated human subjects*. *AIDS Res Hum Retroviruses*, 2006. **22**(11): p. 1081-90.
207. Baran, J., D. Kowalczyk, M. Ozog, and M. Zembala, *Three-color flow cytometry detection of intracellular cytokines in peripheral blood mononuclear cells: comparative analysis of phorbol myristate acetate-ionomycin and phytohemagglutinin stimulation*. *Clin Diagn Lab Immunol*, 2001. **8**(2): p. 303-13.
208. Chardin, P. and F. McCormick, *Brefeldin A: the advantage of being uncompetitive*. *Cell*, 1999. **97**(2): p. 153-155.
209. Chenna, R., H. Sugawara, T. Koike, R. Lopez, T.J. Gibson, D.G. Higgins, and J.D. Thompson, *Multiple sequence alignment with the Clustal series of programs*. *Nucleic Acids Res*, 2003. **31**(13): p. 3497-500.
210. Malik, A., E. Adland, L. Laker, H. Kloverpris, R. Fardoos, J. Roider, M.C. Severinsen, F. Chen, L. Riddell, A. Edwards, S. Buus, P. Jooste, P.C. Matthews, and P.J.R. Goulder, *Immunodominant cytomegalovirus-specific CD8+ T-cell responses in sub-Saharan African populations*. *PLoS One*, 2017. **12**(12): p. e0189612.
211. Bronke, C., N.M. Palmer, G.H. Westerlaken, M. Toebes, G.M. van Schijndel, V. Purwaha, K.E. van Meijgaarden, T.N. Schumacher, D. van Baarle, K. Tesselaar, and A. Geluk, *Direct ex vivo detection of HLA-DR3-restricted cytomegalovirus- and Mycobacterium tuberculosis-specific CD4+ T cells*. *Hum Immunol*, 2005. **66**(9): p. 950-61.
212. Provenzano, M., G. Sais, L. Bracci, A. Egli, M. Anselmi, C.T. Viehl, S. Schaub, H.H. Hirsch, D.F. Stroncek, F.M. Marincola, and G.C. Spagnoli, *A HCMV pp65 polypeptide promotes the expansion of CD4+ and CD8+ T cells across a wide range of HLA specificities*. *J Cell Mol Med*, 2009. **13**(8B): p. 2131-2147.
213. Hanley, P.J., C.R.Y. Cruz, B. Savoldo, A.M. Leen, M. Stanojevic, M. Khalil, W. Decker, J.J. Moldrem, H. Liu, and A.P. Gee, *Functionally active virus-specific T cells that target CMV, adenovirus, and EBV can be expanded from naive T-cell populations in cord blood and will target a range of viral epitopes*. *Blood*, 2009. **114**(9): p. 1958-1967.
214. Nastke, M.D., L. Herrgen, S. Walter, D. Wernet, H.G. Rammensee, and S. Stevanovic, *Major contribution of codominant CD8 and CD4 T cell epitopes to the human cytomegalovirus-specific T cell repertoire*. *Cell Mol Life Sci*, 2005. **62**(1): p. 77-86.
215. Li Pira, G., L. Bottone, F. Ivaldi, R. Pelizzoli, F. Del Galdo, L. Lozzi, L. Bracci, A. Loregian, G. Palu, R. De Palma, H. Einsele, and F. Manca, *Identification of new Th peptides from the cytomegalovirus protein pp65 to design a peptide library for generation of CD4 T cell lines for cellular immunoreconstitution*. *Int Immunol*, 2004. **16**(5): p. 635-42.
216. Gallot, G., R. Vivien, C. Ibsch, J. Lule, C. Davrinche, J. Gaschet, and H. Vie, *Purification of Ag-specific T lymphocytes after direct peripheral blood mononuclear cell stimulation followed by CD25 selection. I. Application to CD4(+) or CD8(+) cytomegalovirus phosphoprotein pp65 epitope determination*. *J Immunol*, 2001. **167**(8): p. 4196-206.

217. Lubke, M., S. Spalt, D.J. Kowalewski, C. Zimmermann, L. Bauersfeld, A. Nelde, L. Bichmann, A. Marcu, J.K. Peper, O. Kohlbacher, J.S. Walz, V.T.K. Le-Trilling, H. Hengel, H.G. Rammensee, S. Stevanovic, and A. Halenius, *Identification of HCMV-derived T cell epitopes in seropositive individuals through viral deletion models*. *J Exp Med*, 2020. **217**(3).
218. Meissner, C.S., P. Köppen-Rung, A. Dittmer, S. Lapp, and E. Bogner, *A "coiled-coil" motif is important for oligomerization and DNA binding properties of human cytomegalovirus protein UL77*. *PLoS One*, 2011. **6**(10): p. e25115.
219. McMahon, T.P. and D.G. Anders, *Interactions between human cytomegalovirus helicase–primase proteins*. *Virus Res*, 2002. **86**(1-2): p. 39-52.
220. Pari, G.S. and D.G. Anders, *Eleven loci encoding trans-acting factors are required for transient complementation of human cytomegalovirus oriLyt-dependent DNA replication*. *J Virol*, 1993. **67**(12): p. 6979-88.
221. AuCoin, D.P., G.B. Smith, C.D. Meiering, and E.S. Mocarski, *Betaherpesvirus-conserved cytomegalovirus tegument protein ppUL32 (pp150) controls cytoplasmic events during virion maturation*. *J Virol*, 2006. **80**(16): p. 8199-210.
222. Schilling, E.M., M. Scherer, N. Reuter, J. Schweininger, Y.A. Muller, and T. Stamminger, *The Human Cytomegalovirus IE1 Protein Antagonizes PML Nuclear Body-Mediated Intrinsic Immunity via the Inhibition of PML De Novo SUMOylation*. *J Virol*, 2017. **91**(4): p. e02049-16.
223. Thimme, R., D. Oldach, K.M. Chang, C. Steiger, S.C. Ray, and F.V. Chisari, *Determinants of viral clearance and persistence during acute hepatitis C virus infection*. *J Exp Med*, 2001. **194**(10): p. 1395-406.
224. Lilleri, D., P. Zelini, C. Fornara, G. Comolli, and G. Gerna, *Inconsistent responses of cytomegalovirus-specific T cells to pp65 and IE-1 versus infected dendritic cells in organ transplant recipients*. *Am J Transplant*, 2007. **7**(8): p. 1997-2005.
225. Seder, R.A., P.A. Darrah, and M. Roederer, *T-cell quality in memory and protection: implications for vaccine design*. *Nat Rev Immunol*, 2008. **8**(4): p. 247-58.
226. Solache, A., C.L. Morgan, A.I. Dodi, C. Morte, I. Scott, C. Baboonian, B. Zal, J. Goldman, J.E. Grundy, and J.A. Madrigal, *Identification of Three HLA-A\*0201-Restricted Cytotoxic T Cell Epitopes in the Cytomegalovirus Protein pp65 That Are Conserved Between Eight Strains of the Virus*. *J Immunol*, 1999. **163**(10): p. 5512-5518.
227. Justesen, S., M. Harndahl, K. Lamberth, L.L. Nielsen, and S. Buus, *Functional recombinant MHC class II molecules and high-throughput peptide-binding assays*. *Immunome Res*, 2009. **5**(1): p. 2.
228. Jackson, S.E., G.X. Sedikides, G.M. Mason, G. Okecha, and M.R. Wills, *Human Cytomegalovirus (HCMV)-Specific CD4(+) T Cells Are Polyfunctional and Can Respond to HCMV-Infected Dendritic Cells In Vitro*. *J Virol*, 2017. **91**(6): p. e02128-16.
229. Hammoud, B., M. Schmueck, A.M. Fischer, H. Fuehrer, S.J. Park, L. Akyuez, J.C. Schefold, M.J. Raftery, G. Schonrich, A.M. Kaufmann, H.D. Volk, and P. Reinke, *HCMV-specific T-cell therapy: do not forget supply of help*. *J Immunother*, 2013. **36**(2): p. 93-101.

230. Peper, J.K., H.C. Bosmuller, H. Schuster, B. Guckel, H. Horzer, K. Roehle, R. Schafer, P. Wagner, H.G. Rammensee, S. Stevanovic, F. Fend, and A. Staebler, *HLA ligandomics identifies histone deacetylase 1 as target for ovarian cancer immunotherapy*. *Oncoimmunology*, 2016. **5**(5): p. e1065369.
231. Steimle, V., C.A. Siegrist, A. Mottet, B. Lisowska-Grospierre, and B. Mach, *Regulation of MHC class II expression by interferon-gamma mediated by the transactivator gene CIITA*. *Science*, 1994. **265**(5168): p. 106-9.
232. Kim, A. and S. Sadegh-Nasseri, *Determinants of immunodominance for CD4 T cells*. *Curr Opin Immunol*, 2015. **34**: p. 9-15.
233. Roy-Proulx, G., M.-C. Meunier, A.-M. Lanteigne, S. Brochu, and C. Perreault, *Immunodomination results from functional differences between competing CTL*. *Eur J Immunol*, 2001. **31**(8): p. 2284-2292.
234. Kedl, R.M., W.A. Rees, D.A. Hildeman, B. Schaefer, T. Mitchell, J. Kappler, and P. Marrack, *T cells compete for access to antigen-bearing antigen-presenting cells*. *J Exp Med*, 2000. **192**(8): p. 1105-13.
235. Kedl, R.M., B.C. Schaefer, J.W. Kappler, and P. Marrack, *T cells down-modulate peptide-MHC complexes on APCs in vivo*. *Nat Immunol*, 2002. **3**(1): p. 27-32.
236. Chudley, L., K. McCann, A. Mander, T. Tjelle, J. Campos-Perez, R. Godeseth, A. Creak, J. Dobbyn, B. Johnson, P. Bass, C. Heath, P. Kerr, I. Mathiesen, D. Dearnaley, F. Stevenson, and C. Ottensmeier, *DNA fusion-gene vaccination in patients with prostate cancer induces high-frequency CD8(+) T-cell responses and increases PSA doubling time*. *Cancer Immunol Immunother*, 2012. **61**(11): p. 2161-70.
237. Todryk, S.M., A.A. Pathan, S. Keating, D.W. Porter, T. Berthoud, F. Thompson, P. Klenerman, and A.V. Hill, *The relationship between human effector and memory T cells measured by ex vivo and cultured ELISPOT following recent and distal priming*. *Immunology*, 2009. **128**(1): p. 83-91.
238. Godkin, A.J., H.C. Thomas, and P.J. Openshaw, *Evolution of epitope-specific memory CD4(+) T cells after clearance of hepatitis C virus*. *J Immunol*, 2002. **169**(4): p. 2210-4.
239. Stemberger, C., P. Graef, M. Odendahl, J. Albrecht, G. Dossinger, F. Anderl, V.R. Buchholz, G. Gasteiger, M. Schiemann, G.U. Grigoleit, F.R. Schuster, A. Borkhardt, B. Versluys, T. Tonn, E. Seifried, H. Einsele, L. Germeroth, D.H. Busch, and M. Neuenhahn, *Lowest numbers of primary CD8(+) T cells can reconstitute protective immunity upon adoptive immunotherapy*. *Blood*, 2014. **124**(4): p. 628-37.
240. Litjens, N.H.R., L. Huang, B. Dedeoglu, R.W.J. Meijers, J. Kwekkeboom, and M.G.H. Betjes, *Protective Cytomegalovirus (CMV)-Specific T-Cell Immunity Is Frequent in Kidney Transplant Patients without Serum Anti-CMV Antibodies*. *Front Immunol*, 2017. **8**(1137): p. 1137.
241. Terlutter, F., R. Caspell, T.M. Nowacki, A. Lehmann, R. Li, T. Zhang, A. Przybyla, S. Kuerten, and P.V. Lehmann, *Direct Detection of T- and B-Memory Lymphocytes by ImmunoSpot® Assays Reveals HCMV Exposure that Serum Antibodies Fail to Identify*. *Cells*, 2018. **7**(5): p. 45.

242. Dargan, D.J., E. Douglas, C. Cunningham, F. Jamieson, R.J. Stanton, K. Baluchova, B.P. McSharry, P. Tomasec, V.C. Emery, E. Percivalle, A. Sarasini, G. Gerna, G.W. Wilkinson, and A.J. Davison, *Sequential mutations associated with adaptation of human cytomegalovirus to growth in cell culture*. J Gen Virol, 2010. **91**(Pt 6): p. 1535-46.
243. Cha, T.A., E. Tom, G.W. Kemble, G.M. Duke, E.S. Mocarski, and R.R. Spaete, *Human cytomegalovirus clinical isolates carry at least 19 genes not found in laboratory strains*. J Virol, 1996. **70**(1): p. 78-83.
244. Akter, P., C. Cunningham, B.P. McSharry, A. Dolan, C. Addison, D.J. Dargan, A.F. Hassan-Walker, V.C. Emery, P.D. Griffiths, G.W.G. Wilkinson, and A.J. Davison, *Two novel spliced genes in human cytomegalovirus*. J Gen Virol, 2003. **84**(Pt 5): p. 1117-1122.
245. Dolan, A., C. Cunningham, R.D. Hector, A.F. Hassan-Walker, L. Lee, C. Addison, D.J. Dargan, D.J. McGeoch, D. Gatherer, V.C. Emery, P.D. Griffiths, C. Sinzger, B.P. McSharry, G.W.G. Wilkinson, and A.J. Davison, *Genetic content of wild-type human cytomegalovirus*. J Gen Virol, 2004. **85**(Pt 5): p. 1301-1312.
246. Buscher, N., C. Paulus, M. Nevels, S. Tenzer, and B. Plachter, *The proteome of human cytomegalovirus virions and dense bodies is conserved across different strains*. Med Microbiol Immunol, 2015. **204**(3): p. 285-93.

## **10 Erklärung zum Eigenanteil**

Diese Arbeit wurde am Interfakultären Institut für Zellbiologie in der Abteilung für Immunologie unter Betreuung von Prof. Dr. Stefan Stevanović durchgeführt.

Die Konzeption des Projekts erfolgte durch Prof. Dr. Stefan Stevanović.

Sämtliche Versuche wurden nach Einarbeitung durch Dr. Maren Lübke und Tatjana Bilich von mir eigenständig durchgeführt. Die Herstellung der Peptide erfolgte durch Ulrich Wulle und Prof. Dr. Stefan Stevanović. Die Qualitätskontrolle der hergestellten Peptide wurde von Ulrich Wulle, Prof. Dr. Stefan Stevanović, Marion Gauger und Dr. Monika Denk durchgeführt. Die statistische Auswertung erfolgte nach Anleitung von Dr. Maren Lübke durch mich. Teile dieser Arbeit wurden bereits in der Publikation von Höttler and März et al. veröffentlicht. Die Generierung und Auswertung dieser Daten erfolgten durch mich und sind mein Anteil an der Publikation.

Ich versichere, das Manuskript nach Anleitung durch Dr. Maren Lübke und Prof. Dr. Stefan Stevanović selbständig verfasst zu haben und keine weiteren als die von mir angegebenen Quellen verwendet zu haben.

Tübingen, den 12.08.2021

Alexander Höttler

## **11 Publications**

Parts of this thesis have been published as an original research article:

Alexander Höttler, Léo März, Maren Lübke, Hans-Georg Rammensee, and Stefan Stevanović, *Broad and Efficient Activation of Memory CD4+ T Cells by Novel HAdV- and HCMV-Derived Peptide Pools*. *Frontiers in Immunology*, 2021. **12**(2691)

### **11.1 Poster presentation**

Parts of this thesis were reported in a poster presentation at the *Forschungskolloquium 2020 der Medizinischen Fakultät, Universität Tübingen* on the 24<sup>th</sup> of January 2020.

## 12 Danksagung

Ich danke Herrn Prof. Dr. Stefan Stevanović für die hervorragende Betreuung während meiner Zeit in der Immunologie. Seine Tür stand mir immer offen, wodurch Fragen und Herausforderungen jederzeit besprochen und angegangen werden konnten. Ich bin sehr dankbar für seine Unterstützung bei der Durchführung und Planung des Projekts und der Publikation der Ergebnisse.

Ich möchte mich herzlich bei Dr. Maren Lübke bedanken, die sich viel Zeit genommen hat, um mich in die Laborarbeit einzuweisen. Ich bin sehr dankbar für ihr Verständnis, wenn einmal etwas nicht funktioniert hat und ihre große Hilfsbereitschaft auch über ihre Zeit am Institut hinaus.

Ich möchte auch Prof. Dr. Hans-Georg Rammensee für wichtige Ratschläge und Rückfragen und die freundliche Unterstützung danken. Mein großer Dank gilt auch dem gesamten Team der Immunologie, das immer sehr hilfsbereit war und für eine freundliche Atmosphäre gesorgt hat. Es hat mir sehr viel Spaß gemacht, ein Teil davon zu sein. Vielen Dank besonders an Dr. Tatjana Bilich und Dr. Ana Marcu, die bei Fragen immer ansprechbar waren und Ulrich Wulle für die Synthese der zahlreichen Peptide für dieses Projekt.

Zudem bedanke ich mich bei der medizinischen Fakultät Tübingen für die finanzielle Förderung im Rahmen des IZKF-Promotionskollegs (2-2018). Ich danke Frau Dr. Montero für lehrreiche Seminare und Workshops, die mich bei der Erstellung meiner Dissertation weitergebracht haben.

Besonders möchte ich meinen Eltern, meiner Familie und Sarah für ihren großen Rückhalt und die verlässliche Unterstützung danken. Vielen Dank auch an Andreas für das Korrekturlesen dieser Arbeit.